January 2013

Application Of Composite Polymeric Membranes For Efficient Regeneration Of Physical Solvents

Alireza Pesaran

Follow this and additional works at: https://commons.und.edu/theses

**APPLICATION OF COMPOSITE POLYMERIC MEMBRANES FOR
EFFICIENT REGENERATION OF PHYSICAL SOLVENTS**

by

Alireza Pesaran
Bachelor of Science, Shiraz University, Shiraz, Iran 2006

A Thesis

Submitted to the Graduate Faculty

of the

University of North Dakota

In partial fulfillment of the requirements

for the degree of

Master of Science

Grand Forks, North Dakota
August
2013

This thesis, submitted by Alireza Pesaran, in partial fulfillment of the requirements for the Degree of Master of Science from the University of North Dakota, has been read by the Faculty Advisory Committee under whom the work has been done and is hereby approved.

_____
Dr. Brian Tande

_____
Dr. Steve Benson

_____
Dr. Gautham Krishnamoorthy

This thesis meets the standards for appearance, conforms to the style and format requirements of the Graduate School of the University of North Dakota, and is hereby approved.

_____
Dr. Wayne Swisher
Dean of the Graduate School

_____
Date

Title   Application of Composite Polymeric Membranes for Efficient
                      Regeneration of Physical Solvents

Department   Chemical Engineering

Degree   Master of Science

In presenting this thesis in partial fulfillment of the requirements for a graduate degree from the University of North Dakota, I agree that the library of this University shall make it freely available for inspection. I further agree that permission for extensive copying for scholarly purposes may be granted by the professor who supervised my thesis work or, in his absence, by the chairperson of the department or the dean of the Graduate School. It is understood that any copying or publication or other use of this thesis or part thereof for financial gain shall not be allowed without my written permission. It is also understood that due recognition shall be given to me and to the University of North Dakota in any scholarly use which may be made of any material in my thesis.

<div align="center">

Alireza Pesaran
07/17/2013

</div>

Table of Contents

List of Figures

x

List of Tables

xiii

ACKNOWLEDGMENTS

To my parents,

for their endless love, support and encouragement.

ABSTRACT

The most dominant CO_2 capture technology used for pre-combustion capture involves the application of physical solvents. Despite the low energy required to regenerate physical solvents and their high capacity for capturing and separating acid gases from the syngas produced in a gasification plant, physical solvents have some disadvantages including CO_2 pressure loss and the energy required to pump the solvent to the high pressure absorber.

The primary objective of this work is to evaluate the use of composite polymeric membranes for the recovery of CO_2 from CO_2-rich solvent streams. To achieve this purpose, an experimental bench-scale setup was built to investigate and quantify CO_2 removal capacity from the rich solvent across different types of membranes.

Dimethyl ether of polyethylene glycol (Selexol) is used as the solvent since it is reputed to be one of the major physical solvents for CO_2 removal. To evaluate the effectiveness of different types of membranes, the CO_2 permeation rate and membrane selectivity were measured for different membranes.

The results of the screening study indicated that PDMS-based membranes (PERVATECH and PERVAP 4060) have higher CO_2 permeability compared to PVOH-based membranes (PERVAP 1211 and PERVAP 1201). The best membrane for further analysis and experiments to find the optimum operational conditions was chosen as PEVAP 4060 from SULZER due to its high CO_2 flux and selectivity compared to other membranes.

Following a two-factor two -level full factorial design with two replicates an three center points, a statistical analysis was also performed to identify the significant factors for each individual response such as permeation rate, leak rate and selectivity. For CO_2 flux, pressure appeared to be strongly significant. However, solvent flow rate had no significant effect on the rate of CO_2 permeation. With respect to the solvent leak, the analysis of Pareto charts suggested pressure to be significant and solvent flow rate to be insignificant. Neither system pressure nor solvent flow rate found to be significant considering the selectivity as the experiment's response. Finally, regarding the percent recovery, both the system pressure and solvent flow rate appeared to be significant.

In order to examine the chemical stability and structural integrity of the membranes after being exposed to the high pressure solvent, a series of post-experiment characteristic tests such as FTIR and DSC were performed. The results of these studies revealed no major changes.

1 Introduction

1.1 Significance of CO_2 capture

Increased levels of greenhouse gases (GHG) in the atmosphere in the past five decades are believed to have caused and further aggravated the adverse effects of global warming. GHG includes a variety of different species such as CO_2, CH_4, SF_6, CF_4 and N_2O. However, CO_2 has the largest contribution among GHG due to its highest concentration in the atmosphere. Yamasaki (Yamasaki, 2003) predicted CO_2's contribution to global warming to be of 60 percent. The International Panel on Climate Change (IPCC) predicts the current atmospheric concentration of CO_2 to be 385 (ppm) which is significantly higher than other GHG such as CH_4: 1.741 (ppm), N_2O: 0.321 (ppm) and CF_4: 74 (ppt). IPCC predicts the CO_2 concentration in the atmosphere by the year 2100 to be 570 (ppm) which may raise the average global temperature by 1.9 ^{o}C (Stewart & Hessami, 2005). Figure 1.1 shows the GHG concentration breakdown in the atmosphere. Clearly, CO_2 with over 80 % accounts for the most significant GHG in atmosphere.
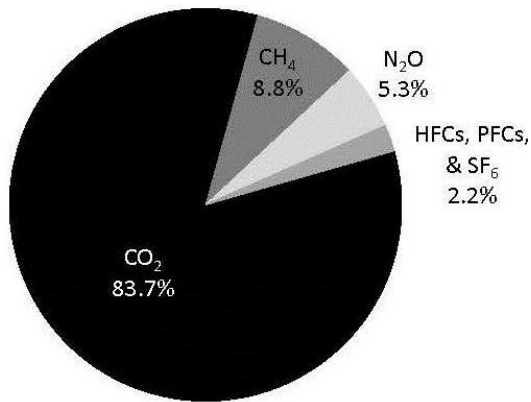
Figure 1.1 2011 Greenhouse Gas Emissions by Gas (Percentages based on Tg
CO_2 Eq.(*INVENTORY OF U.S. GREENHOUSE GAS EMISSIONS
AND SINKS: 1990-2011* .2013).

Compared to other GHG, CO_2 has the highest rate of concentration
change in the atmosphere. While the rate of CO_2 concentration change is 1.4
(ppm/yr), the rates of concentration change for CH_4 and N_2O are 0.005 (ppm/yr)
and (0.26%/yr) respectively. The CO_2 concentration in the atmosphere continues
to increase. Figure 1.2 shows the cumulative change in annual U.S. greenhouse
gas emissions relative to 1990 reported by the Inventory of U.S. Greenhouse
Gas Emissions and Sinks in 2013 (*INVENTORY OF U.S. GREENHOUSE GAS
EMISSIONS AND SINKS: 1990-2011* .2013). The increasing trend of GHG is
quite obvious. The decreased amount of emission in 2009 has been attributed to
the impact of the financial crisis over that period.
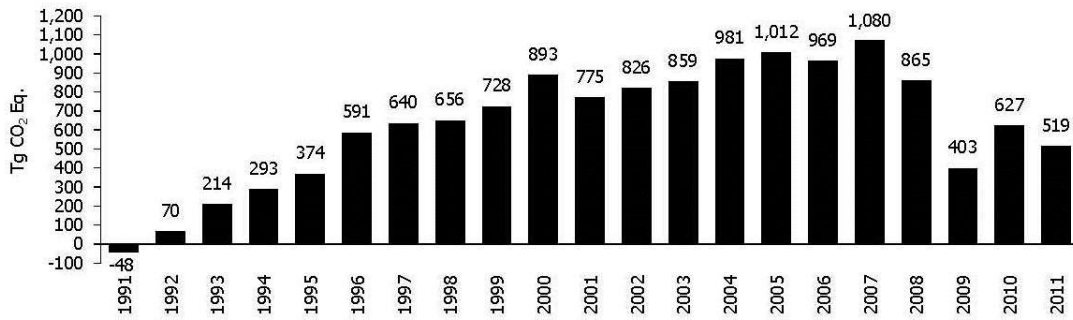
Figure 1.2. Cumulative Change in Annual U.S. Greenhouse Gas Emissions Relative to 1990 (INVENTORY OF U.S. GREENHOUSE GAS EMISSIONS AND SINKS: 1990-2011 .2013).

According to a report by the International Energy Agency (IEA) (*CO₂ EMISSIONS FROM FUEL COMBUSTION.*2012), global CO_2 emissions increased by 1.3 Gt CO_2 between 2009 and 2010. According to the same report the growth rate of CO2 emissions varies for different regions, fuel types and sectors: "The 0.4-GtCO_2 increase in emissions for Annex I countries was primarily due to similar increases in gas and coal demand (demand for oil was almost static). By contrast, the 0.8-Gt CO_2 increase in emissions for non-Annex I countries was more spread out: 50% from coal, 25% from oil and 23% from natural gas." (*CO2 EMISSIONS FROM FUEL COMBUSTION.*2012). Figure 1.3 shows the top ten CO_2 emitting countries in the world which account for nearly two-thirds of the world CO_2 emissions (*CO₂ EMISSIONS FROM FUEL COMBUSTION.*2012).

3
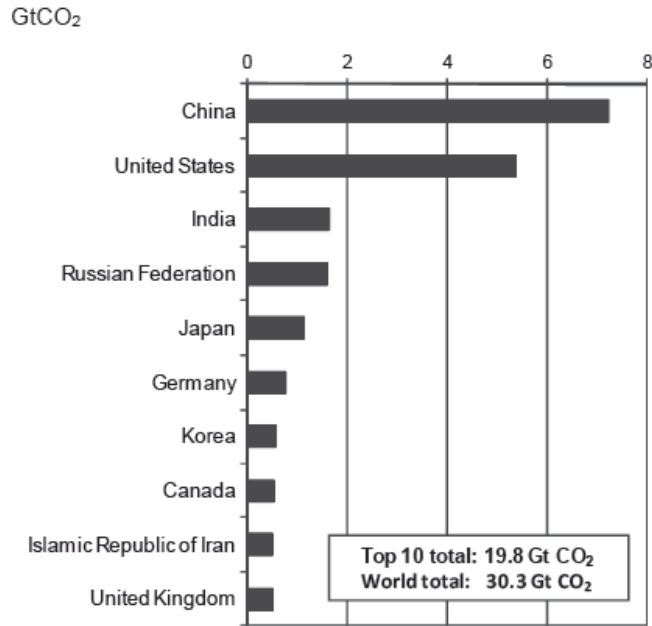
Figure 1.3. Top 10 CO_2 emitting countries in 2010 (CO2 EMISSIONS FROM FUEL COMBUSTION.2012).

An important yet not usually discussed fact about CO_2 is its relatively long atmospheric lifetime. CO_2 has a lifetime of 50-200 years in the atmosphere, which is noticeably longer than many other GHG such as CH_4 (12 years), N_2O (114 years) etc. (*INVENTORY OF U.S. GREENHOUSE GAS EMISSIONS AND SINKS: 1990-2011 .*2013).

Three major strategies may be implemented to reduce total CO_2 emission into the atmosphere, which can be summarized as: (a) reducing energy intensity (b) reducing carbon intensity and (c) using modern CO_2 capture and sequestration technologies. The first option necessitates the use of energy cycles with higher efficiency. The second strategy involves using non-fossil fuels and

4

renewable energies. The last option that is highly studied includes developing and using CO_2 capture technologies from major emission sources. This will be discussed in more detail in the next sections of this chapter.

Considering the high concentration of CO_2 in the atmosphere and the trends of global CO_2 emissions over the past two decades, it is imperative to identify the major CO_2 emission sources to mitigate further CO_2 accumulation in the atmosphere and thus lessen the destructive effects of global warming. In the next section, the major anthropogenic sources of CO_2 emissions will be reviewed.

1.2 The major anthropogenic sources of CO_2 emissions

The total amount of carbon on earth is constant. Carbon in the form of CO_2 is absorbed by oceans and living organisms and emitted to the atmosphere through natural processes. The advent of the industrial revolution in 1750 disrupted the carbon balance on earth. As a result, global atmospheric concentrations of CO_2 has increased by 39 percent (Solomon et al., 2007). Currently over 85 percent of world energy consumption is provided through fossil fuels. Combustion of fossil fuels accounts for the largest source of CO_2 emissions globally. In 2010, 31780 Tg of CO_2 were added to the atmosphere through the combustion of fossil fuels, of which the U.S. accounted for 18 percent (*CO2 EMISSIONS FROM FUEL COMBUSTION*.2012) and (*International energy*

*statistics.*2010). The total amount of CO_2 emissions in 2011 from various anthropogenic sources are shown in Figure 1.4. Among different types of fossil fuels, coal contributes the most CO_2 emissions. In 2010, 43% of CO_2 emissions from fuel combustion were produced from coal, 36% from oil and 20% from gas (*CO2 EMISSIONS FROM FUEL COMBUSTION.*2012). Figure 1.5 shows the profiles of CO_2 emissions versus time for different fuel types.
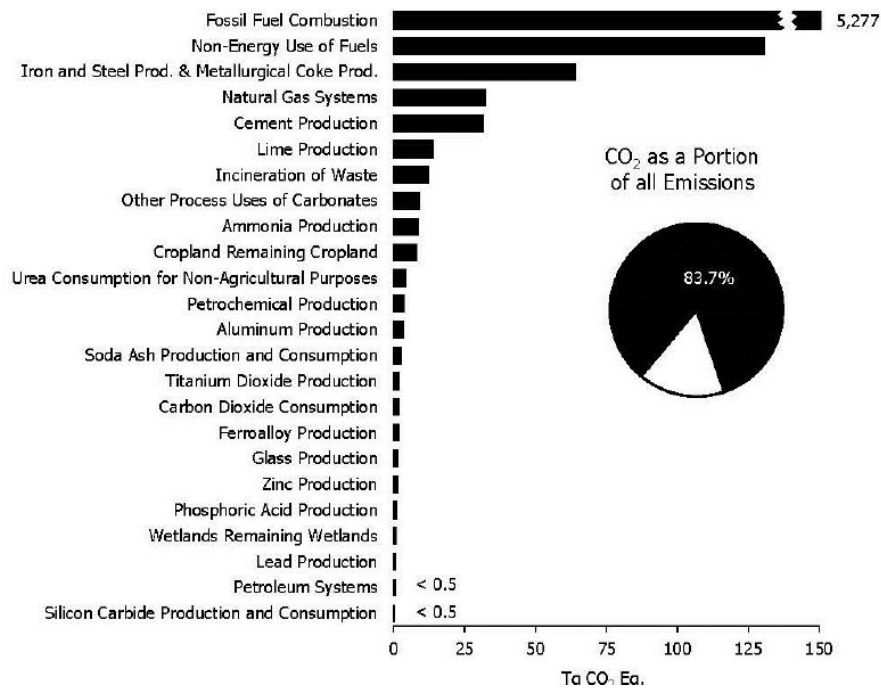
Figure 1.4. 2011 Sources of CO_2 Emissions (INVENTORY OF U.S. GREENHOUSE GAS EMISSIONS AND SINKS: 1990-2011 .2013).

GtCO$_2$
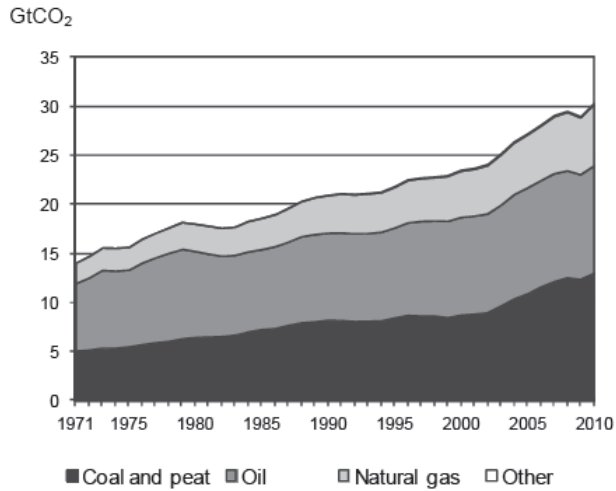
Figure 1.5. CO$_2$ emissions by fuel type (CO$_2$ EMISSIONS FROM FUEL COMBUSTION.2012).

Emissions of CO$_2$ from fossil fuel combustion increased at an average annual rate of 0.5 percent from 1990 to 2011(*INVENTORY OF U.S. GREENHOUSE GAS EMISSIONS AND SINKS: 1990-2011* .2013). The breakdown of CO$_2$ emissions from the combustion of fossil fuels for different sectors and fuel types is shown in Figure 1.6. The data shown in Figure 1.6 clearly demonstrates the fact that electricity generation by coal accounts for the largest point source of CO$_2$ emissions.
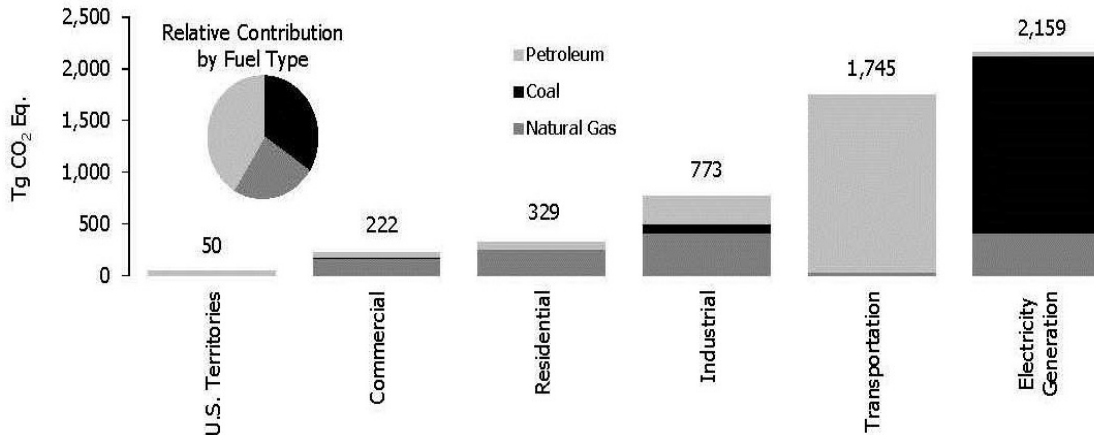
Figure 1.6. 2011 CO_2 Emissions from Fossil Fuel Combustion by Sector and Fuel Type (INVENTORY OF U.S. GREENHOUSE GAS EMISSIONS AND SINKS: 1990-2011 .2013).

According to the 2012 IEA report (*CO2 EMISSIONS FROM FUEL COMBUSTION.*2012), heat and electricity generation is the largest producer of CO_2 emissions and was responsible for 41% of world CO_2 emissions in 2010. The major CO_2 emitting sectors are shown in Figure 1.7.
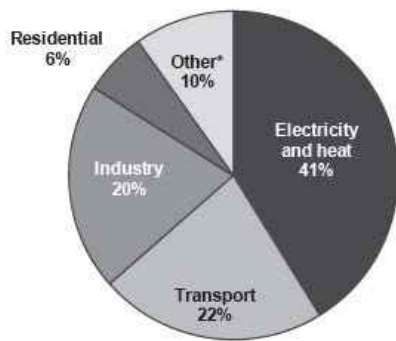
Figure 1.7. World CO_2 emissions by sector in 2010 (CO_2 EMISSIONS FROM FUEL COMBUSTION.2012).

8

The data represented in Figure 6 suggest that electricity generation relies heavily on coal combustion, which is the most carbon-intensive fossil fuel, which in turn explains its significant contribution in global CO_2 emissions. World electricity demand will increase by 70% by 2035 and it is estimated that without using the CO_2 emissions mitigation strategies as explained earlier in section 1.1, CO_2 emissions from coal will grow to 15.3 $GtCO_2$ in 2035 (*CO2 EMISSIONS FROM FUEL COMBUSTION*.2012). Considering the fact that electricity producing power plants are the major point source of CO_2 emissions, along with the ever-increasing demand for electricity, the necessity to further develop CO_2 capture technologies seems crucial and inevitable. In the next section of this chapter, a concise review of the major CO_2 capture approaches will be provided.

1.3   Current CO_2 capture approaches

As outlined by Olajire (Olajire, 2010) and mentioned earlier, the main approaches for reducing the total amount of CO_2 emission include: (1) Reducing energy intensity by increasing the efficiency of power generation cycles, (2) Reducing carbon intensity by using non-fossil fuels such as hydrogen and renewable energy, (3) developing new power production technologies, such as oxy-combustion, Integrated Gasification combined Cycle (IGCC), and chemical looping and (4) Developing advanced and cost effective CO_2 capture technologies. Among these, DOE's Carbon Sequestration Program is focused on the third and fourth approaches to reducing CO_2 emissions. CO_2 capture

9

methods are categorized into three main approaches: (1) pre-combustion capture, (2) post –combustion capture and (3) Oxy-Combustion.

1.3.1 Pre-combustion CO_2 capture

In pre-combustion fuel is reacted with oxygen or air, and in some cases steam, to produce carbon monoxide and hydrogen which is known as syngas. CO_2 emissions can be prevented in a gasification power plant by transferring almost all carbon compounds to CO_2 through the water-gas shift reaction, and then removing the CO_2 before it is diluted in the combustion stage. This can be achieved through syngas scrubbing or applying any other capture technology such as sorbents or gas separation membranes or physical solvents. Since the concentration of CO_2 is increased and because of the high pressure of the syngas, CO_2 removal from IGCC requires considerably smaller and simpler processing equipment than post-combustion CO_2 removal (Herzog, 1999) which, makes pre-combustion CO_2 capture easier and cheaper. The main disadvantages of pre-combustion capture are the need to cool down the syngas in order to capture CO_2 and the efficiency loss in the water-gas shift reaction. The process schematic of pre-combustion CO_2 capture is shown in Figure 1.8 (NETL, May 2011).
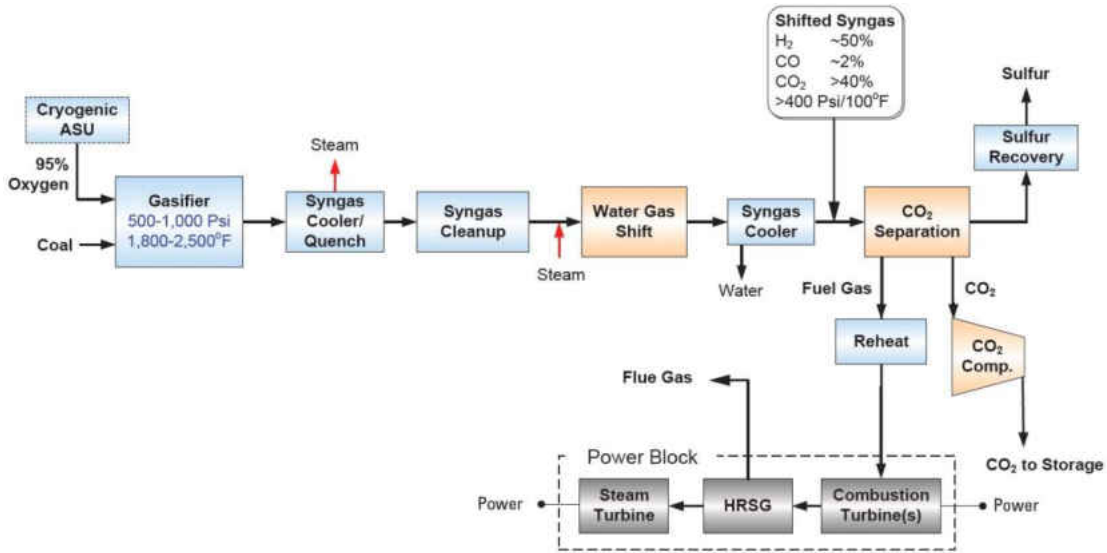
Figure 1.8. Process schematic of pre-combustion CO_2 capture (NETL, May 2011).

1.3.2 Post-combustion CO_2 capture

In the post-combustion technique, CO_2 is removed from the flue gas upstream of the boiler. Chemical solvent-based technologies such as amine scrubbers are currently used in industry to capture CO_2 downstream of the pollutant control facilities. Although post combustion capture provides the greatest near-term potential to capture CO_2, the disadvantages of this method as outlined in the DOE report (NETL, May 2011) are the high cost of solvent regeneration by steam, solvent loss, the difficulties of separating CO_2 from the flue gas (due to high volumes of gas and low CO_2 concentration, low pressure of the flue gas, and trace impurities), and high cost of compressing CO_2 from atmospheric pressure to general pipeline condition (2200 psi). Despite all these

11

challenges, post-combustion CO_2 capture seems to be the most likely near-term solution for reducing CO_2 emissions from power plants due to its capability to be retrofitted to existing power plants. The process schematic of post-combustion CO_2 capture is shown in Figure 1.9 (NETL, May 2011).
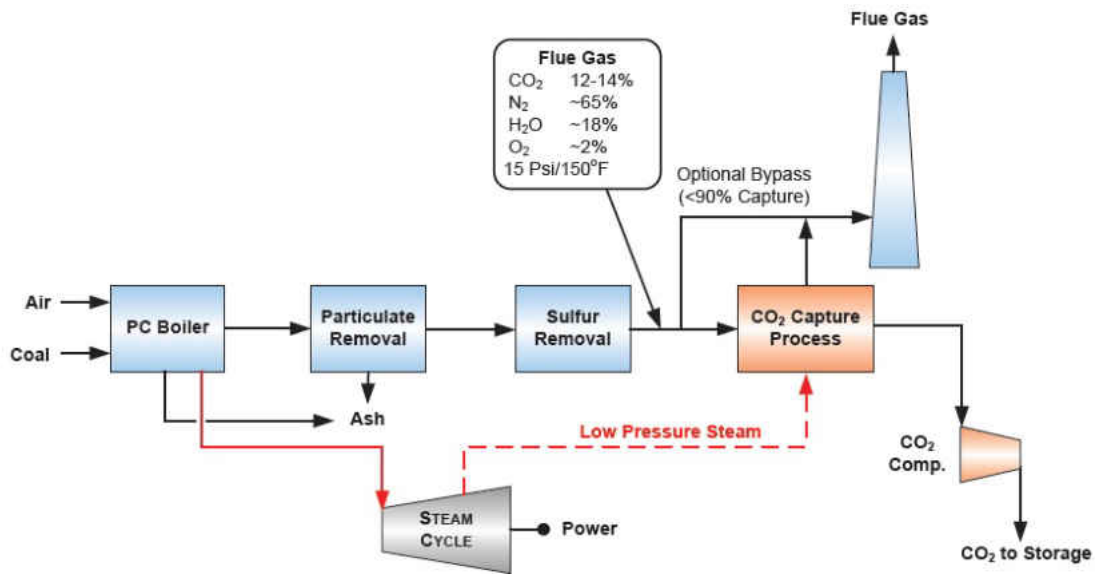
Figure 1.9. Process schematic of post-combustion CO_2 capture (NETL, May 2011).

1.3.3 Oxy-combustion CO_2 capture

In the oxy-combustion approach, fuel is combusted in almost pure oxygen instead of air, which results in a high concentration of CO_2 in flue gases due to the elimination of N_2 from the combustion medium. The main products of oxy-combustion are H_20 and CO_2. CO_2 is separated from the water through condensation and a portion of that is recycled to the boiler. The advantage of oxy-combustion is that the flue gas has a CO_2 concentration of over 80%, so only

simple CO_2 purification is required and less NOx pollutants will be formed. The main challenge of oxy-fuel combustion is that a large quantity of oxygen is required, which is expensive, both in terms of capital cost and energy consumption. The process schematic of Oxy-combustion CO_2 capture is shown in Figure 1.10 (NETL, May 2011).
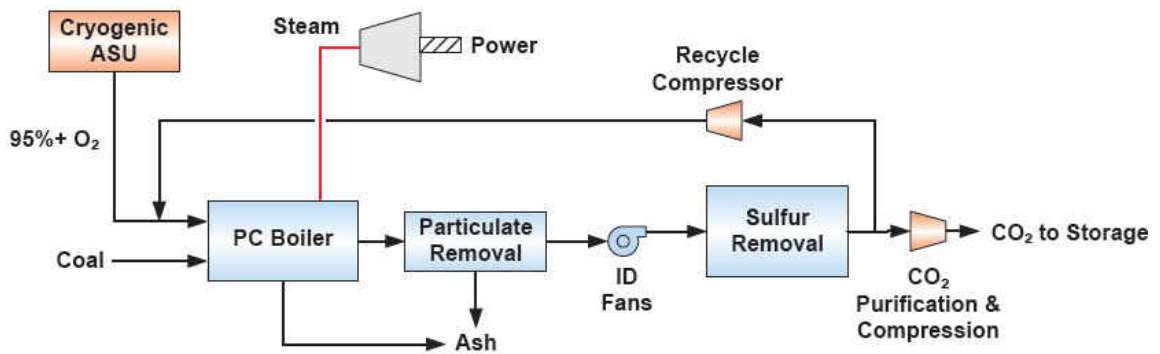
Figure 1.10. Process schematic of oxy-combustion CO_2 capture (NETL, May 2011).

1.3.4 State-of-the-art technologies and future trends for CO_2 capture

The diversity of CO_2 capture technologies is very broad. Many new technologies for CO_2 capture and separation such as membranes, sorbents and novel solvents are under development. Figure 1.11 shows the associated cost of different CO_2 capture technologies used in three approaches discussed previously versus the time to commercialization (Figueroa, Fout, Plasynski, McIlvried, & Srivastava, 2008). It seems that application of amine solvents (post-combustion), physical solvents (pre-combustion) and cryogenic oxygen (oxy-

13

combustion) seem to be the most promising technologies in a close future in terms of technology availability and associated costs (Figueroa et al., 2008).
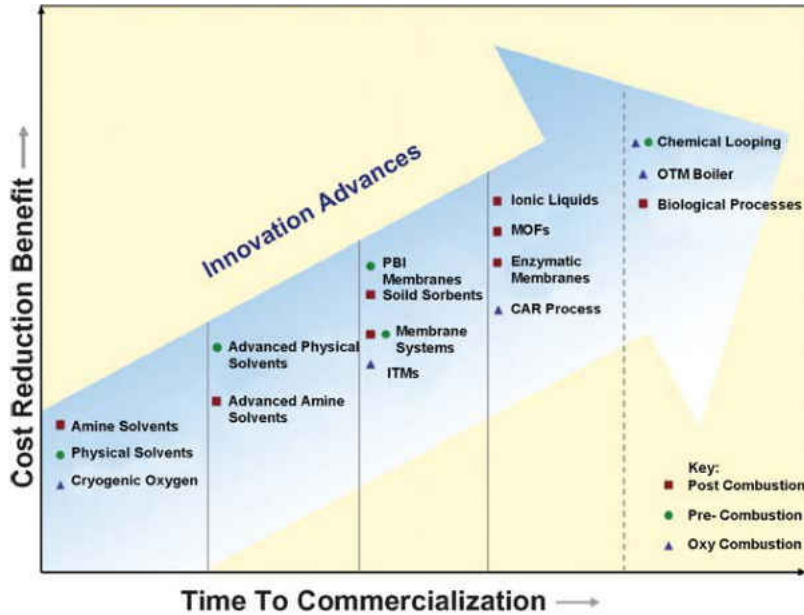
Figure 1.11. Innovative CO_2 capture technologies - cost reduction benefits versus time to commercialization (Figueroa et al., 2008).

Gas purification and separation using solvents is well-established. Two general categories of solvents for gas purification purposes currently exist; physical solvents, which dissolve gas molecules physically without any chemical reaction and chemical solvents which dissolve gas molecules through a certain chemical reaction between the solvent molecules and gas species. Physical solvents tend to have a much higher capacity for acid gases at elevated pressures. Consequently, they are well suited to be used for pre-combustion CO_2

capture from syngas at elevated pressures, whereas chemical solvents are better candidates for Post-combustion CO_2 capture from the low pressure flue gas.

The key parameter that influences the capacity of a solvent for a certain gas separation problem is the solvent selectivity for dissolving different species that exist in the gas mixture. The gas mixture is brought into contact with the lean solvent in the absorber where CO_2 or other gas components are selectively absorbed by the solvent. The rich-solvent regeneration greatly depends on the type of solvent. For chemical solvents, the regeneration step is performed in the stripper column by the help of a stripping gas such as steam to provide the required energy to break the bonds between the solvent and the gas component and then release the gas. For physical solvents, regeneration is usually performed by reducing the pressure in a consecutive series of flash drums. It is quite evident that choosing the appropriate type of solvent for CO_2 capture, significantly depends on the flue gas concentration and pressure which in turn are determined by the type of power plant. The other important factors influencing the gas-liquid absorption process include (NETL, May 2011):

i.   Solvent working capacity: Affects the solvent circulation rate and the incremental sensible heat required to regenerate the solvent.

ii.   Heat of absorption and reaction: Determines the heat required to regenerate the chemical solvent and thus influence the working capacity of the

solvent. Absorber and stripper column temperatures also depend greatly on these variables.

iii.   Reaction rates: the mass transfer rate and chemical reaction rate determine the size of the absorber and stripper. In the case of slow mass transfer and chemical reaction, a larger volume of the solvent needs to be circulated.

iv.   Selectivity: Determines the capacity of a solvent for separating the different species extant in the gas mixture and thus the product purity.

v.   Solvent concentration: Depending on the type of solvent, the concentration of the circulating solvent may vary. Chemical solvents are usually diluted with water. However, physical solvents are used in pure form.

vi.   Contaminant resistance: The chemical stability of the solvent when exposed to high temperatures and different gas components is a very important issue. By-products may form due to the gas and solvent reaction.

DOE/NETL's Clean Coal Power Initiative (CCPI) and restructured FutureGen demonstration plants for CO_2 capture using solvents are summarized in Table 1.1 (NETL, May 2011).

Table 1.1. CO_2 Capture Demonstration Project s Being Conduct ed under CCPI and FutureGen 2.0. (NETL, May 2011).

Performer	Location	Capture Technology	Capture Rate (tonnes/year)	Start Date
Pre-Combustion Capture				
Summit Texas Clean Energy	Odessa, TX	Selexol	3.0×10^6	2014
Southern Company	Kemper county, MS	Selexol	2.0×10^6	2014
Hydrogen Energy California	Kern County, CA	Rectisol	2.0×10^6	2016
Post-Combustion Capture				
Basin Electric	Beulah, ND	Amine	$0.5\text{-}1.0 \times 10^6$	2014
NRG Energy	Thompson, TX	Amine	$.5 \times 10^6$	2015
American Electric Power	New Haven, WV	Chilled	1.5×10^6	2015
Oxy-Combustion Capture				
FutureGen 2.0	Meredosia, IL	Oxy-Combustion	1.0×10^6	2015

1.4   Objectives of this work

The primary objective of this work is to evaluate the application of composite polymeric membranes for the recovery of CO_2 from a CO_2-rich physical solvent stream. To achieve this purpose, an experimental bench-scale setup is built to investigate and quantify CO_2 removal capacity from the rich solvent across different types of membranes. Dimethyl ether of polyethylene glycol (Selexol) is used as the solvent since it is reputed to be one of the major physical solvents for CO_2 removal. To evaluate the effectiveness of various types of membranes, CO_2 permeation rate and membrane selectivity are measured for various membranes.

A basic knowledge of physical solvents and membrane technology is quite essential to design and build the aforementioned experimental setup. In the next chapter of this work, the concept of physical absorption will be discussed briefly along with common physical solvents and processes. A concise review of the common membrane processes and a state-of-the-art literature review will be provided.

2 Physical Absorption, Membrane Technology—Literature Review

2.1 Physical absorption

The major concern regarding using typical chemical solvents such as amines is the heat requirement for solvent regeneration, which can decrease plant efficiency significantly. This has provided the major motive for developing processes that employ nonreactive solvents known as physical solvents. Unlike chemical solvents, physical solvents do not react with the solute and they physically dissolve the acid gases, which are then stripped without the need to be heated, by means of pressure swing techniques.

The performance of a physical solvent depends on its capacity to dissolve different gases. The solubility of an individual gas follows Henry's law—the solubility of a compound in the solvent is directly proportional to its partial pressure in the gas phase. Hence, the capacity of a physical solvent can be enhanced by increasing the partial pressures of gases. This is one of the major advantages of physical solvents over chemical solvents for acid gas removal from high pressure syngas. As shown in Figure 2.1, compared to physical

solvents, chemical solvents have higher absorption capacity at relatively low acid gas partial pressures. However, their absorption capacities are less than those of physical solvents at higher partial pressures. The solubility of an acid gas in a physical solvent increases linearly with its partial pressure. Therefore, chemical solvent technologies are favorable at low acid gas partial pressures and physical solvents are favored at high acid gas partial pressures. Furthermore, physical absorption allows for the solvent to be partially regenerated by pressure reduction, which reduces the energy requirement compared to chemical solvents.
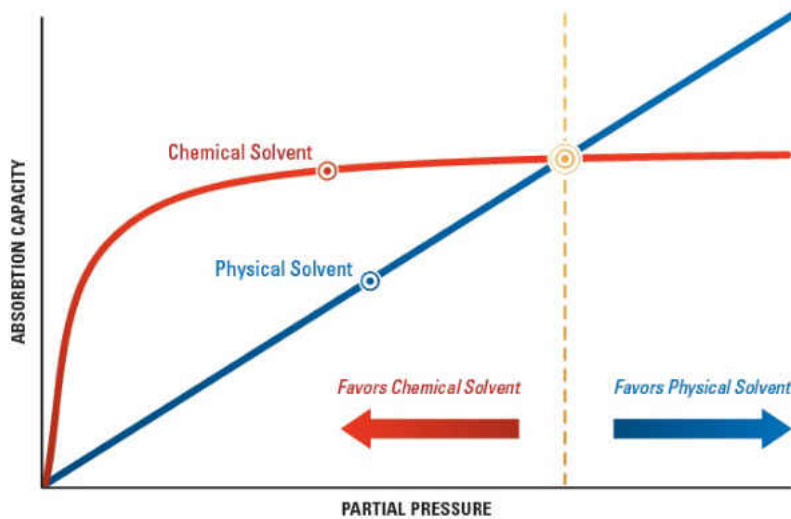
Figure 2.1. Absorption capacity of physical and chemical solvents (NETL, May 2011).

The Rectisol process was the earliest physical solvent commercial process, that has been used in synthesis gas applications. The trend of physical solvents accelerated in 1960 with the introduction of the Fluor solvent process, which was followed by several other physical solvent processes (Kohl & Nielsen,

1997). Table 2.1 shows a list of major physical solvents that have been or are currently offered for commercial use and the solvents used by each.

Table 2.1. Physical Solvent Processes (Epps, R. Union Carbide Chemicals & Plastics Technology Corporation, 1992).

Process Name	Solvent	Process Licensor
Flour Solvent	Propylene carbonate	Fluor Daniel
SELEXOL	Dimethyl ether of polyethylene glycol(DMPEG)	Union Carbide
Sepasolv MPE	Methyl isopropyl ether of polyethylene glycol (MPE)	Badische (BASF)
Purisol	NMP	Lugri and Linde AG
Ifpexol	Methanol	Institut Francais du petrole (IFP)
Etasolvan	Tributyl phosphate	IFP/Uhde
Methylcyanoacetate	Methylcyanoacetate	Unocal
Rectisol	Methanol	Lugri

As mentioned earlier, the most important parameter in designing and selecting the type of process and its associated solvent is the solubility of the gaseous impurities to be absorbed. In order to be practical, the solvents must have an equilibrium capacity for acid gases several times of that of water, coupled with a low capacity for the primary constituents of the gas stream, e.g, hydrocarbons and hydrogen. Additionally, they must have low viscosity to minimize the amount of required work for recirculating the solvent throughout the plant. They must be noncorrosive to common metals as well as nonreactive with all components in the gas (Kohl & Nielsen, 1997). To minimize the amount of solvent loss and obviate the need to scrub the flue gas for solvent recovery, they

must have a very low vapor pressure at ambient temperature and eventually they must be commercially available at a reasonable price. Physical solvent processes are used primarily for acid-gas removal from high-pressure natural-gas streams and for carbon dioxide removal from crude hydrogen and ammonia synthesis gases produced both by partial oxidation and steam-hydrocarbon reforming.

As the molecular weight of the hydrocarbon increases, the solubility also increases. Consequently, hydrocarbons above ethane are also removed to a large extent. This is one of the main reasons why physical solvents are mainly used in gasification when the syngas has no significant amount of hydrocarbon. Physical solvent processes are generally not commercial for the treatment of hydrocarbon streams that contain a substantial amount of pentane-plus hydrocarbons (Kohl & Nielsen, 1997). In their simplest form, physical solvent processes require an absorber, an atmospheric flash vessel and a recycle pump.

After regenerating the solvent by pressure letdown, the lean solution contains acid gas in an amount corresponding to equilibrium concentrations at 1atm is recycled back to the absorber. To obtain a higher degree of purification, vacuum or inert gas stripping or heating of the solvent must be implemented. Design equations and simulation models commonly used for hydrocarbon separations are generally applicable to physical solvent gas purification. The key requirement is adequate liquid/vapor equilibrium data covering all components

and conditions that appear in the process. The selectivity of a physical absorption process can be enhanced by the use of more than one stripping and absorption stage. Many different flow schemes have been developed to meet specific requirements and take advantage of the properties of specific solvents.

One of the key parameters in designing a physical solvent process is the solvent circulation rate, since it affects the size and the cost of every piece of equipment, including the absorber, piping, circulation pumps and flash drums. The main parameter that affects the solvent circulation rate is the contact temperature. At lower temperatures, solvent capacity for acid gases increases and thus less solvent needs to be recirculated. The other advantage of lower temperature is to minimize the amount of hydrocarbon loss due to the fact that the solubility of acid-gases increases much more than that of hydrocarbons as temperature decreases. It should be kept in mind that the temperature to which a solvent may be cooled is limited primarily by its increased viscosity and the resulting decrease in solvent heat and mass transport capabilities.

As outlined by Kohl and Nielsen (Kohl & Nielsen, 1997), the most important factors in selecting a physical solvent process are:

1.   Process performance in terms of acid gas composition and treated gas purity

2.   Loss of light and heavy hydrocarbons,

3.   Experience and ingenuity of the designer in adapting the process to the case at hand

4.   Method of dealing with impurities such as COS, NH_3, aromatic hydrocarbons etc.

5.   Possibility of corrosion, foaming and other operating problems

6.   Cost of initial solvent charge

7.   Cost of replacement solvent

8.   Energy and /or stripping cost

9.   Process royalty cost.

A comparison of common physical solvent processes in terms of power requirements, removal efficiency and equipment required was given by (Burr & Lyddon, 2008) . Among the most common physical solvents, Selexol is one of the most important of the solvents that are widely used both in natural gas processing and gasification applications. Selexol has a very low vapor pressure (0.00073 mm Hg) and a relatively high capacity for CO_2 absorption. In addition, Selexol has an acceptable range of operating temperature and good selectivity for CO_2 and H_2S removal. More details of the solubility data in common physical solvents are available in the literature (Bucklin & Schendel, 1985; Doctor, Molburg, & Thimmapuram, 1994; Epps, R. Union Carbide Chemicals & Plastics Technology Corporation, 1992; Korens, Simbeck, Wilhelm, Longanbach, & Stiegel, 2002; Newman, 1985; Rousseau, Matange, & Ferrell, 1981). Although

different research groups are working in the field of synthesizing new physical solvents with improved capability for absorbing acid gases (Heintz, Sehabiague, Morsi, Jones, & Pennline, 2008; Porter, Sitthiosoth, & Jenkins, 1991), the primary focus of this research is on the application of Selexol process to the IGCC power plants. More details of the Selexol process will be discussed in the next section.

2.2   Selexol process

2.2.1 Selexol process history and current practices

The Selexol process, patented by Allied Chemical Corp., has been used since the late 1960s. The process was sold to Norton in 1982 and then bought by Union Carbide in 1990 (R. Epps, 1994). The Dow Chemical Co. acquired gas processing expertise, including the Selexol process, from Union Carbide in 2001. The process is offered for license by several engineering companies—the most experienced of which with the process is Universal Oil Products (UOP) (Breckenridge, Holiday, Ong, & Sharp, 2000). The Selexol process has been used commercially for 30 years and has provided reliable and stable operation. Over 60 Selexol units have been put into commercial service (*Meeting staged CO2 capture requirements with the UOP SELEXOL™ process.*2009), which cover a wide variety of applications, ranging from natural gas to synthetic gas. By now, the Selexol process has been the dominant acid-gas removal system in gasification projects. Moreover, increasing interest into

25

controlling CO_2 emissions in the world may lead to the Selexol process being applied widely, particularly in coal gasification plants. Relevant experiences for gasification are Sarlux – Italy (IGCC-Power plus H_2), API-Italy (IGCC Power), Coffeyville Resources – USA(NH_3/UAN), OptiCanada - Oil Sands Canada (H_2 plus fuel) (*Meeting staged CO2 capture requirements with the UOP SELEXOL™ process.*2009). The 100 MW Texaco/Cool Water (California) 1,000 t/d coal gasifier plant for IGCC demonstration was operated continuously for about five years in the 1980s and the Selexol unit performed extremely well. The TVA/Muscle Shoals (Alabama) 200 t/d coal gasifier demonstration plant was operated continuously for about five years in the early 1980s and used the Selexol process to convert coal to clean synthesis gas, and CO_2 as an alternative feed to an existing ammonia-urea plant. In addition, multiple large units are in the engineering phase, such as Residue gasification for H_2 production (Oil Sands Canada) and other gasification projects. According to Union Carbide as of 1992, a total of 53 Selexol plants had been installed. These comprise 10 for CO_2 removal from various synthesis gas, 12 for CO_2 removal from natural gases, 15 for selective H_2S removal, 8 for the desulfurization of synthesis gas and 8 for landfill gas purification (Kohl & Nielsen, 1997).

2.2.2 Solvent properties

The solvent used in the Selexol acid removal system is a mixture of dimethyl ethers of polyethylene glycol (DMEPG) (with the formulation of

$CH_3(CH_2CH_2O)_nCH_3$, where n is between 3 and 9. 3-9 PEG repeat units enable the solvent to have vapor pressure and viscosity values low enough to inhibit evaporative losses and lower pumping costs respectively. The oligomers end groups are methyl ether groups rather than the CO_2-phobic hydroxyl groups. The oxygen of the methyl ether group increases the CO_2 solubility by providing an additional site for Lewis acid: Lewis base interaction with CO_2. Selexol solvent is a yellow to brown liquid with a mild odor. The general properties of the DMPEG are given by (Newman, 1985; Sciamanna & Lynn, 1988) and summarized in Table 2.2.

Table 2.2. DMPEG Basic properties

Property	Value
Vapor pressure, mm Hg @25 ^{o}C	0.00073
Viscosity, cp @25 ^{o}C	5.8
Maximum feasible operating temperature, ^{o}C	175
Density, kg/m^3	1,030
Boiling point, ^{o}C	240
Freezing point, ^{o}C	-28
Molecular weight	250
Specific heat @ 25 ^{o}C , Btu/(lb)(^{o}F)	0.49
Thermal conductivity, Btu/hr(ft^2)((^{o}F/ft)	0.11

Solvents containing DEPG are licensed and/or manufactured by several companies including Coastal Chemical Company, Dow (Selexol) and UOP (Selexol). Other process suppliers such as Clariant GmbH of Germany offer

similar solvents (Burr & Lyddon, 2008). The performance of a physical solvent can be predicted by its solubility.

As explained previously, the solubility of a physical solvent follows Henry's law. This explains the reason why physical solvents are favorable in gasification applications where the partial pressure of acid-gas is high enough for the solvent capacity of acid-gases to increase. The major advantage of the Selexol solvent over other physical solvents is that it has a favorable solubility for acid gases versus other light gases. Table 2.3 shows the relative solubility of different compounds in Selexol solvent (Doctor et al., 1994). As shown in Table 2.3, CO_2 is 75 times more soluble than H2, and H2S is 670 times more soluble than H_2 in Selexol. Also H_2S solubility is almost 9 times CO_2 solubility. This characteristic facilitates use of Selexol in removing H_2S and CO_2 selectively from the gas stream to be purified. DMEPG also dehydrates the gas and removes HCN.

Table 2.3. Relative solubility of gases in Selexol solvent (Doctor et al., 1994).

Gas	CO_2	H_2	CH_4	CO	H_2S	COS	SO_2	NH_3	N_2	H_2O
Solubility	1	0.01	0.0667	.028	8.93	2.33	93.3	4.87	0	733

The regeneration step for Selexol can be carried out either thermally, or by flashing or stripping the gas depending on the process design, specifications of the treated gas and acid-gas composition. In addition to the advantage of high capacity for acid-gases, other advantages of Selexol solvent and the Selexol

process that make it the most promising candidate for gasification applications are:

1. very low vapor pressure, which limits its losses to the treated gas

2. Low viscosity to avoid large pressure drop

3. High chemical and thermal stability

4. Nontoxic, non-corrosive and inherently non-foaming

5. Compatibility with gasifier feed gas contaminants

6. High solubility for HCN and NH_3

7. Low heat requirements for regeneration

8. High flash point ensures ease and safety in handling

9. Requires no mixing, formulating, diluting or activating agents and can be used as received.

10. DEPG has a fairly wide range of operating temperatures (0 to 347 $^{\circ}$ F).

11. High loadings at high CO_2 partial pressure, which reduces solvent recirculation rate

12. High affinity for water so it simultaneously dehydrates the gas stream

2.2.3 Selexol process flow schemes

The design and configuration of a Selexol process depends on the requirements for the level of H_2S/CO_2 selectivity, the depth of sulfur removal, the

need for bulk CO_2 removal, and whether the gas needs to be dehydrated or not. However, all the Selexol processes have some elements in common including acid gas absorption, solvent regeneration/acid gas recovery, and solvent cooling and recycle. The Selexol process has been discussed extensively in the literature (Epps, R. Union Carbide Chemicals & Plastics Technology Corporation, 1992; Judd, 1978; Kohl & Nielsen, 1997; Raney, 1976; J. W. Sweny, 1976; J. W. Sweny, 1980; J. Sweny, 1976). Due to the diversity of flow schemes and design configurations the two most common flow schemes are discussed in more details.

2.2.3.1   *Selexol process for H$_2$S and CO$_2$ removal*

Selexol solvent processes can be configured to capture H_2S and CO_2 together with high levels of CO_2 recovery. This is usually achieved by staging absorption for a high level of H_2S removal, followed by CO_2 removal. Figure 2.2 shows a Selexol process for synthesis gas treating where a high level of both sulfur and CO_2 removal are required. H_2S is selectively removed in the first column by a lean solvent, and CO_2 is removed from the H_2S-free gas in the second absorber. The second-stage solvent can be regenerated with air or nitrogen if very deep CO_2 removal is required. Solvent regeneration is carried out both by air stripping for CO_2 and applying heat to regenerate the absorbed H_2S.
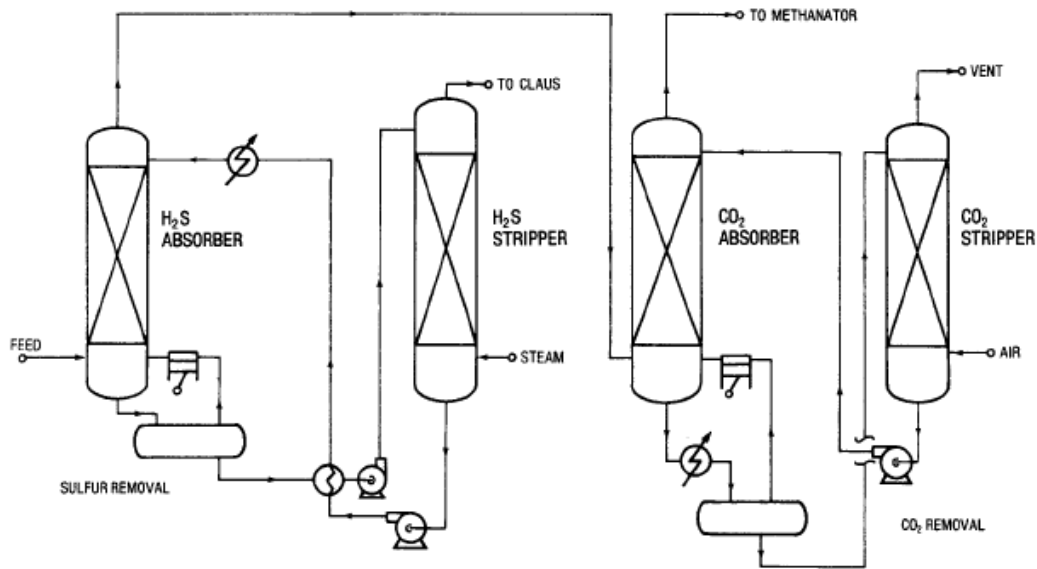
Figure 2.2. Selexol process for CO_2 and Sulfur removal (Kohl & Nielsen, 1997).

2.2.3.2 *An optimal design for Selexol process for sulfur and CO_2 capture*

The following is a description of an optimal design for a Selexol process that removes sulfur and CO_2 from syngas from IGCC systems. Recent DOE/NETL systems analysis studies assume that a water-gas Shift (WGS) reactor combined with a two-stage Selexol process will be used for CO_2 capture in IGCC applications. This optimal design is based on modifying an original design by UOP, for H_2S and CO_2 removal from syngas for the production of ammonia from IGCC systems. A simplified schematic diagram of this design is showed in Figure 2.3 (NETL, May 2011).
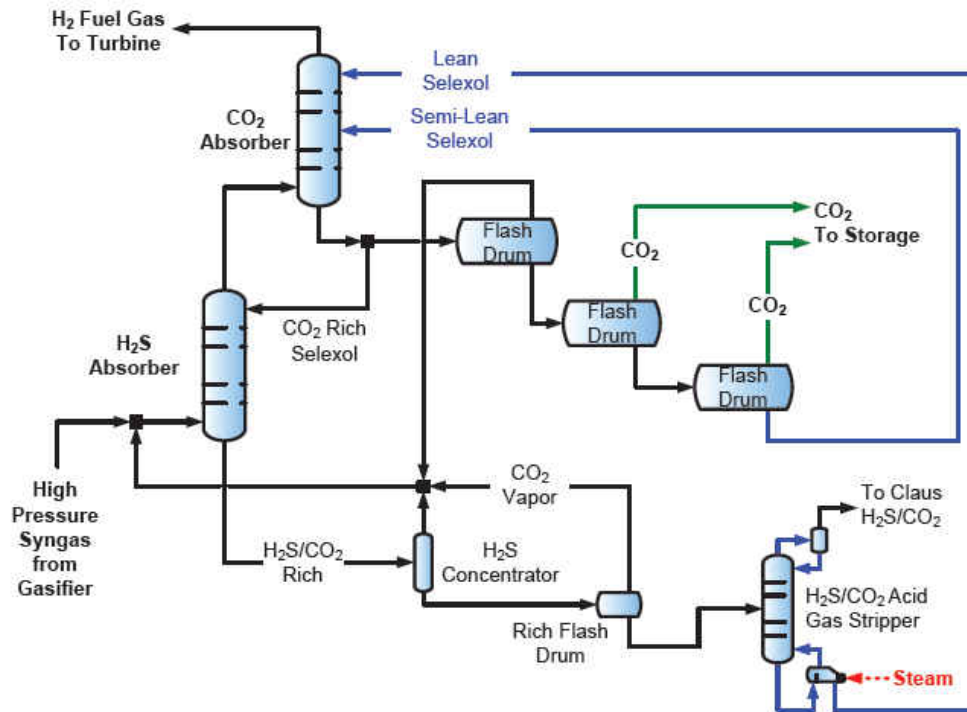
Figure 2.3. Schematic diagram of CO_2 pre-combustion capture with Selexol (NETL, May 2011).

Untreated syngas enters the H_2S absorber and is brought into contact with solvent that is preloaded with CO_2 in a CO_2 absorber and H_2S is preferentially removed using this CO_2-rich solvent. The use of pre-loaded solvent prevents additional CO_2 absorption in the H_2S absorber, and it also minimizes the temperature rise across the tower. The H_2S absorber overhead stream enters the CO_2 absorber where CO_2 is absorbed into the fresh solvent. The rich solvent from the H_2S absorber is fed to the H_2S solvent regeneration facility. The H_2S regeneration facility consists of an H_2S concentrator where its pressure is set so that if any CO_2 has been absorbed into the solvent, it would be degassed from

the rich solvent and recirculated back to the feed gas stream. Then the rich solvent from the H_2S concentrator passes through a stripping column where H_2S is regenerated from the solvent using high pressure steam. The rich solvent at the bottom of the CO_2 absorber is partially sent through the H_2S absorber and the other proportion is regenerated by consecutive flash drums. The flash drums operate at progressively lower pressures, ranging from several hundreds of psia down to near-atmospheric pressure in the final flash drum. Because a significant fraction of the CO_2 is produced at elevated pressures, the total compression energy requirement is lower than for post-combustion processes that typically generate their entire CO_2 product stream at near atmospheric pressure. As explained previously, the key factor in designing the absorption towers as well as the regeneration facilities is the solubility data of the gas components in the solvent under different conditions that may be encountered in the plant. In the case of the Selexol process, many studies have been performed regarding the solubility of different gases in DMPEG (Gainar & Anitescu, 1995; Henni, Tontiwachwuthikul, & Chakma, 2006; Miller et al., 2009). More details on the design conditions and simulations of the Selexol process can be found in (*Power plant carbon capture with CHEMCAD.*; Strube & Manfrida, 2011)

2.3 Challenges and barriers of the current physical solvent technology

Despite the low energy required to regenerate physical solvents, and their high capacity to capture and separate acid gases from the syngas produced in a gasification plant, physical solvents have some disadvantages as outlined below:

1. CO_2 pressure is lost during flash recovery. If the captured CO_2 needs to be transported and sequestered in geological formations it has to adhere to certain specifications: it must be dry, and near pure CO_2 at high pressures approximately 13 MPa. Since the pressure swing technique is often used to regenerate physical solvents, the last flash drum is usually operating at atmospheric pressure. As a result of that, more energy is required to compress the CO_2 to meet pipeline specifications.

2.   In order to increase the solubility of acid gases and minimize the solvent circulation rate, physical solvent absorption usually takes place at ambient temperatures or even lower temperatures. This requires the syngas to be cooled down and then heated back up again and re-humidified for firing turbines, and this can impose significant energy penalties on the plant performance.

3.   The absorption process may require some refrigeration.

4.   Another disadvantage of physical solvents, not as important as previously listed, but still challenging, is the energy required to circulate the

solvent from atmospheric pressure (at the outlet of the last flash drum) to the high pressures of the absorber column.

5.   Simultaneous absorption of the heavier hydrocarbons may occur in the process gas stream.

6.   Some hydrogen may be lost with the CO_2.

It seems that the main challenges of the physical solvents originate from the regeneration step. Pressure swing techniques lead to pressure loss on both the solvent side and in the captured CO_2, which requires a significant amount of pressure to reach the operational pressures of both the CO_2 transport line and the high pressure absorber column. Novel techniques need to be investigated for regenerating physical solvents while avoiding pressure loss on both the solvent and CO_2 sides.

A section of the "Efficient Regeneration of Physical and Chemical Solvents for CO_2 Capture" project entails the use of polymeric membranes for regeneration of physical solvents. The goal of this work will be the development of materials and processes that reduce the capital and operating costs of the solvent regeneration process; particularly the energy expended in regeneration. The primary advantage of membranes over other vapor-liquid mass transfer processes is its significantly higher interfacial contact area. While packed and trayed columns possess ~30-300 (m^2/m^3) of interfacial area, membranes can

provide over 6000 (m^2/m^3). In the next section of this chapter, a more detailed description of the membrane technology will be given.

2.4 Membrane technology

Membrane technology is a competitive alternative to conventional separation processes. Membrane filtration and separation is a fast emerging field and was not considered a technically feasible method of separation 25 years ago (Mulder, 1991). As outlined by Li and Chen (Li & Chen, 2005) the major advantages of membrane separation compared to other conventional methods such as bubble columns and trayed columns include: (a) Operational flexibility, (b) Economics (c) Linear scale-up and (d) Easier prediction of the membrane performance. The size reduction and higher energy efficiency of membrane processes compared to other conventional separation processes are well studied for many separation problems in literature (Bhide, Voskericyan, & Stern, 1998; Feron & Jansen, 1995; Kumar, Hogendoorn, Feron, & Versteeg, 2002; Yan et al., 2007). Separation via membrane technology can be performed continuously. Membranes can be combined with other separation processes in a hybrid system. Membrane properties are variable and depending on the application, can be tailored for a certain separation problem. The major drawbacks of membrane technology include: (a) Concentration polarization/ membrane fouling, (b) low membrane lifetime and (c) generally low selectivity (Mulder, 1991). One of the main disadvantages of the membrane technology is its high manufacturing cost.

36

Membranes can be expensive not only to manufacture but also to maintain. Certain solvents and chemicals can quickly and permanently disintegrate the membrane structure due to the chemical reaction between the solvent and membrane material. Consequently, an appropriate selection of the membrane material can improve the purity of the final product and the economics of the process significantly.

2.4.1 Membrane definition

Wankat (Wankat, 2006) has defined the membrane as "a physical barrier between two fluids (feed side and product side) that selectively allows certain components of the feed fluid to pass". The term selective is the inherent feature of any membrane processes. Figure 2.4 shows a schematic of a membrane process (Stanojević, Lazarević, & Radić, 2003).
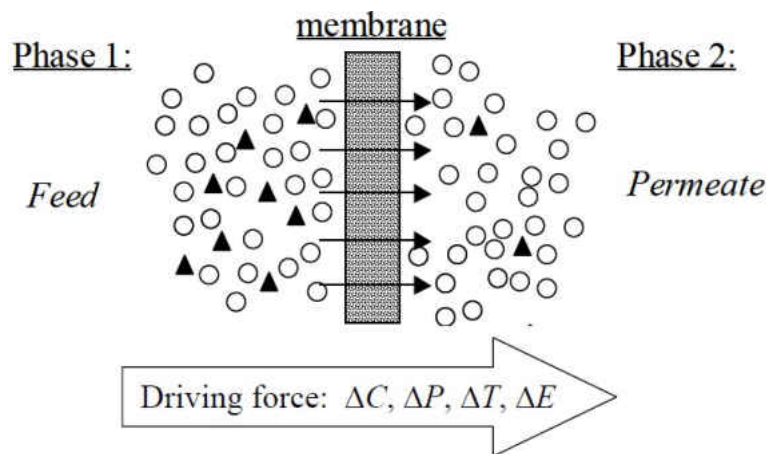
Figure 2.4 Schematic of a membrane separation process (Stanojević et al., 2003)

Membranes exist in many forms, structures and materials. They could be natural or synthetic. The synthetic membranes are widely used in industry and they can be classified as symmetric and asymmetric. Commercial membranes are made out of polymers, metals and ceramics. Baker (R. Baker, 2012) classified the membrane types into three categories: (a) Metal membranes (b) Polymeric membranes (c) Ceramic and zeolite membranes. Membranes used in most of commercial applications are polymeric (solution-diffusion) membranes (Meindersma & Kuczynski, 1996; Puri, 1996).

2.4.2 Membrane flux and selectivity

The performance of any membrane process is determined by two parameters; membrane selectivity and flux. Flux is defined as the volume flowing through the membrane per unit area and time. Higher permeability results in smaller membrane surface area required for a separation process and this, in turn, leads to a more economical process. An ideal membrane, needs to have a high flux for the permeate and low flux for the retentate.

Selectivity is the ability of a membrane to separate a mixture and thus the purity of the permeate and retentate streams. The selectivity of a membrane can be defined by one of the two parameters; the retention (R) or the separation factor (α) (Mulder, 1991). R is usually used for dilute aqueous mixtures consisting of a solute and a solvent. The retention (R) is given by

38

$$R = \frac{C_P - C_f}{C_p} = 1 - \frac{C_f}{C_P}$$ Eqn (2.1)

Where Cf is the solute concentration in the feed and C_p is the solute

concentration in the permeate (Mulder, 1991). For the gas mixtures and liquid

mixtures, selectivity is usually defined as the separation factor (α). For a binary

mixture of A and B, α $_{A/B}$ is given by equation 2.2 as

$$\alpha_{A/B} = \frac{y_A/y_B}{X_A/X_B}$$ Eqn (2.2)

Where y_A and y_B are the concentrations of components A and B in the permeate

and X_A and X_B are the concentrations of the components in the feed (Mulder,

1991).

2.4.3 Transport through dense membranes

As mentioned earlier, membranes have the ability to transport one

component of a mixture more readily compared to the other components of that

mixture. The differences in the chemical / physical properties of different species

in the feed stream and different interactions between the membrane material and

the permeating components, result in different rates of transport and hence the

separation of the components. For a specific gas molecule, diffusivity and

solubility are intrinsic properties of the membrane material. Transport through the

membrane occurs as a result of a driving force that exists on the two side of the

membrane (feed side and the permeate side). The relationship between the flux and the driving force is given by

$$J = -A\frac{dX}{dx}$$

where A is the diffusion coefficient (D, Fick's law) and dX/dx is the driving force perpendicular to the transport barrier. Depending on the membrane separation process, the nature of the driving force may vary. For gas separation membranes, the driving force is defined as the difference in the partial pressure of the transferring species across the membrane. For Reverse Osmosis (RO), the driving force is the pressure difference minus the osmotic pressure difference across the membrane. Table 2.4 summarizes the driving forces for different membrane processes.

Two models are commonly used to describe the permeation through the membranes. The first model is known as the solution-diffusion model, where different species in the mixture dissolve in the membrane material and then diffuse through the membrane. The separation is achieved as a result of differences between the solubility and diffusivity of different constituents of the mixture (Wijmans & Baker, 1995).

Table 2.4.Membrane processes and driving forces (Mulder, 1991).

Membrane Process	Phase 1	Phase 2	Driving Force
Microfiltration	L	L	ΔP
Ultrafiltration	L	L	ΔP
Hyperfiltration	L	L	ΔP
Piezodialysis	L	L	ΔP
Gas separation	G	G	ΔP
Dialysis	L	L	ΔC
Osmosis	L	L	ΔC
Pervaporation	L	G	ΔP
Eelctrodialysis	L	L	ΔE
Thermo-osmosis	L	L	ΔT/ ΔP
Membrane distillation	L	L	ΔT/ ΔP

The second model is pore-flow in which permeants are separated by pressure-driven convective flow through tiny pores. The separation is achieved because one of the components of the mixture is excluded from some of the pores, through them, the other component is moving (Wijmans & Baker, 1995). Currently, solution-diffusion is the dominating model for modeling of many membrane processes such as gas permeation, pervaporation, reverse osmosis, and dialysis.

Wankat (Wankat, 2006) defined the flux of permeate through the membrane as

$$\text{Flux} = \frac{\text{Transfer Rate}}{\text{Transfer Area}} = \frac{\text{Permeability}}{\text{Separation Thickness}}(\text{Driving Force}) \qquad \text{Eqn (2.4)}$$

Membrane permeability is defined as the product of the solubility and the diffusivity of the permeant in the membrane and is given by

41

$$P_a = H_a . D_{m,a}$$ Eqn (2.5)

where, *Pa* is the permeability, *Ha* is the solubility parameter similar to Henry's

coefficient and *Dm,a* is the diffusivity. Diffusivity and solubility depends greatly

on the size of the molecules. As the size increases, the diffusion coefficient

decreases. However, the capability of the component to be absorbed on the

membrane surface and then diffuse through the membrane increases. Molecules

with a smaller collision diameter have higher diffusion coefficient and lower

solubility parameter. However, larger molecules like CO_2 have lower diffusion

coefficient values and higher solubility parameter.

In addition to the permeants properties, the type of the membrane material

(polymers in most cases) and the state of the polymer (glassy vs. rubbery)

determines the diffusivity and solubility of different components in the membrane.

In glassy polymers, the selectivity is basically derived from the molecular

dimension difference of the molecules and thus different diffusion rates through

the polymer (mobility selectivity) where smaller molecules diffuse faster and thus

are selectively removed. In rubbery polymers, selectivity is derived from the

difference of condensability of the molecules, where larger molecules are more

likely to dissolve and diffuse through the membrane. For instance, almost all

industrial gas separation membranes are glassy polymers because in rubbery

polymers, the segmental motions of the chains are not rigid enough to allow a

desirable separation of the gas mixture and unless the solubility difference of the

gas mixture compounds in the polymer matrix is significant (as in vapors/gases separation), rubbery polymers are not promising candidates for gas-separation membranes.

It is quite evident that a judicious choice of the membrane material can significantly influence the efficiency of the separation and process economy. In the next section of this chapter a short review of the membrane types and materials will be given.

2.4.4 Membranes: types and materials

Selection of membrane material depends on the application of the membrane and the nature of the feed stream. While a certain type of membrane material achieves a desired level of separation for a gas or liquid mixture, the same membrane may totally fail the task of separating another mixture. Mulder (Mulder, 1991) classified the polymeric membranes into porous and dense nonporous membranes. Table 2.5 shows the types of the membranes used for different membrane processes (Perry, Green, & Maloney, 2008).

2.4.4.1   Porous membranes

Porous membranes are usually used in microfiltration and ultrafiltration. They contain fixed pores in the range of 0.1-10μm for microfiltration and of 2-100 nm for ultrafiltration (Mulder, 1991).

Table 2.5. Membrane separation Process for Porous/Nonporous membranes

Process Name	Applied Driving Force	Type of Membrane
Pervaporation	Vapor Pressure	Nonporous
Vapor Permeation	Vapor Pressure	Nonporous
Gas Permeation	Partial pressure difference	Nonporous
Reverse Osmosis	Pressure difference	Nonporous
Dialysis	Concentration difference	Nonporous or Microporous
Electrodialysis	Electric Potential difference	Nonporous or Microporous
Microfiltration	Pressure difference	Porous
Ultrafiltration	Pressure difference	Porous

For this type of membranes, selectivity is determined by the dimensions of the pores. The type of membrane material only affects the chemical integrity of the membrane over its operational lifetime. Fouling and chemical/thermal resistance is the most important factors in selecting this type of membrane material. Table 2.6 summarizes the most common polymers used for microfiltration and ultrafiltration membranes (Mulder, 1991).

Table 2.6. Polymers for microfiltra**tio**n and ultrafiltration membranes (Mulder, 1991).

Microfiltration membranes	Ultrafiltration membranes
polycarbonate	polysulfone/poly (ether sulfone)
Poly(vinylidene-fluoride)	polyacrylonitrile
polytetrafluoroethylene	Cellulose esters
polypropylene	Polyimide/poly (ether imide)
polyamide	Polyamide (aliphatic)
Cellulose-esters	Poly (vinylidene fluoride)
polysulfone	---

For microfiltration membranes, polycarbonate is the most common polymer due to its mechanical stability. Hydrophobic polymers such as PTFE, PVDF and PP are commonly used due to their excellent thermal and chemical

44

stability. Despite the great thermal and chemical resistance of such hydrophobic membranes, hydrophilic membranes are gaining more attention. This is mainly due to the fact that hydrophilic polymers have reduced adsorption tendencies (Mulder, 1991). The best example of these types of polymers is cellulose and its derivatives. Cellulose and its derivatives are very common membrane materials not only for microfiltration and ultrafiltration membranes but also for other membrane processes such as hyperfiltration, gas separation and dialysis. In fact, cellulose acetate is the most common membrane material for gas separation membranes (Nunes & Peinemann, 2006) because of its crystalline structure which makes it a glassy polymer.

Ultrafiltration membranes pores are within the range of nanometer size. Phase inversion is usually used to create such small pores. Polysulfones (PSf) and poly (ether sulfones) (PES) are the basic materials for ultrafiltration membranes (Mulder, 1991). These polymers have very good thermal and chemical stability. Polyimdes and polyacrylonitriles are also used as ultrafiltration membrane materials.

2.4.4.2   Nonporous membranes

Nonporous membranes are used for gas separation and pervaporation purposes. In order to combine the high selectivity of a dense membrane with the high permeation rate of thin porous membranes, nonporous membranes are usually made in form of composite membranes. Unlike the porous membranes,

nonporous membranes performance (selectivity and permeation rate) depends greatly on the intrinsic properties of the polymer used in the membrane fabrication.

Much attention is given to investigate and develop membrane materials with higher permeability and selectivity. Both of these factors significantly affect the economy of the membrane process. Substantial amount of research has been performed to modify the chemical and physical structure of the membranes for improved permeability and selectivity. It is well-established that polarity and steric characteristics of the polymer backbone affect the basic properties of the membrane such as structural regularity, packing density, fractional free volume, and rigidity of the polymer chain, which in turn alter the permeation properties of the membrane. Many researchers investigated the structure-property relationship in glassy polymers such as polyimides (Coleman & Koros, 1990; Freeman, Yampolskii, & Pinnau, 2006; Hu, Xu, & Coleman, 2007; Nunes & Peinemann, 2006; Stern, Mi, Yamamoto, & Clair, 1989), PTMSP(Jia & Baker, 1998; Kelman et al., 2008) and polycarbonates(Chern, Sheu, Jia, Stannett, & Hopfenberg, 1987; Hellums, Koros, Husk, & Paul, 1991; Muruganandam & Paul, 1987; Percec, 1987; Story & Koros, 1992) and rubbery polymers such as PDMS (Coleman & Koros, 1990; Kesting et al., 1990; Kim, Koros, Husk, & O'brien, 1988). Comprehensive reviews of relationship between membrane materials and permeation properties of gases have been published by Koros and Fleming

46

(Koros & Fleming, 1993), Pixton and Paul (Pixton & Paul, 1994) and Stern (Alexander Stern, 1994).

2.4.4.3 Inorganic membranes

Another category of the membranes is inorganic membranes. Inorganic-based membranes have superior chemical and thermal stability compared to conventional polymeric membranes, which enables them as suitable candidates for special separation purposes such as high-temperature gas separation or membrane reactors. Three different types of inorganic materials are generally used for the synthesis of inorganic membranes: (a) ceramic, (b) glass, and (c) metal. Ceramic membranes are used for microfiltration and ultrafiltration applications. They are usually made through the sintering process by the combination of a metal with a non-metal compound to form an oxide, nitrite or carbide (Mulder, 1991). Alumina (Al_2O_3) and Zirconia (ZrO_2) are the most important materials used for ceramic membranes. Glass membranes are often made from silica (SiO_2) by the leaching technique. Metallic membranes are obtained by the sintering of the metal powders. A good example of the application of metallic membranes includes hydrogen separation and purification by the Palladium-based alloys membranes.

2.4.5 State-of-the-art industrial applications of the membranes

Commercial application of membranes for different separation problems in industry is well-established (Bessarabov, 1999; Matsuura, 1994). Novel applications of the membranes can be categorized in 4 distinct groups: (1) Gas separation, (2) Liquid separation (3) Membrane reactors, and (4) Membrane contactors.

The first industrial application of gas separation membranes was to separate hydrogen from ammonia-plant purge-gas by Monsanto company (Henis & Tripodi, 1980). After that, many other companies such as Cynara, Separex, Dow and Air Liquide developed membranes for many industrial gas separation applications. Baker (R. W. Baker, 2002) predicted the market of gas separation membranes in 2020 to be five times of that of year 2000. Current gas separation membranes cover a variety of applications including: (a) supply of pure enriched gases such as He, N_2 and O_2 from air, (b) acid gas removal from natural gas, (c) the separation of H_2 in the petrochemical and chemical industries, (d) natural gas and air dehydration, and (e) hydrocarbons recovery from process streams. One of the rapidly emerging fields of membrane-based gas separation is to separate olefin/paraffin gases. Many scholars studied and outlined the advantages of the application of the membranes for the separation of olefin/paraffin gases (Eldridge, 1993; Ilinitch, Semin, Chertova, & Zamaraev, 1992; Park, Won, & Kang, 2001). Comprehensive reviews on the application of gas separation

membranes are available in literature (R. Baker, 2012; Mulder, 1991; Spillman, 1989; Toshima, 1992).

Membranes can be used for certain liquid/liquid separation problems in a process called pervaporation. In this process, a liquid mixture enters the feed side of the membrane and the permeate is removed as a vapor. Pervaporation is generally used for separating liquids with close boiling points or azeotrpic mixtures. The first industrial pervaporation system was installed by Gesellschaft fur Trenntechnik Gmbh, Germany (GFT) in 1982 for separating water from alcohol by polyvinyl alcohol (PVOH) composite membranes. Currently, pervaporation membranes are widely used in petrochemical industries for variety of applications such as, volatile organic compounds (VOCs) removal from water and aromatic/aliphatic separation. Pervaporation membranes are also used for removing the toxic phenolic (Han, Ferreira, & Livingston, 2001) and aromatic compounds (Dastgir, Ferreira, Peeva, & Livingston, 2004; Dastgir, Peeva, & Livingston, 2005; Han, Puech, Law, Steinke, & Livingston, 2002; Lebo, Zajicek, Huckins, Petty, & Peterman, 1992) from the waste effluent of industrial units.

Membrane reactor is another application of membranes. Membrane reactor is a generic name for reactors that are coupled with the membranous walls. The membrane usually removes one of the products and thus shifts the reaction toward products, and so increases the conversion of the reaction. The very initial applications of membrane reactors involved gas/vapor phase

49

reactions by using the inorganic microporous or mesoporous membranes such as alumina or zirconia. In most cases, membrane reactors perform the product purification as well (Mulder, 1991). Membrane reactors cover a wide range of applications such as pervaporation and vapor permeation for esterification reactions (Okamoto et al., 1992; Okamoto, Semoto, Tanaka, & Kita, 1991; Zhu, Minet, & Tsotsis, 1996), dehydrogenation (Collins et al., 1996; Itoh, 1987; Kikuchi, 1995) and many other processes.

Membrane contactor is a device that provides an interface between two components such as two liquids or two gases or a liquid and a gas without the dispersion of the phases within each other. The membrane facilitates the mass transfer between the phases. Gabelman and Hwang (Gabelman & Hwang, 1999) outlined the major advantages of the membrane contactors as: absence of emulsions, no flooding at high flow rates, no unloading at low flow rates, no density difference between fluids required and very high interfacial area compared to conventional dispersed phase contactors (30 times more than the gas absorbers and 500 times more than liquid/liquid extraction columns). Membrane contactor technology has applications in wastewater treatment (Pankhania, Stephenson, & Semmens, 1994; Prasad & Sirkar, 1987), pharmaceuticals (Prasad & Sirkar, 1990; Prasad & Sirkar, 1989), semiconductor manufacturing (Wikol, Kobayashi, & Hardwick, 1998), Liquid/liquid extraction

(Basu & Sirkar, 1991; COONEY & POUFOS, 1987) and other types of processes (Gabelman & Hwang, 1999; Stanojević et al., 2003).

2.5   Membrane approach in this work

In this work, a hybrid approach to capture the CO_2 will be utilized. The ultimate goal of this work is to test the feasibility of regenerating a physical solvent via the application of composite polymeric membranes. In a conventional Selexol plant to capture the CO_2 or other acid gases, the regeneration of the solvent is carried out via the pressure swing technique in a series of consecutive flash drums. In this work, the pressure letdown is replaced by a membrane module where the high pressure pre-saturated solvent flows over the membrane surface. Physical solvent regeneration via the composite polymeric membranes has not been done before and no relevant or similar studies were found in the literature. In the next chapter, the experimental setup and procedures will be explained in detail.

3 Experimental Apparatus - Procedures and Materials

3.1 System overview

The physical solvent regeneration setup consists of a high pressure absorber vessel for saturating the solvent with CO_2 and the membrane module where CO_2 permeates across the membrane. The schematic of the experimental setup is shown in Figure 3.1. Initially, the absorber is charged with solvent. The absorber is equipped with a relief valve on top for safety purposes and degassing the solvent at the end of the experiments via the pressure letdown technique. During the solvent saturation process, this relief valve is kept open initially for a couple of minutes to push air out of the absorber. The absorber is equipped with a home-made cooling water coil to control the absorber temperature. The absorber pressure and temperature are measured and recorded continuously. Solvent recirculates through the membrane module and then returns back to the absorber. In order to study the effect of feed-side pressure and temperature, the feed-line pressure and temperature, upstream of the membrane module are measured and recorded continuously. Solvent circulation flow rate is adjustable using a variable speed pump. Solvent temperature can be controlled using inline pencil heaters coupled with a temperature controller. To increase the driving

force across the membrane, N_2 is used as the sweep gas. To investigate the effect of sweep gas flow rate, a mass flow controller is used to adjust the N_2 flow rate. To quantify the amount of CO_2 permeation across the membrane, the concentration of CO_2 in the sweep gas is measured using a Non-Dispersive Infrared CO_2 analyzer or an Agilent 7850A GC with Flame Ionization Detector (FID) and Thermal Conductivity Detector (TCD), depending on the CO_2 concentration. To prevent damage to the GC and the CO_2 analyzer and to measure solvent permeation through the membrane and thus calculate the selectivity, the sweep gas is filtered using a Parker coalescing filter from Cole-Parmer.

Knowing the exact solvent flow rate to the membrane module is critical for calculating the percentage recovery of the solvent by the membrane. The rotameter readings are calibrated using the pump calibration module as will be discussed in section 3.2.7.

In order to better understand the required time to saturate the solvent with CO_2 and evaluate the capacity of the membrane to regenerate the solvent, it is necessary to measure the concentration of CO_2 in the solvent under different operating conditions. This is achieved by taking solvent samples downstream and upstream of the membrane module and measuring the CO_2 concentration in the sampling module. The sampling module will be explained in detail in section 3.2.7.1.
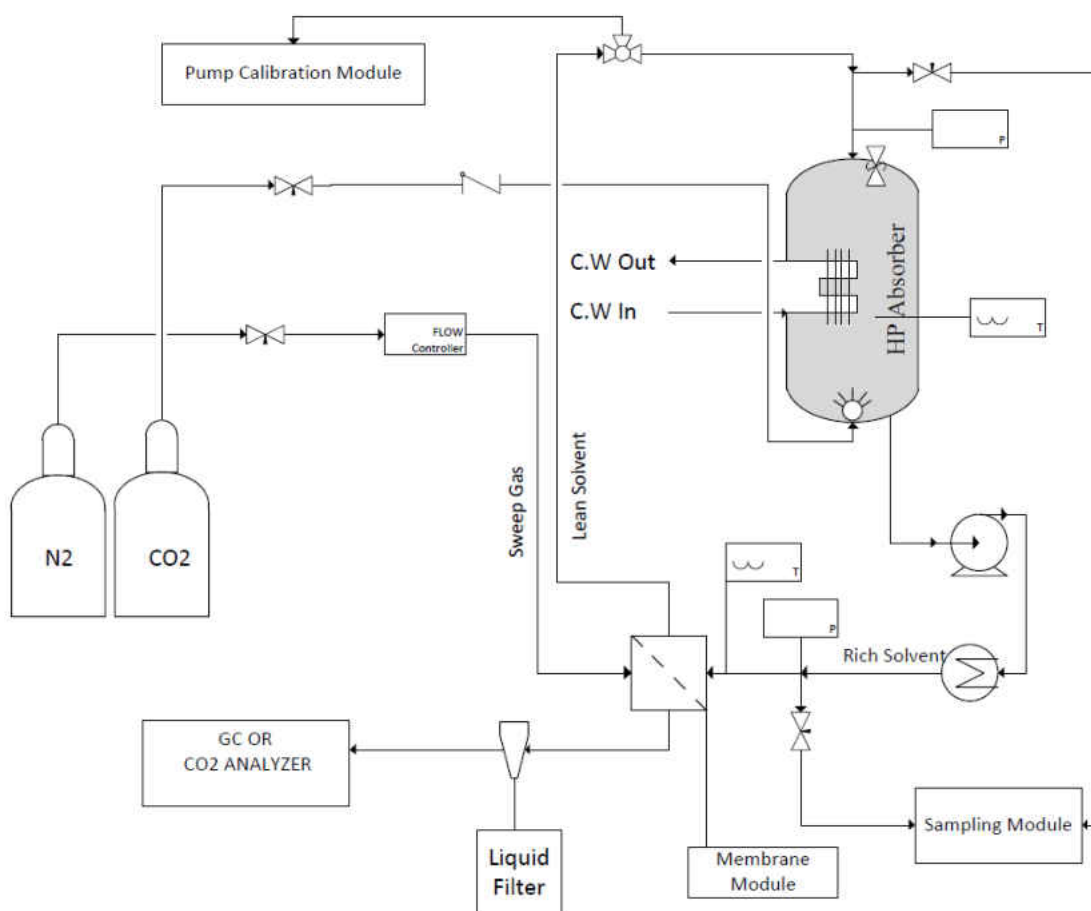
Figure 3.1 .Schematic of high pressure permeation system for physical solvent regeneration.

3.2   Equipment list

The following equipment and materials were used for building the high pressure permeation setup.

3.2.1 Pervaporation equipment

- Membrane unit: Millipore® 47mm High Pressure Stainless Steel

  Membrane Holder XX4504700

- Pump head: Micropump high-flow pressure-loaded pump compatible with type 56 c-face motors from Cole-Parmer, Part Number: EW-07003-41

- Pump motor: Leeson NEMA Type 56C-face TEFC motor, 1/3 hp, 1750 rpm, 90 VDC from Cole-Parmer, Part Number: EW-70071-00

- Motor speed controller: Basic Variable-Speed DC Motor Controller for 1/4 to 2 hp motors, from Cole-Parmer, Part Number: EW-70100-10

- Cartridge heaters: Stainless steel construction, ¼" diameter, 6" length, ¼" NPT thread, 400 W, 120V, ID Number: HR25060R from Big Chief, Inc.

- Heater controller: Cal controller 9400

- Pressure transducer: Omega, 0-1000psi, 5 VDC regulated input, 0-100mV output, Part Number : PX309-1KGV

- Pressure gauges: Cole-Parmer, Part number: PGI-63C-PG800-LAOX

- Thermocouple: 1/8", 1/4" diameter, K type from Omega

- Mass flow controller: Brooks 4800 series, N_2 (0-10 SLPM).

- Swagelok tubing and fittings

- Liquid and particulate filter: Parker coalescing filter from Cole-Parmer, ¼" NPT Ports, Part Number: EW-02917-00

- Rotameter: Brooks Metal Tube Rotameter Model 3750CA5A11DCAAAAA0, Valve on Inlet, +/- 5% full scale accuracy.

3.2.2 Data logger

- National Instruments 9219 4 CH-CH ISOLATED, 24-BIT, +/-60V, UNIVERSAL AI MODULE, Part Number: 779781-01.

- National Instruments USB SINGLE MODULE CARRIER FOR C SERIES MODULES, Part Number: 779471-01.

3.2.3 CO_2 Analyzer

- Li-cor 820 Non-Dispersive Infrared CO_2 analyzer, 0-20,000ppm, ± 1ppm

- Agilent 7850A GC- FID with methanizer, TCD

3.2.4 Computers and software

- Computer: Dell Precision T3200, Microsoft ^{TM} Windows 7

- Data acquisition: Labview ^{TM} software, version 2010 from National Instruments

- GC control and analysis: Chemstation, Agilent

- CO_2 analyzer: LI-820 v2.0.0

3.2.5 Absorption vessel

The 4 liter absorption vessel was built by the University of North Dakota Chemical Engineering Department workshop from a 6" stainless steel pipe. Two class 300 flanges coupled with gaskets are used to seal the absorption tank. This absorption vessel is equipped with a home-made cooling water coil to maintain the absorption temperature at a certain value. A pressure transducer is

mounted on top of the absorber to record the pressure inside the absorber. CO_2 is injected into the solvent via a sparger installed at the bottom of the absorber to increase the contact time between the liquid and gas bubbles. To discharge the air during the period when the absorber is loaded with solvent, and also to regenerate the physical solvent inside the absorption tank at the end of the experiment, a relief valve is mounted on top of the absorber. Using a 1/4" diameter, K type thermocouple, the absorber temperature is measured and recorded continuously.

3.2.6 Membrane Module

The membrane module is modified from the original Millipore® 47 mm stainless steel membrane holder XX4504700. Figure 3.2 shows different parts of the original filter holder. This membrane holder can hold filters of 47 mm diameter and the inlet pressure is rated up to 10,000 psi. Its diameter and height are 8.6 and 4.4 cm respectively. It is sealed by a fluoroelastomer O-ring. The inlet and outlet fittings are 7/16 in.-20 (UNF-3B) female. To apply this filter holder to our application, the central inlet and outlet adaptors on the top and bottom plates were plugged and two new 1/8" holes were drilled on each plate to allow the solvent to recirculate in the upper chamber and the sweep gas to flow in the bottom chamber of the membrane holder.

57
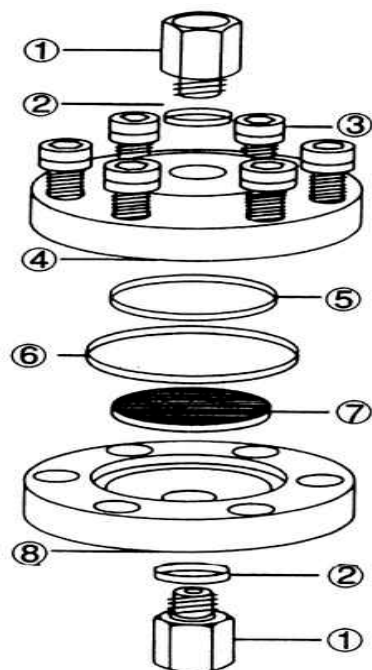
Figure 3.2. (Adopted from www.millipore.com/catalogue/module/C263) Original configuration of the membrane holder (Upper and bottom plates were modified with an inlet and outlet) 1. Inlet/Outlet Adapter, 2. Adapter O-ring, 3. Hex-cap Screw, 4. Top plate, 5. Inner O-ring, 6. Outer O-ring, 7. Support Screen, 8. Bottom plate.

3.2.7 Pumping system

Initially, a reciprocating pump was used to circulate the solvent through the setup. The pump was a 500-A-N3 stainless steel pump from Neptune (Available at UND Chemical Engineering Research Lab). Two major difficulties were encountered with this pump. First, the flow rate of the Neptune pump was very limited, 3.7 LPH at 100 psi. The system is supposed to operate at significantly higher pressures and, since the flow rate decreases by 10% for each 100 psi pressure increase (based on personal communication with the factory), it

became clear that using this pump would prevent us from looking into different flow rates at different pressures.

The second important issue regarding the Neptune pump was its pumping method. Neptune pumps are reciprocating pumps, and thus much pulsation is expected in the flow. Such pulsations made the flow rate measurements difficult and inaccurate. The rotameter calibration needs a rather smooth flow with much a lower level of fluctuations. Furthermore, if the flow is pulsing in the membrane chamber, it is likely to cause fluctuations in the sweep gas CO_2 concentration.

To address these pump-related issues, a container filled with solvent and pressurized air on top of the liquid was added to the solvent line to dampen flow fluctuations. However, later investigations of the system indicated that running the system would deplete the dampener and eventually result in pump cavitation. Additionally, it was assumed that the liquid CO_2 loading of the solvent in the container would not be equal to the CO_2 loading of the solvent circulating in the system and this could decrease the accuracy of the calculations.

For the mentioned difficulties, a new gear pump that delivers the fluid more smoothly with a wider range of flow rates was purchased. The new installed pump includes the following items:

- Micropump® high-flow pressure-loaded pump head. This pump head is a magnetically driven, precision-geared pump that delivers the fluid smoothly and with very low pulsation and an acceptable

59

range of flow rates (0.85 ml/revolution). The pump head was purchased through Cole Parmer, part No: EW-07003-41.

- Leeson NEMA Type 56C-face TEFC motor, 1/3 hp, 1750 rpm, 90 VDC. (Purchased through Cole Parmer, part No: EW-70071-00)

- Basic Variable-Speed DC Motor Controller to adjust the speed of the motor and thus the desirable flow rate. (Purchased through Cole Parmer, part No: EW-70100-10).

3.2.7.1 Pump calibration module

In order to confirm the readings of the rotameter and calibrate the pump delivery flow rate versus the speed of the motor, an apparatus was designed and incorporated into the system. The schematic of the calibration module is shown in Figure 3.3.

The calibration system includes a collection vessel that is pressurized with CO_2 from the same CO_2 line that is used to load the absorber. Once the valve on the CO_2 line that goes to the collecting vessel is opened, both the collecting vessel and the absorber will have the same pressure. The collection vessel is equipped with a pressure gauge to ensure that both the collection vessel and the absorber are at the same pressure. After pressurizing the collection vessel, it is isolated from the CO_2 line by closing the valve. Following that, for a specific period of time (30 seconds), the solvent flow is diverted from the main solvent line to the collecting vessel using a three way valve. Next, the collecting vessel is

60

depressurized using the relief valve mounted on top of the collection vessel. Finally, the valve installed on the bottom of the collection vessel is opened and the volume of the collected solvent is measured with a graduated cylinder. The collection vessel and the absorber are both mounted on the rack at the same elevation from the pump centerline. Since the delivery pressure and the elevation of both the absorber and the collection vessel are exactly the same, the delivery flow rate to the collection vessel should be exactly the same as the delivery flow rate to the absorber and thus the rotameter readings can be calibrated using this module.
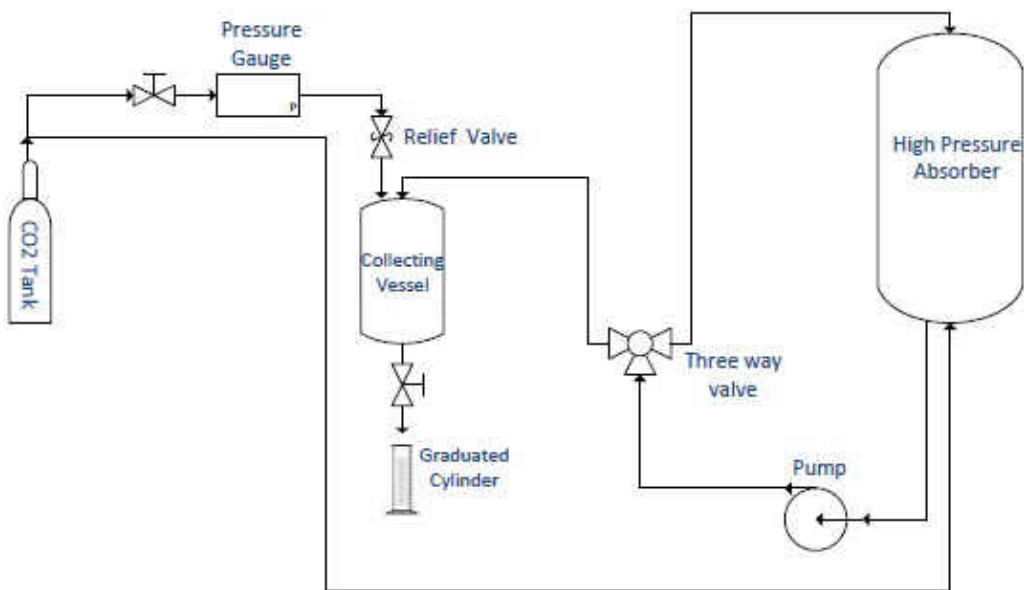
Figure 3.3. Pump calibration apparatus.

3.2.8 Physical solvent sampling module

In order to calculate the amount of CO_2 recovered from the rich solvent stream by the membrane module and determine the efficiency of the absorber in term of solvent saturation at different pressures and temperatures, it is necessary to design and develop a method to measure the amount of dissolved CO_2 in the solvent. As discussed earlier, unlike chemical solvents, physical solvents do not react with the solute and they physically dissolve the acid gases, which are then stripped by means of pressure swing techniques or a combination of heat and pressure letdown. The performance of a physical solvent can be predicted by its solubility. The solubility of an individual gas follows Henry's law—the solubility of a compound in the solvent is directly proportional to its partial pressure in the gas phase. Hence, the capacity of a physical solvent is enhanced by increasing the partial pressures of the acid gases. Since there is no reaction between the solvent and the solute in the case of physical solvents, desorption of the gas from the liquid can be achieved by reducing the pressure. Pressure reduction is used as a mean to measure the concentration of the CO_2 in the solvent stream. The sampling apparatus is shown schematically in Figure 3.4.

The apparatus consists mainly of a small sampling cylinder (10 ml) (purchased from Swagelok, part No: SS-4CD-TW-10) and a 1 liter expansion vessel (purchased through Swagelok, part No: 304L-HDF4-1000) connected to the sampling cylinder
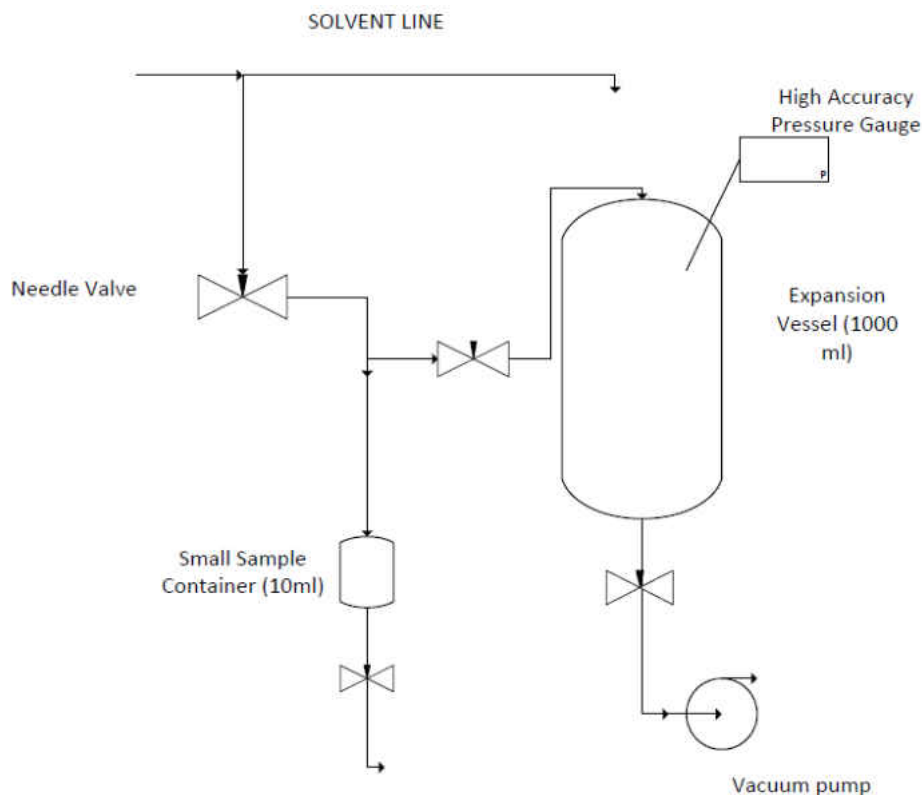
Figure 3.4. Schematic of physical solvent sampling apparatus

The expansion vessel is equipped with a high accuracy 0.08% pressure gauge from Omega (part No: DPG409-030A). Both the sampling cylinder and the expansion vessel are connected to a 1.1cfm vacuum/pressure diaphragm pump (purchased from Cole-Parmer, part No: EW-07061-40). Before drawing the sample from the solvent line, the whole sampling module is vacuumed and isolated using the valves. The initial pressure of the expansion vessel is recorded. Following that, using an on-off valve, the expansion vessel is isolated from the sampling cylinder and, using a metering valve, a few cubic millimeters of the solvent from the solvent line is injected into the sampling cylinder. Next, the

valve that isolates the expansion vessel from the sampling cylinder is opened and the desorbed gas from the solvent enters the expansion vessel and increases the pressure in the expansion vessel. Approximately two hours after the sample injection, the final pressure of the expansion vessel is recorded. Following that, the valve at the bottom of the sampling cylinder is opened and the collected solvent is weighed to calculate the number of moles of the solvent using the average molecular weight of the solvent. To ensure all solvent collected in the sampling cylinder is drained, the entire sampling module is purged with 50psi N_2 gas. It is assumed that all the CO_2 content of the solvent desorbs under vacuum conditions.

By using: (1) an equation of state such as the ideal gas law or SRK equation of state, (2) the expansion vessel pressure difference before and after the sample injection and (3) the volume of the sampling system, the number of moles of CO_2 desorbed from the solvent sample is given by equations 3.1 and 3.2

$$n_{CO2} = \frac{[P_2(V_T - V_S) - P_1V_T]}{RT}$$ Eqn (3.1)

$$X_{CO2} = \frac{n_{CO2}}{n_{CO2} + \frac{m_s}{M_n}}$$ Eqn (3.2)

where:

R: Universal Gas Constant (cm^3.Psi.g mol^{-1}.K^{-1})

T: Temperature (K)

P_1: Sampling module pressure after evacuation (Psi)

P_2: Sampling module final Pressure after sample injection (Psi)

V_T: Sampling module total volume (cm^3)

V_S: Sample volume (cm^3)

m_S: Sample weight (gr)

M_n: Average molecular weight of the solvent (gr)

3.3   Materials

- Poly (Ethylene Glycol) Dimethyl Ether, Average Mn CA. 250, 10L from SIGMA-ALDRICH, SKU No: 445878).

- PREVAP^{TM} 1201/2235 Polymeric Membrane Sheets, Sulzer Chemtech.

- PREVAP^{TM} 1211/2203 Polymeric Membrane Sheets, Sulzer Chemtech.

- PERVAP^{TM} 4060 Polymeric Membrane Sheets, Sulzer Chemtech.

- PDMS Selective Layer Polymeric Membrane Sheet, PERVATECH.

- SYLGARD 184$^{®}$ silicon elastomer base and silicon elastomer curing agent, from SIGMA-ALDRICH, SKU No: 761036-5EA.

- Membrane holder inner O-ring (TFE packed VITON) from Millipore$^{®}$, part No: XX4504705.

- Membrane holder inner O-ring (Perfluoroelastomer) from CHEMRAZ®, part No: 9030-SD505.

- Membrane Holder Outer O-ring (VITON), from Millipore®, part No: XX4504713.

Due to the high operating pressure of this physical solvent system, only composite polymeric membranes with a dense selective layer on top can be utilized. Two different types of material for the dense selective layer were chosen to study their capacity for capturing CO_2 from the pre-saturated solvent: (a) PERVAP 1201 and PERVAP 1211 which have a polyvinylalcohol (PVOH)-based selective layer and (b) PERVAP 4060 and PERVATECH which have a polydimethylsiloxane (PDMS)-based selective layer. The structures of these two polymers are given in Figure 3.5.

(a)   (b)
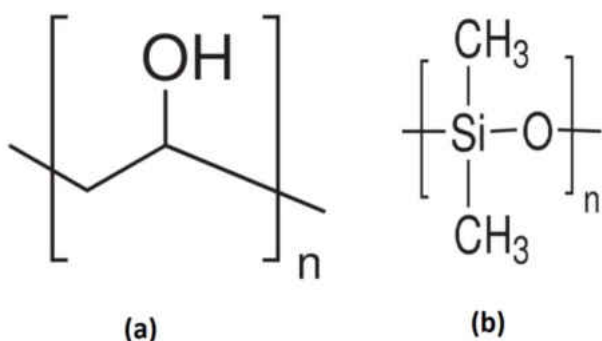
Figure 3.5 (a) PVOH and (b) PDMS structures.

PDMS is an elastomer with a glass transition temperature of -123 °C (Mulder, 1991). PDMS is known to have a high permeability for CO_2. The

permeability of CO_2 in different polymeric membranes is shown in Table 3.1. It is clear that except Poly [1-trimethylsilyl-1-propyne] (PTMSP), all other polymeric membranes have significantly lower permeabilities for CO_2 (Wankat, 2006).

Table 3.1. CO_2 permeability in different polymeric membranes (Wankat, 2006).

Membrane	Permeability cm^3 (STP).cm/[cm^2.s.cm Hg]
PTMSP	28,000
PDMS	4550,3240
Natural rubber	99.6, 153, 131
Silicone rubber	2700
Polystyrene	10.0, 12.4, 23.3
Polycarbonate	8.0
Butyl rubber	5.2,5.18
Nylon 6	0.16
Nylon 66	0.17
Poly(4-methyl pentene)	93
Cellulose acetate	7.75

Brunetti et al. (Brunetti, Scura, Barbieri, & Drioli, 2010) summarized the permeability of CO_2 in different polymers. Except for a very few polymers such as PTMSP and PTMGP, all other polymers have lower CO_2 permeabilities compared to PDMS.

The polymeric membranes used in this work consist of a very thin separation layer (e.g. PDMS or PVOH), a porous support (e.g. polyacrylonitrile) and a mechanical support (e.g. polyester). The schematic of the composite membranes used in this work is shown in Figure 3.6.
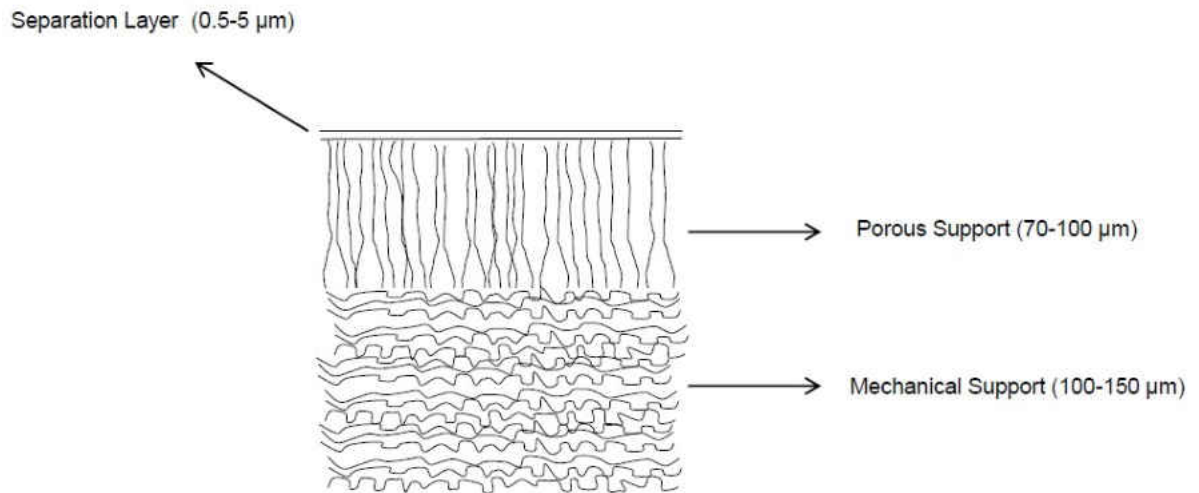
Figure 3.6 Structure of the composite membranes used in this work.

3.4 Experimental procedure

The following procedure is used to measure the permeation rate of CO_2 through different polymeric membranes:

- Membranes are cut using a variable diameter circular cutter set to the diameter of 47mm.

- Membrane holder O-rings are inspected visually to make sure they can seal the membrane properly. If any corrosion or defect is observed, the O-rings will be replaced.

- The membrane sheet is placed on top of the screen in the bottom chamber of the filter holder.

- The upper chamber is placed over the bottom chamber and screwed down tightly. For even sealing, the screws are tightened with the same number of turns.

- The pump motor speed controller is set to 10% and the pump is turned on.

- N_2 mass flow controller is set to 500 (sccm/min) and N_2 tank pressure regulator is opened and set to 50 psi (The allowed pressure for the mass flow controller).

- The sweep gas coalescing filter is checked to make sure no significant leaking is occurring in the membrane chamber.

- The Data Acquisition program is run using NI LabView.

- The relief valve mounted on the absorber vessel is opened

- The CO_2 tank is opened and the pressure is set as low as 30 psi for five minutes (This is to flush the absorber with CO_2 to ensure no air is trapped in the system).

- The relief valve on top of the absorber is closed.

- The absorber is pressurized to the desirable pressure by increasing the outlet pressure of the CO_2 tank pressure regulator and monitoring the readings of the absorber pressure transducer via LabView. (This step has to be done slowly to avoid hydraulic shock to the membrane sealing and the pump).

69

- The desirable solvent flow rate is set by adjusting the DC motor speed controller and using the calibration charts for any pressure.

- The solvent flow rate is confirmed by measuring it via the pump calibration module as explained in section 3.2.7.1.

- The sweep gas is diverted to the CO_2 analyzer and the LI-820 v2.0.0 is run to monitor and record the measured CO_2 concentration in the sweep gas (Two measurements per second).

- If the CO_2 analyzer readings are over the analyzer limit (20000 ppm), then the sweep gas CO_2 concentration is measured using the GC.

- The CO_2 mole fraction is measured via the sampling module and procedure explained in section 3.2.8.

- The permeation experiment is run for about 6-8 hours.

- The sweep gas filter is drained once per hour for the "membrane selectivity calculations".

- The system is depressurized by opening the relief valve, stopping the pump, opening the chamber and removing the membrane for post-experiment characterization tests.

3.5   Design of Experiment

In this work, a two-level, two-factor full-factorial design with two replicates and three center points was set up to determine which factors influence the

70

permeation properties of the membrane. The two factors were the system pressure and solvent circulation flow rate. The responses measured were the CO_2 permeation rate, rate of solvent leakage, membrane selectivity, and percentage of solvent recovery. The design was replicated and the order of experiments was randomized. The three center points were added to study the curvature in the system. The original experimental factors (uncoded units) along with the coded units designated as −1 (low) and +1 (high) are summarized in Table 3.2.

Table 3.2 Experimental factors and their uncoded set point values

Factor	Low Values (-1)	High Values (+1)	Center Point
Pressure (psi)	300	600	450
Solvent Flow rate (mL/min)	80	160	120

For each individual response, the net effect was obtained by using the difference between the average responses at the high and low levels of each factor. A larger absolute value for an effect signifies a greater impact on the response. To evaluate the statistical significance of effects of various factors, a two-sample t-test using the means at the high and low settings was performed and a probability value (p-value) was calculated. For the effect to be statistically significant at a 95% confidence level, the p-value should be less than or equal to 0.05. The statistical software package, Minitab^{TM} 15 was used to calculate the t value for each factor. The calculated t value is compared with the critical t value and if it is greater than the critical t value, that specific factor is identified as a

significant factor. The Pareto chart demonstrates the t value for each factor along with the critical t value and thus is used as a mean to identify the significant factors for each response. The main effects plots are utilized to better understand the effect of each factor on the responses of the experiment.

3.6   Post experiment characterization tests

In order to examine the chemical stability of the membranes after being exposed to the high pressure solvent stream, a series of post-experiment characterization tests are performed to better understand the chemical stability and structural of the membranes.

3.6.1   FTIR analysis

A Fourier transform infrared (FTIR) spectrum is generally a useful tool for investigating the structure and chemical changes of a membrane after it has been used in the permeation setup. A Nicolet IR-200 spectrometer (Thermo-Nicolet Corp, Madison, WI) was used to analyze the original and post-experiment membrane samples. Analysis was performed on a Thunderdome Swap-Top operation module equipped with ZnSe crystal. All spectra were recorded in the absorbance mode in the wave number range of 400-4000 cm^{-1} with a detection resolution of 16 and 16 scans per sample. OMNIC 6.0 software (Madison, WI.) was used to determine peak positions and intensities. Two replicates of each

sample were run to ensure reproducibility of the results. Figure 3.7 shows the FTIR settings used for both the original and post-experiment membranes.

3.6.2 Differential Scanning Calorimetry (DSC)

DSC is used to measure transitions or chemical reactions in a polymer (Mulder, 1991). DSC curves are used to identify the glass transition temperature and the degree of crystalinity.
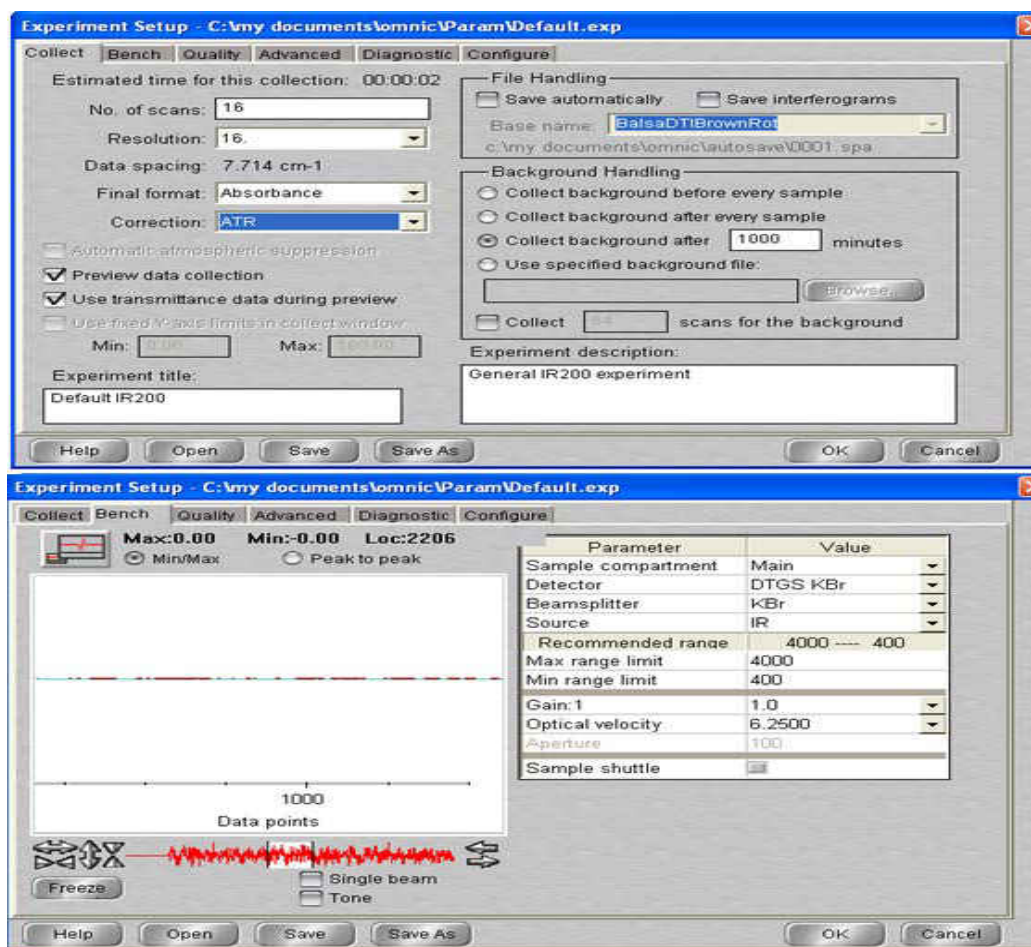
Figure 3.7 FTIR settings.

In this work, a Perkin Elmer 7 Series Diamond DSC was used to analyze the membrane samples. The analysis was performed for both the original and post-experiment samples for each type of membrane. The polymer samples, each approximately 7 mg, were sealed in aluminum pans. For each sample, two thermal scans were conducted. The first scan erased the thermal history of the sample. Only the second scan was used to compare the structural integrity of membrane samples after being exposed to the high pressure solvent stream. The following temperature profile was defined for the DSC experiments. Only the sixth step was used for thermal analysis of the membranes.

1) Hold for 1.0 min at -20.00°C

2) Heat from -20.00°C to 240.00°C at 10.00°C/min

3) Hold for 1.0 min at 240.00°C

4) Cool from 240.00°C to -120.00°C at 10.00°C/min

5) Hold for 1.0 min at -120.00°C

6) Heat from -120.00°C to 240.00°C at 5.00°C/min

3.6.3 Scanning electron microscope (SEM)

An SEM is a microscope that uses a focused beam of high-energy electrons to form an image. The signals from electron-sample interactions give information about the sample morphology, chemical composition, and crystalline

74

structure of the sample. In this work, the surface and cross-section SEM images of the membrane samples were captured using a JEOL SEM (Model No: JSM-7600F).

3.7   Sorption experiment

One of the major challenges of the membrane processes that prevent the membrane technology from being used commercially is the fouling effect. Fouling may occur due to the blocking of the pores of the membrane or adsorption of the fluid particles on the surface of the membrane. Fouling causes the flux to decline and eventually decreases the performance of the membrane significantly. A comprehensive review of flux decline in membrane processes has been given by van den BERG and Smolders (VAN DEN & Smolders, 1988). The following procedure was used to carry out the sorption experiment:

- Polymeric membranes were cut in a circular shape with the diameter of 47mm.

- Membrane thickness was measured (average of three points) using a digital micrometer (Fowler IP54, ±0.00001in) and weighed on a microbalance (Fisher Scientific, ±0.00001g).

- Duplicate polymer samples were immersed in 1L of the solvent in a water bath (Precision Microprocessor, Controlled 280 series Water Bath) at a constant temperature of 25 ^{o}C for 20 hours.

- Following that, the membranes were removed from the bath and the excessive solvent on the membranes' surface were wiped off using dry filter papers.

- The membranes were weighed immediately.

- The weight changes of each membrane sample were recorded in 30 minutes intervals till no detectable change was observed.

Using the criteria developed by Yamaguchi et al, the solubility coefficient was calculated using equation 3.3.

$$S = \frac{\frac{\Delta W}{\rho 1}}{(\frac{\Delta W}{\rho 1} + \frac{1}{\rho 2})} \qquad \text{Eqn (3.3)}$$

where ΔW is the weight of liquid dissolved in the membrane (g of solvent/g of dry membrane) and ρ1 and ρ2 are the densities of the solvent and dry membrane respectively.

4 Results and Discussions

4.1 System verification

In order to compare the permeation properties of different membranes, it is imperative to verify the consistency and accuracy of operational parameters measurements. System temperature and pressure is measured and recorded using the pressure transducers, thermocouples and the data logger from National Instruments. Accurate measurements of the solvent flow rate and its CO_2 concentration are also critical to the calculations of the membrane effectiveness in separating the CO_2 from the solvent. In this section, the verifications of various operational parameters will be presented.

4.1.1 Pump Calibration

Figure 4.1 shows the pump calibration curves at different system pressures. The calibration curves were generated using the pump calibration module explained in section 3.2.7.1. As the curves in Figure 4.1 indicate, at a given pumping speed, solvent flow rate decreases as the pressure of the system increases. The effect of pressure on flow rate drop becomes more pronounced

as the motor speed increases. At the lower pumping speeds, solvent flow rate does not change significantly with pressure.
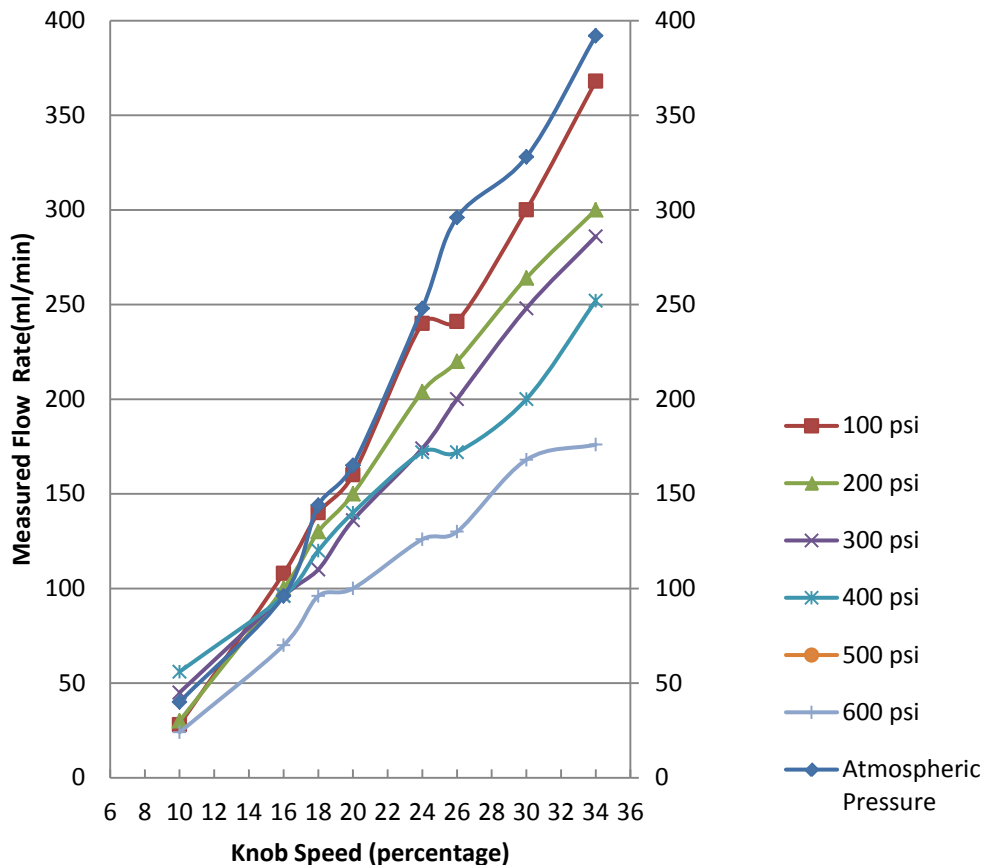
Figure 4.1 Pump calibration curves at different pressures (The horizontal axis represents the percentage of the maximum pump motor speed, 1750 rpm).

Figure 4.2 shows the rotameter readings versus the actual flow rate in the system. These graphs will be used to adjust the actual solvent delivery at different pressures using the rotameter readings.
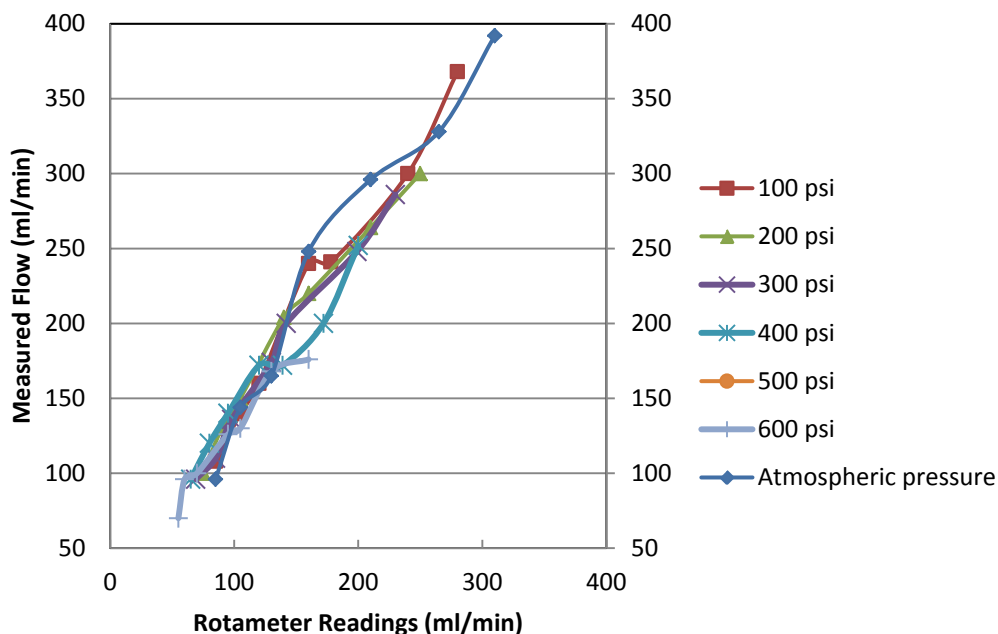
Figure 4.2 Measured solvent flow rate versus rotameter readings.

4.1.2 Absorber pressure and temperature

Figure 4.3 and Figure 4.4 show the stability of the absorber pressure and temperature with respect to time. The measured pressure and temperature variations were acceptable for the purposes of the permeation experiments. To study the stability of the pressure in the system, the absorber was pressurized with CO_2 at 335 psi and the pressure of the absorber was recorded. The pressure in the absorber remained within an acceptable range of 335.5±.2 Psi over a two hour period.
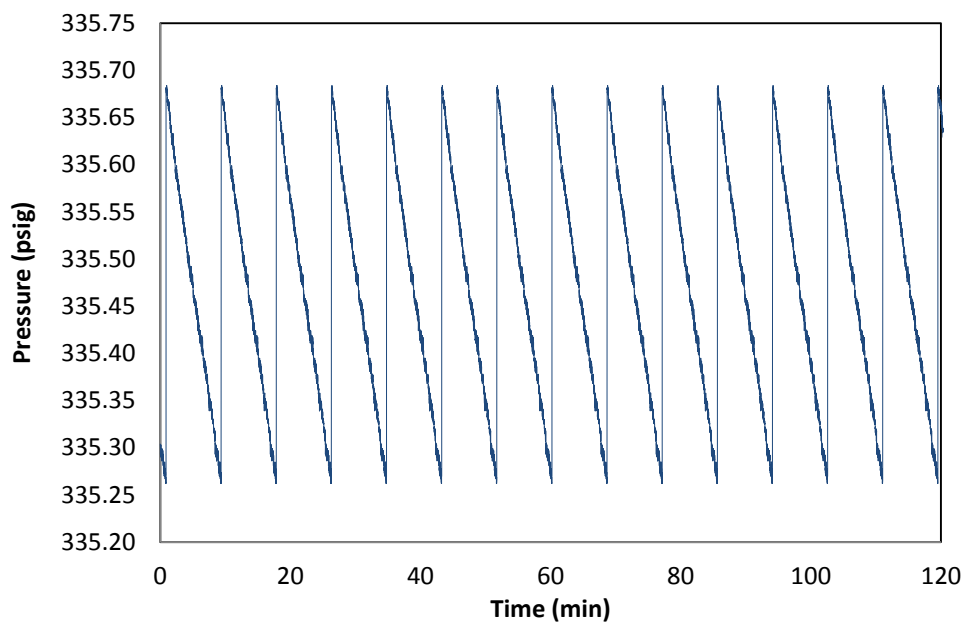
Figure 4.3 Absorber pressure versus time.

Figure 4.4 shows the temperature fluctuations in the absorber. The temperature was measured using a K-type Omega thermocouple mounted on top of the absorber. It is clear that the temperature of the system remained within an acceptable range with respect to time. Using the temperature controller and the pencil heaters, the temperature of the solvent line can be adjusted upstream of the membrane module. Using the home-made cooling water coil installed in the absorber, the temperature of the absorber can be controlled within an acceptable range.

80
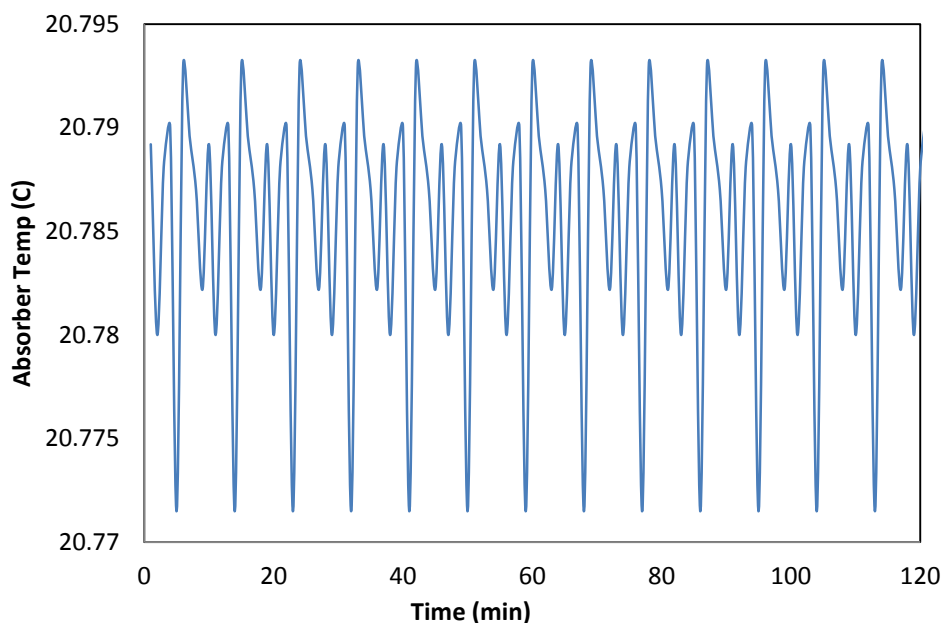
Figure 4.4 Absorber temperature versus time.

4.2 CO_2 concentration measurement

Using the sampling module explained in section 3.2.8 and equations 3.1 and 3.2, the concentration of CO_2 in the solvent was measured at different pressures. The absorber was pressurized to the desired pressure and the pump was turned on. Solvent samples were drawn into the sampling module at different time intervals after absorber pressurization. The measured CO_2 mole fractions in Selexol at different pressures are shown in Figure 4.5. Clearly, the CO_2 mole fraction increases as the pressure of the system increases. Additionally, the concentration of CO_2 in the solvent reaches a steady state value approximately 2 hours after the absorber pressurization. This is important with

respect to the calculations of the permeation properties of the membrane. Only steady state CO_2 concentrations in the sweep gas will be considered in the calculations. Tabulated values for the mole fractions with respect to time at different pressures are shown in Table 4.1.
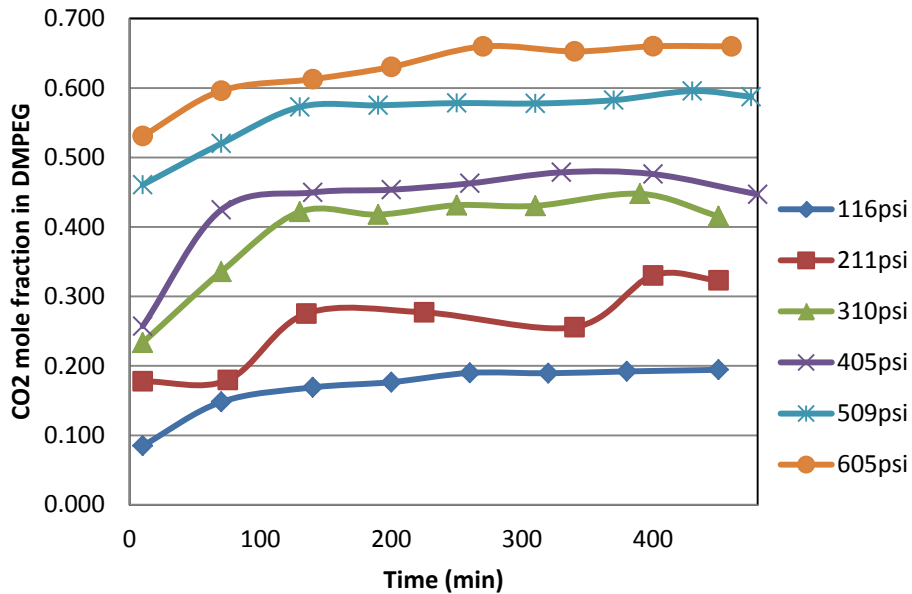
Figure 4.5 CO_2 mole fraction in Selexol at different pressures

Table 4.2 compares the steady state values for the CO_2 mole fraction in the solvent obtained from the sampling module with the literature values (Gainar & Anitescu, 1995). The values from Gainar and Anitescu were interpolated and reported in Table 4.2. The results are fairly close, with an average absolute deviation of 5.87%. A sample calculation of the CO_2 mole fraction in the solvent is given in Appendix A.

Table 4.1. CO_2 mole fraction in DMPEG at diferent presures.

Time (min)	Mole Fraction	Time(min)	Mole Fraction
116 (psi)		211 (psi)	
10	0.085	10	0.178
70	0.148	75	0.180
140	0.169	135	0.275
200	0.177	225	0.277
260	0.190	340	0.256
320	0.189	400	0.330
380	0.192	450	0.323
450	0.194		
310 (psi)		405 (psi)	
10	0.233	10	0.257
70	0.335	70	0.425
130	0.422	140	0.450
190	0.418	200	0.454
250	0.431	260	0.463
310	0.430	330	0.479
390	0.448	400	0.476
450	0.415	480	0.447
509 (psi)		605 (psi)	
10	0.461	10	0.531
70	0.520	70	0.596
130	0.573	140	0.613
190	0.575	200	0.630
250	0.578	270	0.660
310	0.578	340	0.653
370	0.582	400	0.660
430	0.596	460	0.660

Table 4.2 Comparison of CO_2 mole fractions in this work with the literature values (Gainar & Anitescu, 1995).

Pressure (psi)	This work	Gainar Work (Interpolated)
116	0.191	0.175
211	0.297	0.28
310	0.431	0.382
405	0.466	0.465
509	0.586	0.547
605	0.658	0.639

4.3   Permeation results

4.3.1 Verification of the membrane stripping performance

Prior to the screening study, sample runs were carried out with a PVOH-based membrane (PERVAP 1211/2203) and a PDMS-based membrane (PERVATECH). The absorber was pressurized with CO_2 to 400 Psi. Using the pump calibration curves and the pump motor speed controller, the solvent flow rate was set to 120 (mL/min). The sweep gas flow rate was adjusted to 500 (sccm). Figure 4.6 and Figure 4.7 show the CO_2 concentration in the sweep gas. The PDMS-based membrane (Figure 4.7) has a significantly higher CO_2 flux compared to the PVOH-based membrane. As mentioned earlier, PDMS has a very high affinity for CO_2 compared to other polymers and this explains the higher CO_2 flux in our permeation experiments.
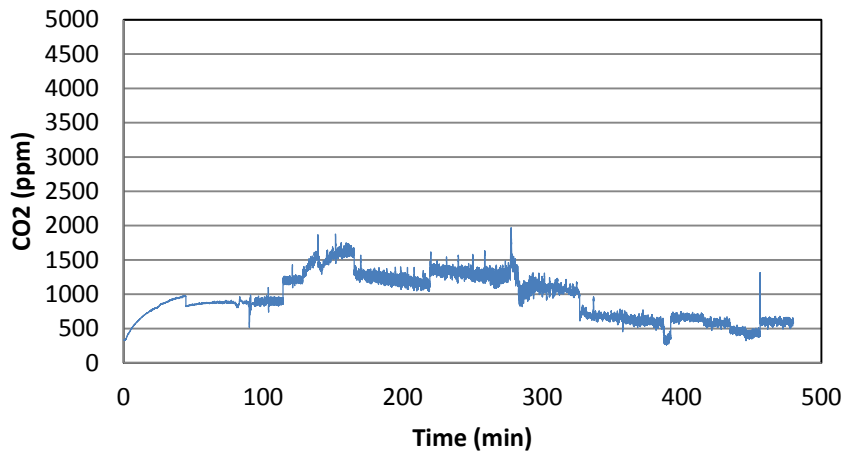
Figure 4.6 CO_2 concentration in the sweep gas. (PERVAP1211, PVOH-based membrane).
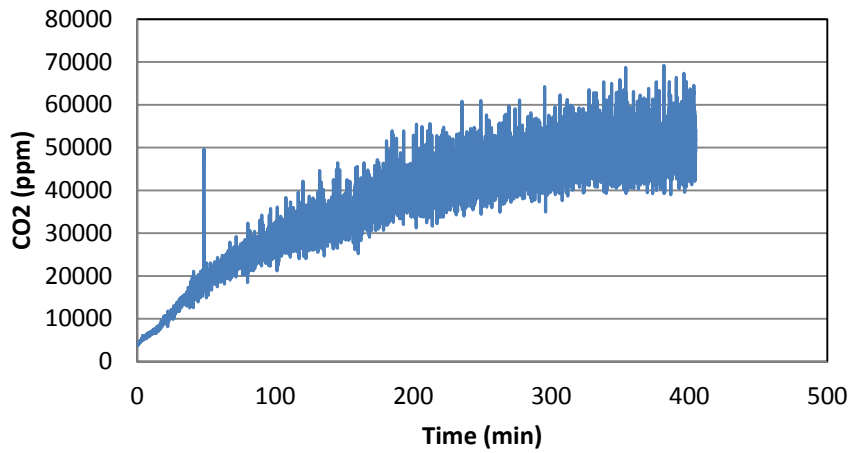
Figure 4.7. CO_2 concentration in the sweep gas, (PERVATECH, PDMS-based membrane).

4.3.2 Screening study

Following the same procedure outlined in section 3.4, the candidate membranes including PERVAP 4060 (SULZER), PERVAP 1201 (SULZER), PERVAP 1211 (SULZER) and PERVATECH were tested in the permeation setup. All the membranes were tested at 400 Psi. The solvent flow rate was adjusted to 100 (mL/min) and the sweep gas flow rate was 500 (sccm). The absorber temperature was controlled at 17±1 ^{o}C. The permeation properties of the membranes were calculated and shown in Table 4.3. The results of the screening study are shown in Table 4.3. These results, along with the CO_2 profiles in the sweep gas, suggest the following preliminary conclusions:

Table 4.3 Screening study results.

Membrane	PERVAP 4060 (SULZER)	PERVAP 1201 (SULZER)	PERVAP 1211 (SULZER)	PERVATECH
Thickness (mm)	0.24	0.19	0.19	0.19
Average CO_2 concentration (ppm)	167000 (From GC)	910	952	36475 (From GC)
CO_2 Flux (cm^{3}STP $(CO_2)(cm2)^{-1}.S^{-1}$	0.14	0.79×10-3	8.26×10-4	32.00×10-3
Solvent Flux $(cm^3)(cm^2)^{-1}.S^{-1}$	3.88×10-5	0	1.80×10-6	9.87×10-5
Selectivity	3608.25	Perm-selective	456.74	320
Percent Recovery	0.79	4.14×10-3	4.69×10-3	0.17

- The CO_2 profile in the sweep gas reaches its steady state condition, two hours after absorber pressurization.

- PDMS-based membranes (PERVATECH and PERVAP 4060) show higher CO_2 permeability compared to PVOH-based membranes (PERVAP 1211 and PERVAP 1201).

- PERVAP 4060 was chosen as the candidate membrane for further analysis and design of engineering experiments to find the optimum operational conditions, due to its high CO_2 flux and selectivity compared to the other membranes.

The term "perm-selective" in Table 4.3 does not necessarily indicate that the membrane is absolutely impermeable to the solvent and only CO_2 can diffuse across the membrane. Rather, it implies no measurable amount of solvent has been collected by the sweep gas filter.

4.3.3 Effect of regeneration temperature

As mentioned earlier, unlike chemical solvents, physical solvents do not react with the solute and they physically dissolve the acid gases, which are then stripped by means of pressure swing techniques or a combination of heat and pressure letdown. Consequently, CO_2 absorption/desorption in a physical solvent process is mainly dominated by the pressure of the process. To validate this assumption and to investigate the effect of temperature, solvent stream temperature was raised and the concentration of CO_2 in the sweep gas was measured. The CO_2 concentration in the sweep gas for PERVAP 1211 (PVOH based) and PERVAP 4060 (PDMS based) at different temperatures is shown in

Figure 4.8. The experiments started at room temperature and then temperature was increased by 20 ^oC for consecutive 2-hours periods. As shown in Figure 4.8, increasing the solvent temperature upstream of the membrane module did not affect the amount of CO_2 liberated. The results of this experiment indicate that increasing the temperature at a constant pressure cannot alter the permeation properties of the membranes studied in this work. For both membranes, sweep gas flow rate was set to 500sccm and pressure was constant at 400 psi. For PERVAP 4060 membrane, the CO_2 concentration in the sweep gas was measured using the Agilent 7850A GC (CO_2 concentration > 20000 ppm) and for PERVAP 1211, CO_2 concentration was measured using Li-cor 820 Non-Dispersive Infrared CO_2 analyzer (CO_2 concentration < 20000ppm).
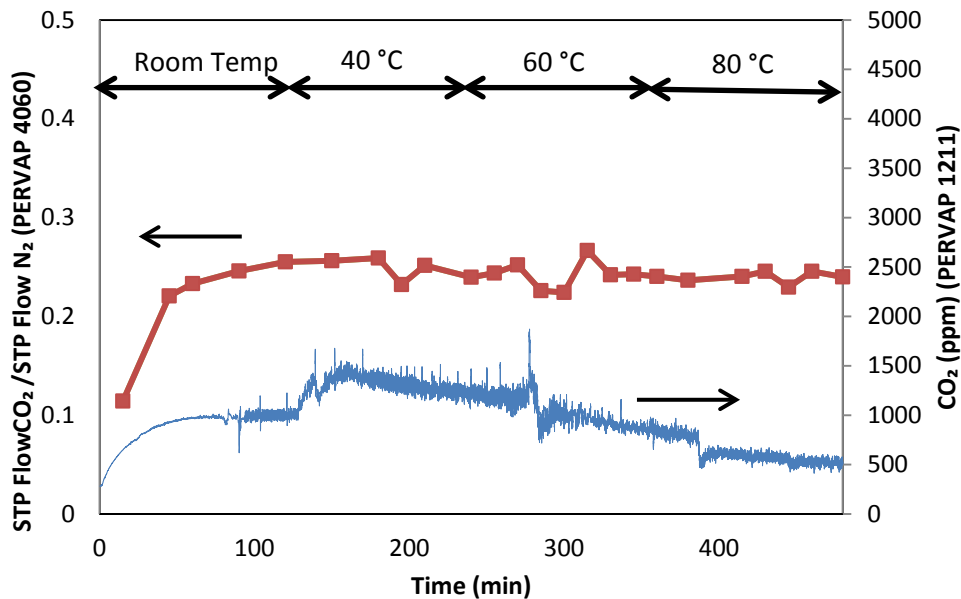
Figure 4.8 Effect of temperature on the rate of CO_2 permeation.

4.3.4 Effect of sweep gas flow rate

The primary objective of using the sweep gas is to sweep away the permeated CO_2 and thus maintaining the driving force for CO_2 permeation across the membrane at its maximum possible level. However, considering the size of the membrane chamber and the small amount of CO_2 permeation due to the small membrane area, it is expected that changing the sweep gas flow rate will not affect the CO_2 permeation. To test this hypothesis, PERVAP 4060 membrane was used at two different sweep gas flow rates of 500 and 1000 (sccm) and the CO_2 concentration in the sweep gas was measured using the GC. The profiles of the CO_2 permeation rate for the two different sweep gas flow rates are shown in

Figure 4.9 and Table 4.4. It appears that changing the sweep gas flow rate has no significant effect on the rate of CO_2 permeation within the range of the experimental conditions in this study.
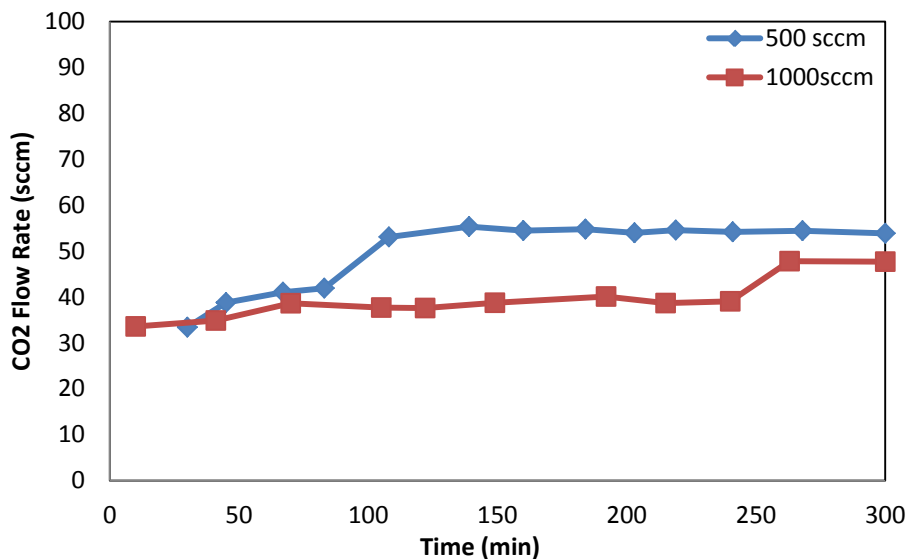
Figure 4.9 CO_2 Permeation rate for two different sweep gas flow rates.

Table 4.4 Effect of sweep gas flow rate on CO_2 permeation rate

Sweep Gas Flow Rate(sccm)	CO_2 Flux (cm^{3}STP CO_2/cm^2.S)	Avg Solvent Leak (mL/cm^2.S)	% Recovery
500	0.087	3.18×10^{-5}	0.582
1000	0.069	3.47×10^{-5}	0.847

4.4   Design of experiment runs

To better understand the effects of system pressure and solvent flow rate on different experiment responses, CO_2 Flux, selectivity, % recovery, and solvent leakage, a two-factor two-level full factorial design with two replicates and three center points were performed on PERVAP4060 membrane, which appeared to

be the most promising membrane in the screening study. The summary of the experimental conditions along with the responses are given in Table 4.5. A sample calculation of Table 4.5 is given in Appendix B.

Table 4.5 Design of experiment runs- operating conditions and permeation properies.

Pressure (psi)	Solvent Flow rate (mL)	CO_2 Flux (cm^3STP CO_2/cm^2.s)	Avg Solvent Leakage (mL/cm^2.sec)	Selectivity	%Recovery
300	160	0.097	4.10×10^{-5}	2365	0.60
300	80	0.087	3.18×10^{-5}	2741	1.08
600	160	0.442	1.77×10^{-4}	2497	0.9
600	80	0.367	1.67×10^{-4}	2197	1.50
450	120	0.205	4.58×10^{-5}	4470	0.97
300	160	0.095	4.70×10^{-5}	2020	0.59
600	80	0.464	1.93×10^{-4}	2405	1.90
450	120	0.250	9.16×10^{-4}	2733	1.19
450	120	0.356	7.11×10^{-5}	5005	1.69
300	80	0.069	3.47×10^{-5}	1976	0.85
600	160	0.439	2.11×10^{-4}	2080	0.90

A statistical analysis was performed to identify the significant factors for each individual response. To achieve this purpose, the last four columns of Table 4.5 along with the corresponding experimental conditions were imported to Minitab^{TM} 15 statistical software. The Pareto charts and main effect plots for different responses of each experiment including: (a) CO_2 flux, (b) average solvent leakage, (c) selectivity, and (d) % recovery are shown in Figure 4.10 - Figure 4.13 respectively.

Analysis of the Pareto charts in Figure 4.10 clearly indicates the significance of pressure. With respect to CO_2 flux, pressure appears to be strongly significant.

91

As pressure inside the absorber increases, the solubility of CO_2 in the solvent stream is enhanced. A greater pressure difference across the membrane, signify a higher driving force and thus higher CO_2 flux should be expected. The Main Effects plot in Figure 4.10 confirms the aforementioned hypothesis. However, the solvent flow rate has no significant effect on the CO_2 flux. The immediate conclusion from this observation is that the mass transfer is mainly controlled by the membrane. Increasing the solvent flow rate should cause more turbulence inside the membrane chamber, which, in turn, increases the rate of CO_2 diffusion into the boundary layer, adjacent to the membrane surface. However, since the dominant mass transfer resistance exists in the membrane, the rate of CO_2 permeation does not change significantly.

Regarding solvent leakage, the Pareto chart in Figure 4.11 indicates pressure to be significant. However, the solvent flow rate has no effect on the rate of solvent leakage through the membrane. As the pressure of the system increases, the liquid in the upper chamber of the membrane module forces itself into the membrane and hence, the rate of solvent leakage increases.
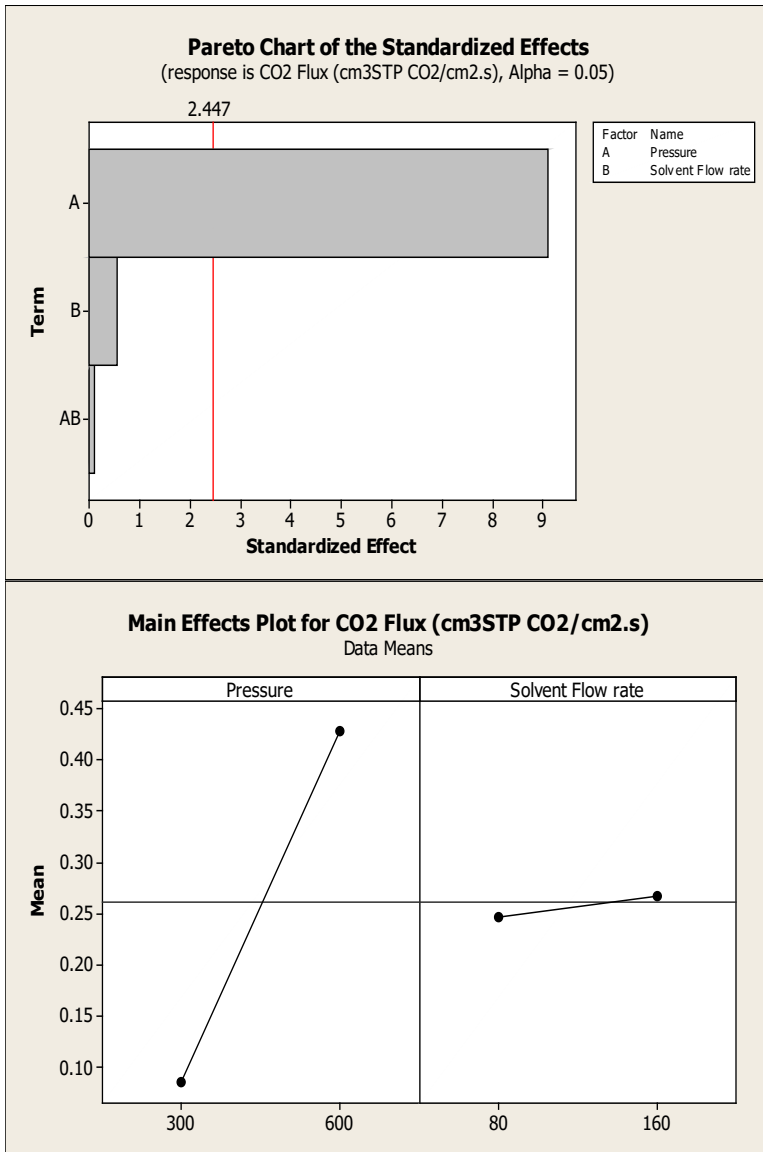
Figure 4.10 Pareto and main effects plot for CO_2 flux.
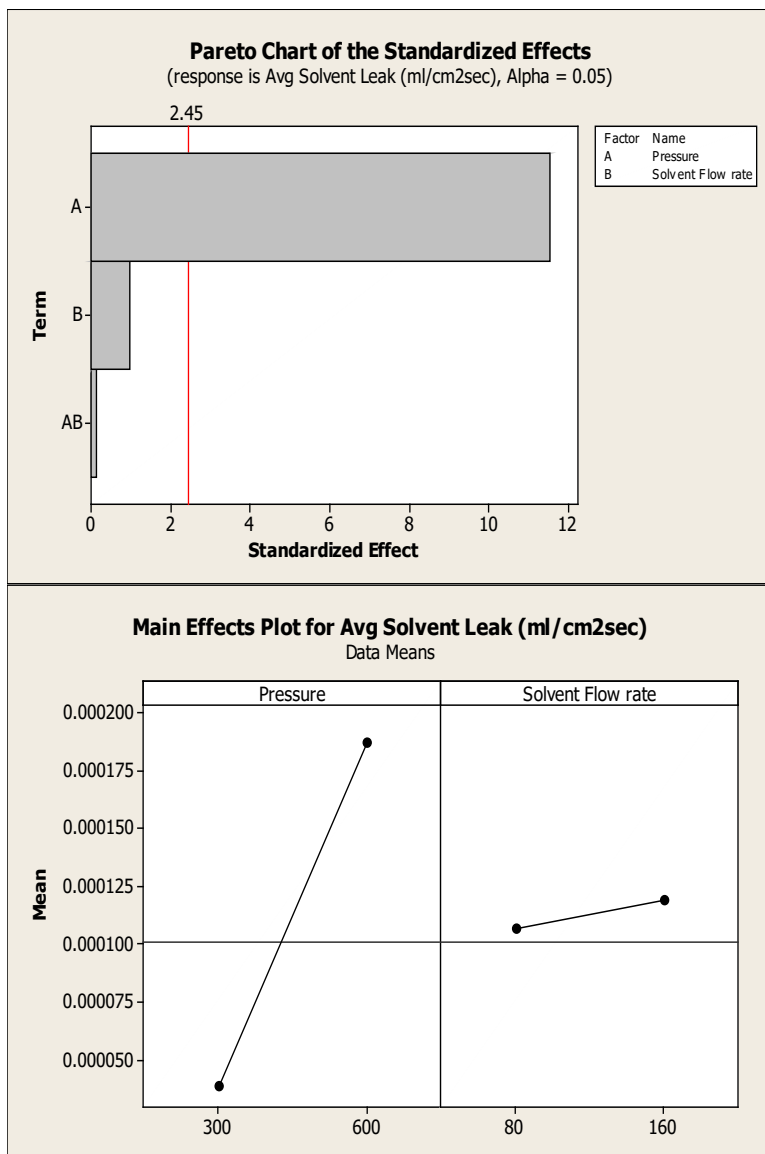
Figure 4.11 Pareto and main effects plot for solvent leakage.

Neither the pressure of the system nor the solvent flow rate were found to significantly influence the selectivity of the membrane (Figure 4.12). As explained earlier, membrane selectivity is an intrinsic property of the membrane material for a given separation problem. The system operational parameters such as

pressure and solvent flow rate cannot influence the intrinsic properties of the membrane material and thus membrane selectivity remains unchanged.

Finally, regarding the percent recovery of the solvent, both system pressure and solvent flow rate appeared to be significant. At elevated pressures, the mole fraction of CO_2 in the solvent increases, thus suggesting that the higher pressure creates a higher driving force for CO_2 permeation. As a result of this, the percent of recovery increases by pressure as confirmed by the Main Effects plot in Figure 4.13.

Furthermore, by increasing the solvent flow rate, more CO_2 is introduced to the upper membrane chamber. However, mass transfer resistance through the membrane prevents more CO_2 from being transported. Thus, introducing more CO_2 to the upper chamber eventually decreases the percent recovery of the solvent due to the slow mass transport through the membrane and reduced residence time of the solvent in the membrane module. The residual plots for various responses along with analyses of variance and model parameters are given in Appendix C.
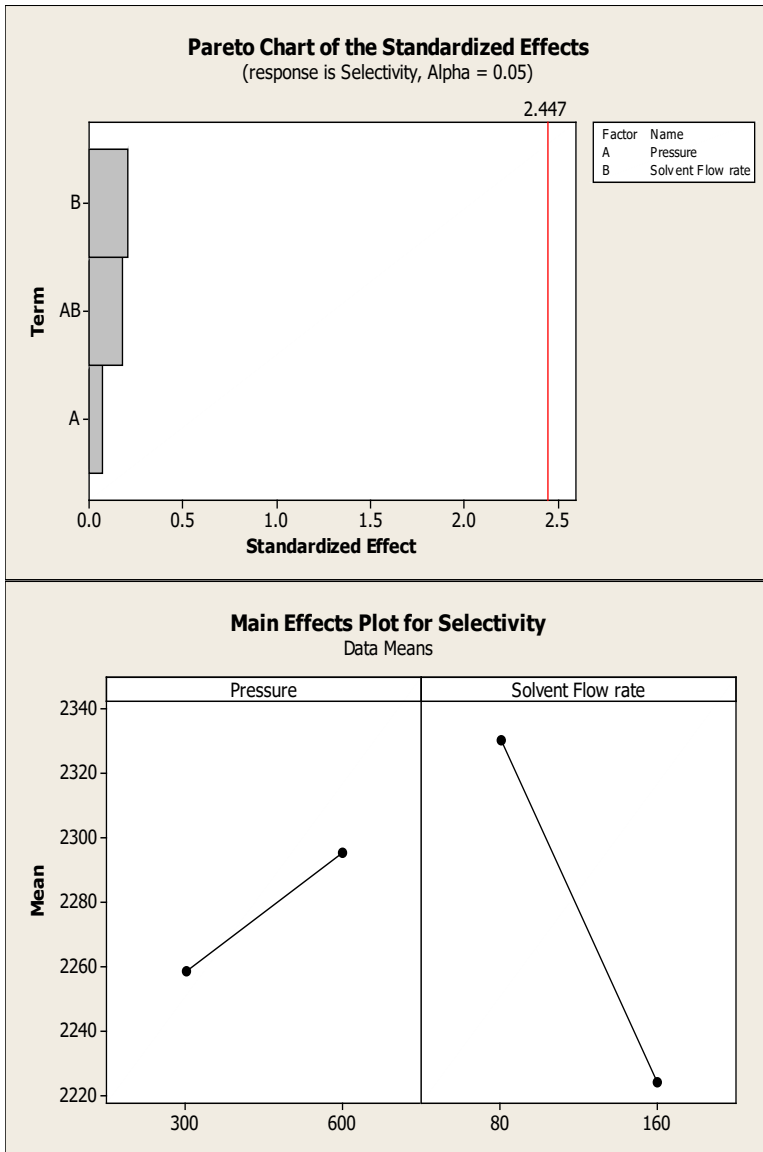
Figure 4.12 Pareto and main effects plot for selectivity.
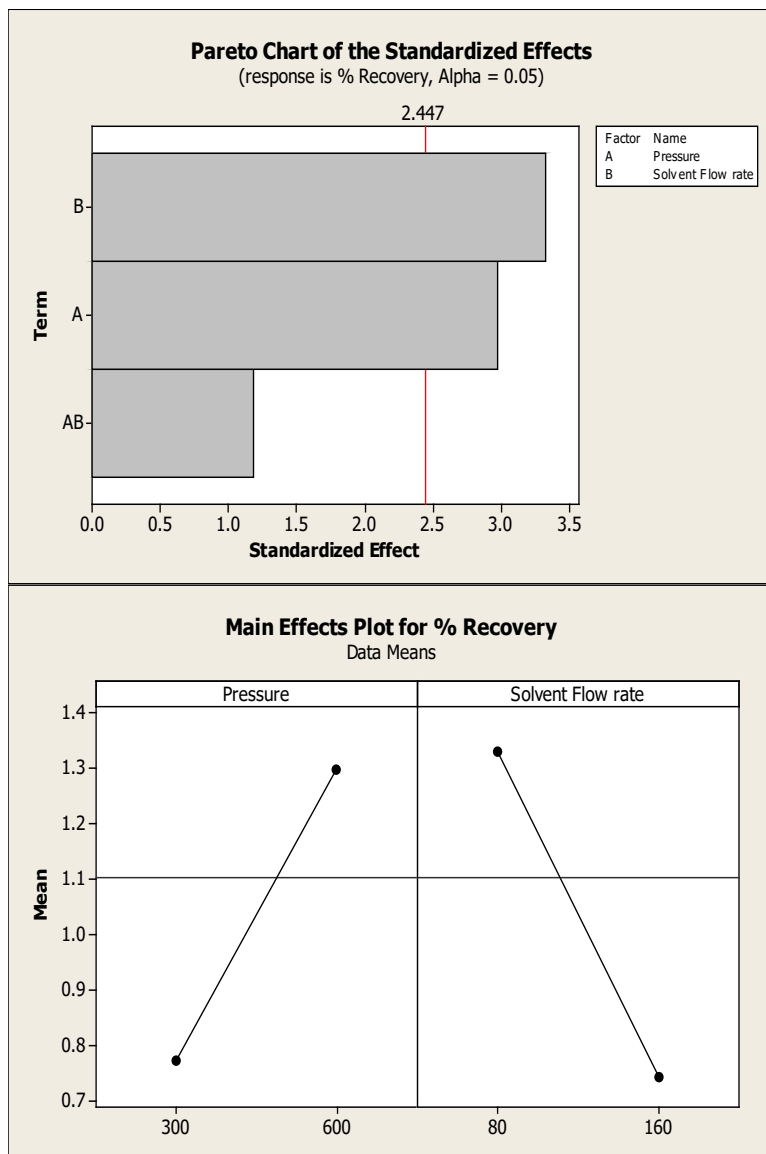
Figure 4.13 Pareto and main effects plot for percent recovery of solvent.

4.5   Post experiment characterization tests

In order to examine the chemical stability and structural integrity of the membranes after being exposed to the high pressure solvent stream, a series of

post-experiment characteristic tests were performed. In this section the FTIR, DSC and SEM results will be presented.

4.5.1 FTIR results

FTIR results for the membranes used in this work are shown in Figure 4.14. For each type of membrane, FTIR test was performed for both the original and post-experiment membranes. A Comparison of the spectra of the original and post-experiment membranes revealed no major differences. The only detectable difference was observed at higher wavelengths, which could be attributed to solvent deposits on the membrane surface. To better understand the origin of this peak, FTIR test was performed for a solvent sample (Selexol). The spectrum obtained from the solvent sample is shown in Figure 4.15. It appears that the minor differences observed at a wavelength of approximately 3000 (cm-1), could be attributed to solvent deposits on the membrane surface. The FTIR test showed no significant chemical changes of the membrane surface for the running period of approximately 8 hours. However, it is likely that longer contact times may cause chemical degradation of the membrane materials. This hypothesis may be confirmed by using the membranes in the permeation setup over significantly longer periods.
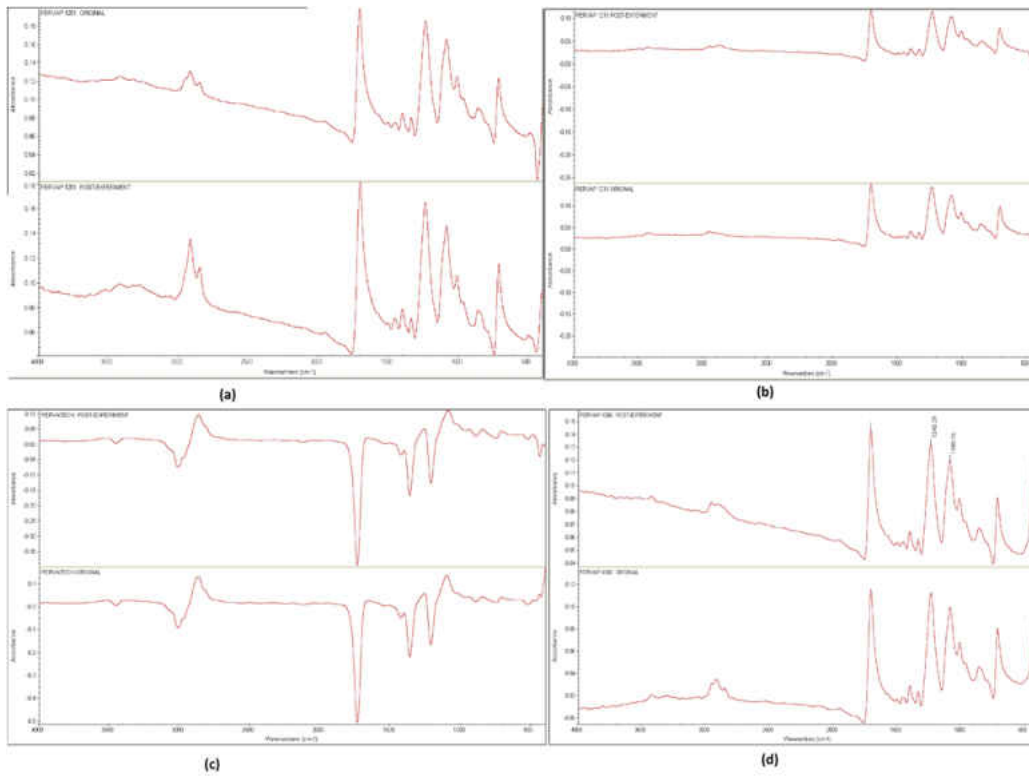
Figure 4.14 FTIR spectra for different membranes: (a) SULZER 1201 (b) SULZER 1211 (c) PERVATECH (d) PERVAP 4060 (For each graph, the upper section shows the post-experiment membrane and lower section shows the original membrane).
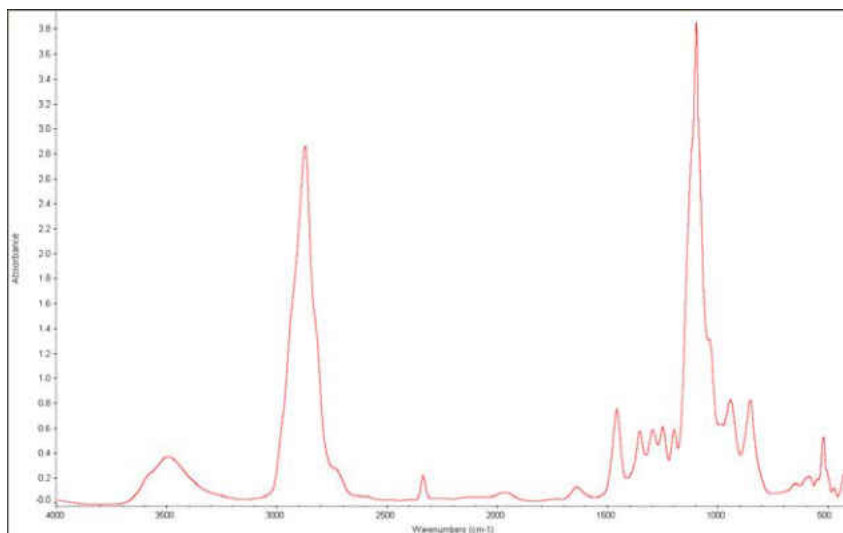
Figure 4.15 FTIR spectrum for the solvent sample.

4.5.2 DSC results

Results of the DSC measurements are shown in Figure 4.16 through Figure 4.19. Except for the peaks at the lower temperatures of -80 ^{o}C for the post experiment membranes, no significant structural changes are detectable. The aforementioned peaks could be attributed to solvent deposits on the membrane surface.
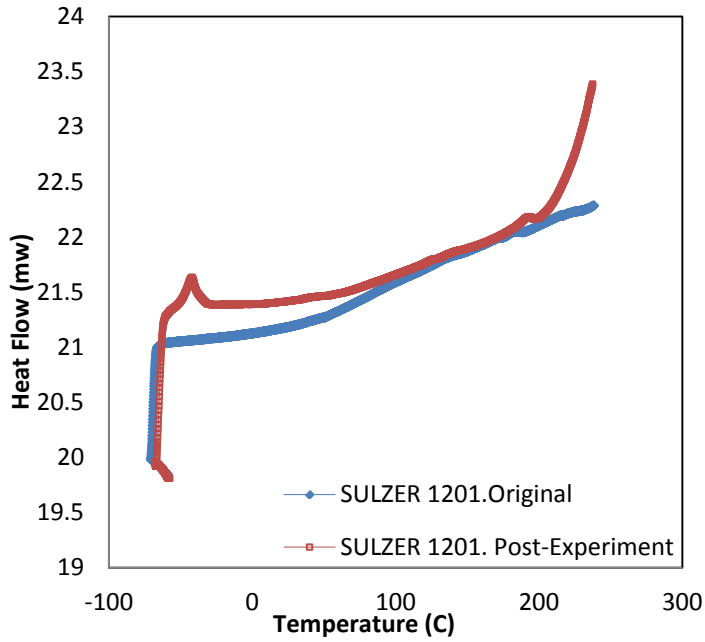
Figure 4.16 DSC results. PERVAP 1201, SULZER.
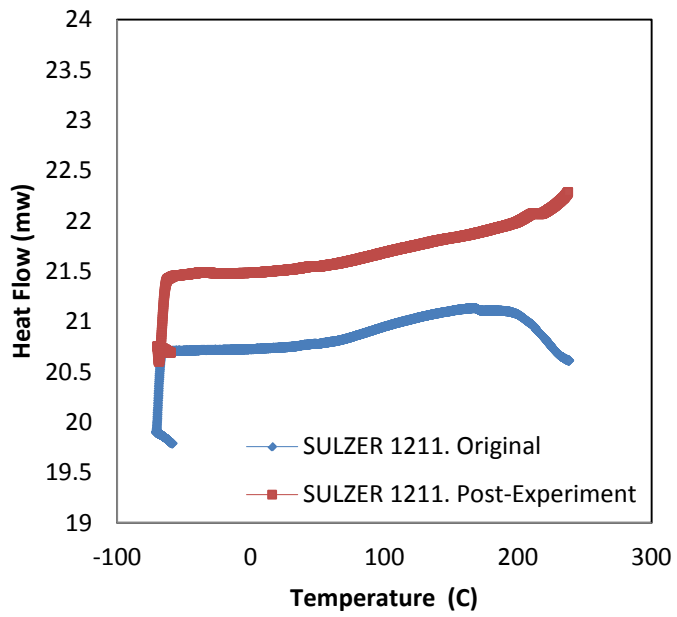
Figure 4.17 DSC results. PERVAP 1211, SULZER.
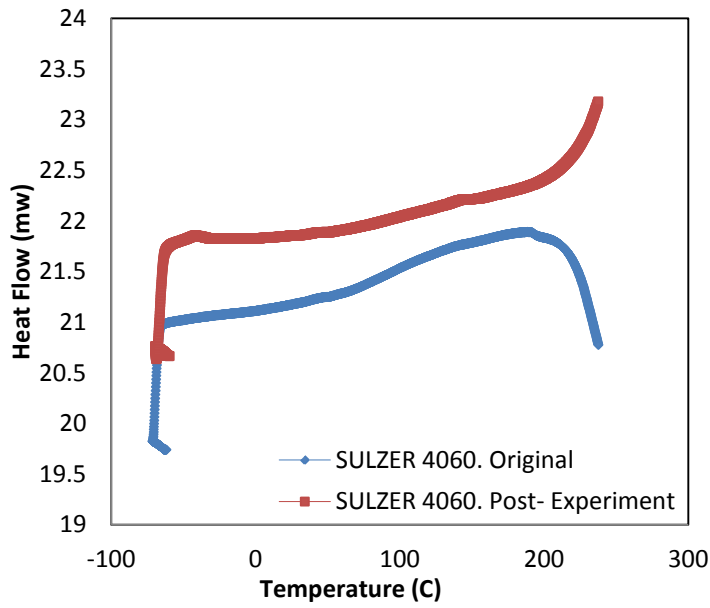
Figure 4.18 DSC results. PERVAP 4060, SULZER.
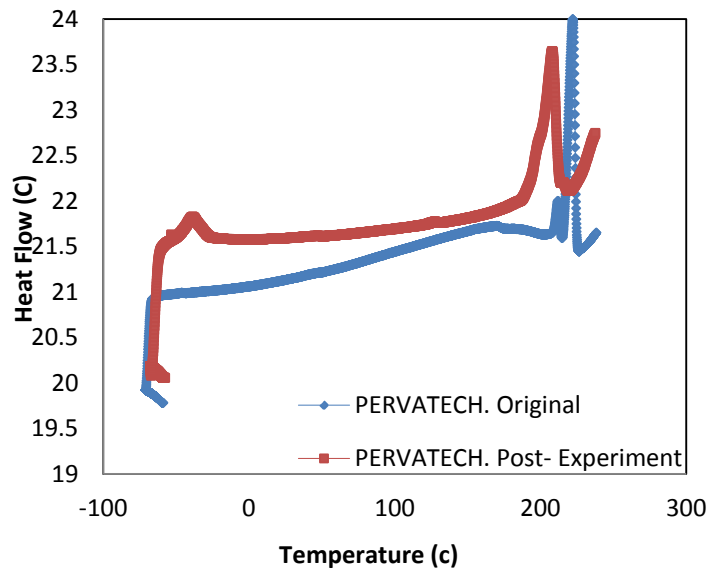
Figure 4.19 DSC results. PERVATECH.

4.5.3 SEM results

Top view and cross-section view images of PERVAP 4060 membrane are shown in Figure 4.20 and Figure 4.21 respectively.

(a)   (b)
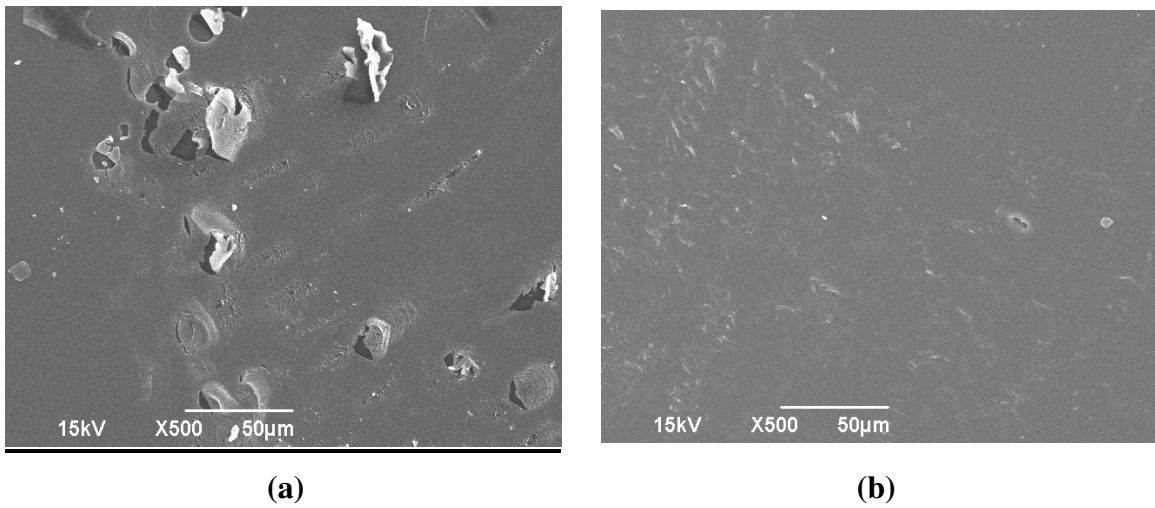
Figure 4.20 PERVAP 4060 top view comparison. (a) Original Membrane (b) Post experiment Membrane.

(a)   (b)
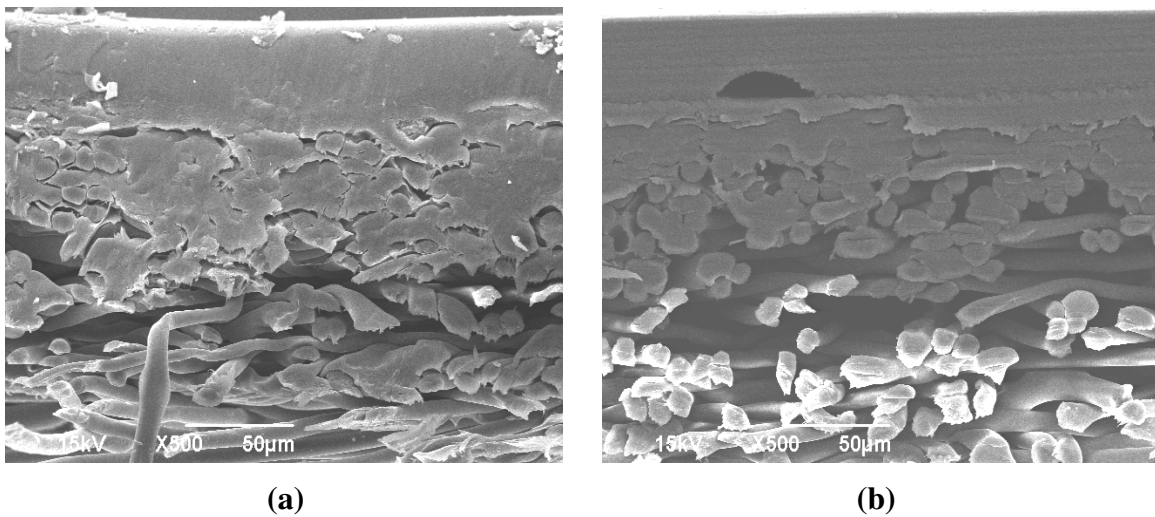
Figure 4.21 PERVAP 4060 cross-section view comparison. (a) Original Membrane (b) Post experiment Membrane.

A comparison of the SEM images shows no significant changes in the membrane after being exposed to the high pressure solvent stream in the permeation setup. The pores of the membrane in the porous support section of the membrane are not blocked or filled by solvent deposits or any membrane degradation product. The top surface of the membrane also appears to be the same after the permeation experiment.

4.6   Sorption experiment results

The physical properties of the membranes before the sorption experiment are summarized in Table 4.6. Figure 4.22 shows the mass gain for different membranes versus time. It is clear that no change of mass gain with respect to time was observed. This is mainly caused by the very low vapor pressure of the Selexol (0.00073 mm Hg). The highest mass gain of the PERVATECH membrane could explain the highest rate of solvent flux in Table 4.3

Table 4.6. Physical properties of the membrane before the sorption experiment.

Membrane	Mass (gr)	Thickness (cm)	Volume (cm^3)	Density (gr/cm^3)
PERVAP 1201	0.21440	0.020	0.346813	0.618201
PERVAP 1211	0.19896	0.018	0.312132	0.637423
PERVAP 4060	0.20419	0.021	0.364154	0.560725
PERVATECH	0.21845	0.023	0.398835	0.54772
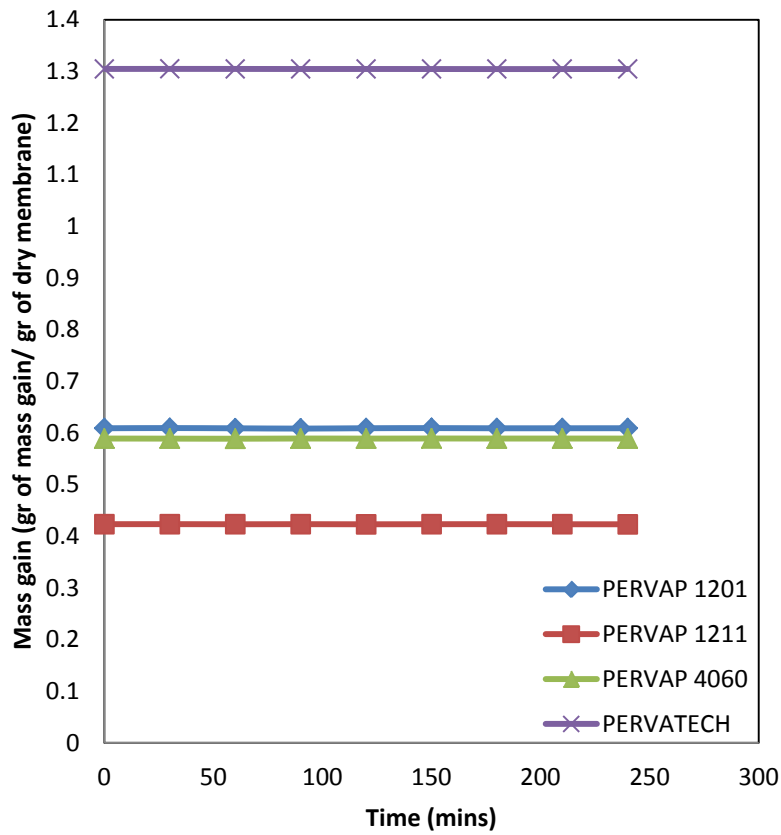
Figure 4.22 Mass gain of different membranes versus time.

Using equation (3.3), the calculated values of the solubility coefficient for different membranes are shown in Table 4.7.

Table 4.7 Solubility coefficient of different membranes.

Membrane	Solubility coefficient (S)
PERVAP 1201	0.072693
PERVAP 1211	0.049527
PERVAP 4060	0.061465
PERVATECH	0.366147

The calculated values of the solubility coefficient are in agreement with the calculated mass gains shown in Figure 4.22.

5 Conclusions

The primary objective of this thesis was to study the feasibility of the application of composite polymeric membranes for efficient regeneration of physical solvents. The bench-scale high pressure permeation setup was built and used to study the capacity of common commercial membranes for separating CO_2 from pre-saturated solvent. The primary conclusions from this work are as follows:

1. The CO_2 mole fraction in the solvent was measured using the sampling module. As the pressure of the system is elevated, the mole fraction of CO_2 in the solvent increases. Additionally, the concentration of CO_2 in the solvent reaches a steady state value approximately 2 hours after the absorber pressurization.

2. The CO_2 profile in the sweep gas reaches its steady state condition two hours after absorber pressurization.

3. PDMS-based membranes (PERVATECH and PERVAP 4060) have higher CO_2 permeability compared to PVOH based membranes (PERVAP 1211 and PERVAP 1201).

4. PEVAP 4060 was chosen as the candidate membrane for further analysis and design of engineering experiments to find the optimum operational conditions, due to its high CO_2 flux and selectivity compared to the other membranes.

5. The effects of temperature on the rate of CO_2 permeation was investigated. It was found that increasing the solvent temperature, upstream of the membrane module, does not enhance the rate of CO_2 concentration in the sweep gas stream.

6. To study the effects of sweep gas flow rate on the rate of CO_2 permeation, PERVAP 4060 membrane was used at two different sweep gas flow rates of 500 and 1000 (sccm) and CO_2 concentrations in the sweep gas were measured using the GC. The sweep gas flow rate did not affect the rate of CO_2 permeation significantly within the range of the experimental conditions in this study.

7. The results of the design of experiment's runs were used to perform a statistical analysis with Minitab^{TM} and the significant factors for various permeation responses such as, CO_2 flux, solvent leakage, and the percent recovery were identified.

8. With respect to CO_2 flux, pressure appeared to be strongly significant. However, solvent flow rate did not have any significant effect on the rate of CO_2 permeation. The primary conclusion based

on this observation is that the mass transfer is controlled by the membrane.

9. In terms of solvent leakage, pressure was found to be significant. Solvent flow rate did not have any influence on the rate of solvent leakage.

10. Neither the pressure of the system nor the solvent flow rate was found to be a significant factor in membrane selectivity.

11. Regarding the percent recovery of the solvent, both system pressure and solvent flow rate appeared to be significant.

12. The post-experiment characterization tests such as FTIR, DSC, and SEM were performed to study the chemical stability and structural integrity of the membranes after exposure to the high pressure solvent stream in the permeation setup. None of such tests showed any major change in the membrane material or structure.

6   Recommendations and Future Works

- Synthesizing CO_2-philic membranes with higher flux and selectivity to be tested in the permeation setup.

- Using higher surface area membrane modules, such as hollow-fiber modules and spiral membrane holders. Higher surface area might increase the percentage recovery of the solvent.

- Testing the candidate membranes with a real syngas to study the effect of impurities and other gas components extant in the gas stream.

- Economic analysis that compares the cost per avoided ton of CO_2 emissions for the membrane technology and pressure swing technique.

- Designing and building a pilot plant to regenerate a physical solvent at higher flow rates and pressures.

- Testing other commercial physical solvents to study the feasibility of solvent regeneration via the membrane technology.

- Running the permeation setup for significantly longer periods to study the structural integrity, chemical stability, and reliability of membrane technology.

7 Appendices

Appendix A. Sample calculation of CO_2 mole fraction in the solvent.

The detail of the sampling module was explained in section 3.2.8. A sample calculation of the CO_2 mole fraction at 400 psi is given here.

The following parameters were used in all calculations:

Universal Gas Constant:	1205.91	$(cm^3.psi/gmol.k)$
Solvent Density:	1.03	(gr/cm^3)
Solvent Average Molecular weight	250	(gr)
Sampling Module Total Volume:	1010	(cm^3)

For the sample taken at 400 Psi, the following data were collected from the sampling module:

Initial Pressure	2.16 (psi)
Final Equilibrium Pressure	5.07 (psi)
Sample Weight	2.57911(gr)
Temperature	291.15 (k)

The following equations are used to calculate the mole fraction of CO2 in the solvent sample.

$$n_{CO2} = \frac{[P_2(V_T - V_S) - P_1 V_T]}{RT}$$
Eqn (3.1)

$$X_{CO2} = \frac{n_{CO2}}{n_{CO2} + \frac{m_s}{M_n}}$$
Eqn (3.2)

so the mole fraction of CO_2 at 400 psi can be calculated as follows:

$$n_{CO2} = \frac{[5.07(1010 - 2.57911/1.03) - 2.16 \times 1010]}{1205.91 \times 291.15} = 8.3349 \times 10^{-3}$$

$$X_{CO2} = \frac{8.3349 \times 10^{-3}}{8.3349 \times 10^{-3} + \frac{2.57911}{250}} = 0.4468$$

Appendix B. Sample calculation of CO_2 flux and permeability.

The calculation procedure for PERVAP 4060 membrane at 300 psi and solvent flow rate of160 (mL/min) is given here. Table 6.1 summarizes the peaks area of CO_2 and N_2, given by the GC, with respect to the time.

Table 7.1. CO_2 and N_2 peaks areas with respect to time.

Time(min)	Area CO_2	Area N_2	Area (CO_2/N_2)	Flow (CO_2/N_2)	Flow CO_2 (sccm)
30	677.50	9457.36	0.072	0.082	41.1487
60	842.91	9338.77	0.090	0.104	51.8454
90	832.58	9293.28	0.090	0.103	51.4607
120	862.21	9321.43	0.092	0.106	53.1308
135	780.96	9391.40	0.083	0.096	47.7658
150	817.39	9353.19	0.087	0.100	50.1983
165	886.39	9278.80	0.096	0.110	54.8718
180	945.70	9282.52	0.102	0.117	58.5204
210	927.07	9254.31	0.100	0.115	57.5420
240	989.97	9264.24	0.107	0.123	61.3805
280	932.14	9266.83	0.101	0.116	57.7784
300	923.95	9299.85	0.099	0.114	57.0680
315	897.86	9320.06	0.096	0.111	55.3363
330	903.34	9293.90	0.097	0.112	55.8305
345	923.38	9284.28	0.099	0.114	57.1284
360	919.38	9276.89	0.099	0.114	56.9257
				Average Flow CO_2	55.8622

The first 120 minutes were excluded in taking the average of the CO_2 flow. Conversion of the peak area ratio to flow ratio was done using the calibration curve.

$$CO_2 \ Flux = \frac{\text{Average CO2 Flow}}{\text{Membrane Area}} \times \frac{1}{60} = \frac{55.862}{9.6} \times \frac{1}{60} =$$

$0.09698 \ (cm^3 \ (STP) \ CO_2/cm^2.s)$

Average solvent leak = $4.1 \times 10^{(-5)}$

Selectivity = (CO_2 Flux) / (Solvent Flux) = 2365.43

Using the same procedure explained in Appendix A, mole fraction of CO2 was calculated to be 0.3694.

Molar flow rate of solvent=

(solvent flow rate) × (solvent density)/(M.W solvent)= 0.01098 (moles/sec)

Moles of CO_2 entering the membrane module = N_{in}=

$$\frac{X_{CO2} \times (\text{Molar flow rate of solvent})}{(1-X_{CO2)}} = 0.006435 (\text{moles CO2/sec})$$

Moles of CO_2 permeating through the membrane= $N_{permeation}$

$$1(\text{atm}) \times \frac{(\text{CO2 flux}) \times (\text{Membrane Area})}{(82.057 \times (273.15 + 21.1))} = 3.85 \times 10^{(-5)} (\text{moles CO2/sec})$$

Percent Recovery= ($N_{permeation}$) / (N_{in}) ×100= 0.599 %

Appendix C. Statistical analysis

The residual plots for different responses are shown in Figure 7.1-Figure 7.4.
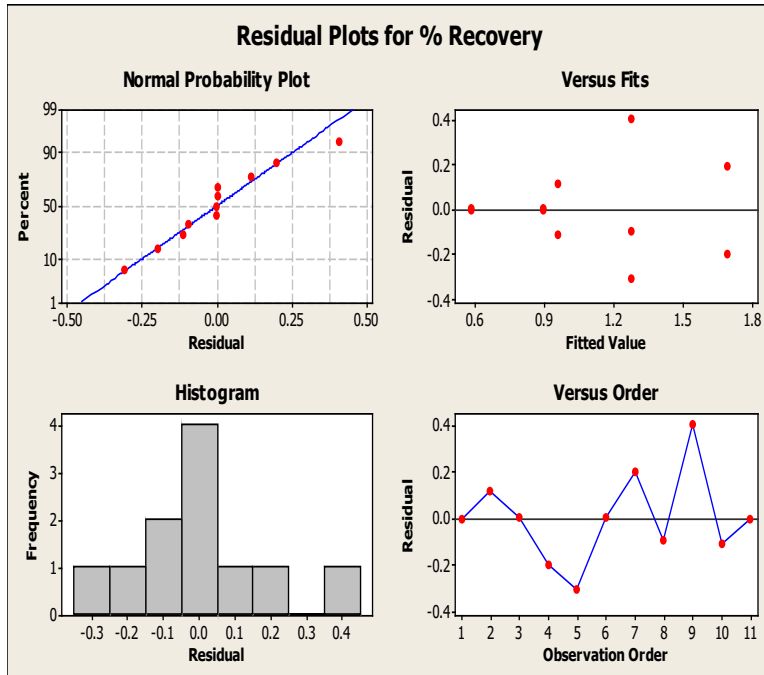
Figure 7.1. Residual plots for % recovery.
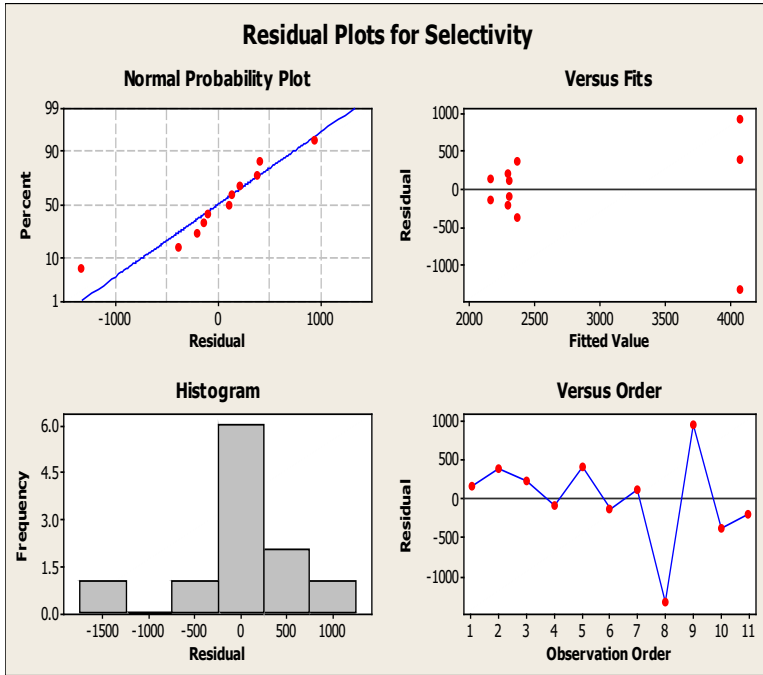
Figure 7.2. Residual plots for selectivity.
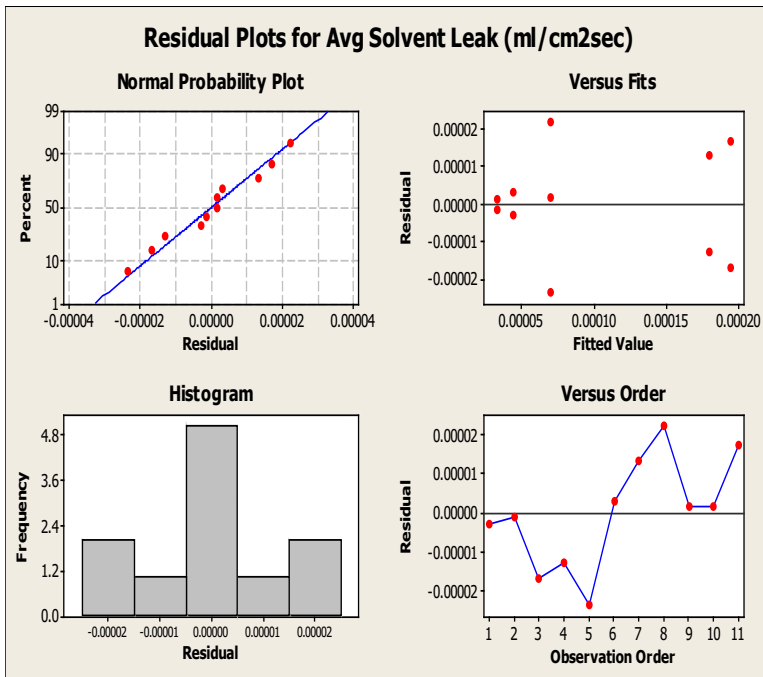
Figure 7.3. Residual plots for average solvent leakage.
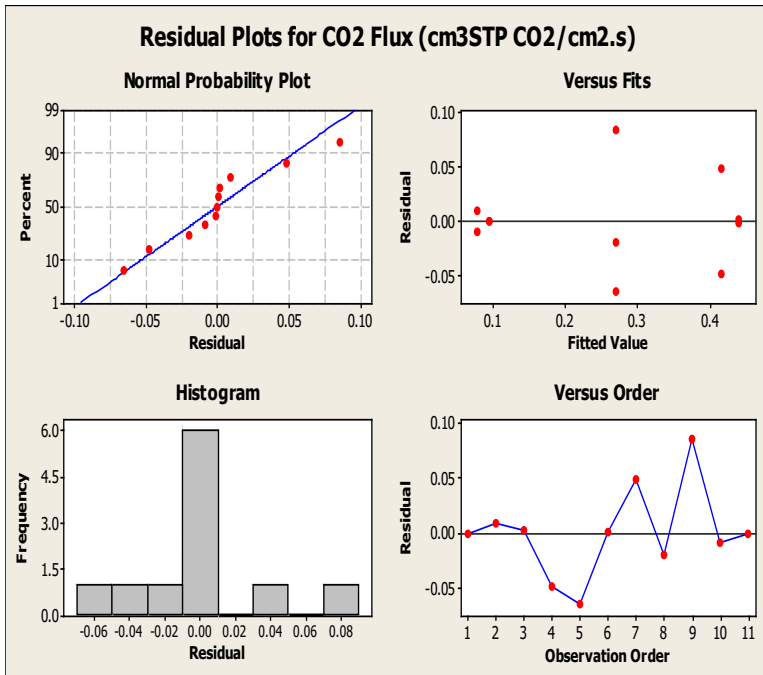
Figure 7.4. Residual plots for CO_2 flux.

Analysis of Variance for CO₂ Flux (cm³STP CO₂/cm².s) (coded units)

Analysis of Variance for CO_2 Flux (cm^{3}STP CO_2/cm^2.s) (coded units)

```
Source                        DF    Seq SS    Adj SS    Adj MS      F      P
Main Effects                   2  0.234630  0.234630  0.117315  41.55  0.000
  Pressure                     1  0.233764  0.233764  0.233764  82.80  0.000
  Solvent Flow rate            1  0.000866  0.000866  0.000866   0.31  0.600
2-Way Interactions             1  0.000034  0.000034  0.000034   0.01  0.916
  Pressure*Solvent Flow rate   1  0.000034  0.000034  0.000034   0.01  0.916
  Curvature                    1  0.000379  0.000379  0.000379   0.13  0.727
Residual Error                 6  0.016939  0.016939  0.002823
  Pure Error                   6  0.016939  0.016939  0.002823
Total                         10  0.251982
```

Estimated Coefficients for CO_2 Flux (cm^{3}STP CO_2/cm^2.s) using data in uncoded units

```
Term                               Coef
Constant                      -0.268329
Pressure                      0.00109839
Solvent Flow rate             0.00010558
Pressure*Solvent Flow rate  3.43407E-07
Ct Pt                         0.0131863
```

Least Squares Means for CO_2 Flux (cm^{3}STP CO_2/cm^2.s)

```
                            Mean   SE Mean
Pressure
 300                     0.08622   0.02657
 600                     0.42810   0.02657
Solvent Flow rate
  80                     0.24676   0.02657
 160                     0.26757   0.02657
Pressure*Solvent Flow rate
 300   80                0.07788   0.03757
 600   80                0.41564   0.03757
 300  160                0.09457   0.03757
 600  160                0.44057   0.03757


Mean for Center Point = 0.27035
```

Analysis of Variance for Avg Solvent Leak (mL/cm^2.sec) (coded units)

```
Source                           DF      Seq SS      Adj SS      Adj MS       F
Main Effects                      2  0.00000004  0.00000004  0.00000002   66.81
  Pressure                        1  0.00000004  0.00000004  0.00000004  132.70
  Solvent Flow rate               1  0.00000000  0.00000000  0.00000000    0.92
2-Way Interactions                1  0.00000000  0.00000000  0.00000000    0.02
  Pressure*Solvent Flow rate      1  0.00000000  0.00000000  0.00000000    0.02
  Curvature                       1  0.00000000  0.00000000  0.00000000   12.34
Residual Error                    6  0.00000000  0.00000000  0.00000000
  Pure Error                      6  0.00000000  0.00000000  0.00000000
Total                            10  0.00000005

Source                            P
Main Effects                  0.000
  Pressure                    0.000
  Solvent Flow rate           0.374
2-Way Interactions            0.904
  Pressure*Solvent Flow rate  0.904
  Curvature                   0.013
Residual Error
  Pure Error
Total
```

Estimated Coefficients for Avg Solvent Leak (mL/cm^2.sec) using data in uncoded units

```
Term                          Coef
Constant               -1.21000E-04
Pressure                4.78333E-07
Solvent Flow rate       9.37500E-08
Pressure*Solvent Flow rate  1.35417E-10
Ct Pt                  -4.33125E-05
```

Least Squares Means for Avg Solvent Leak (mL/cm^2.sec)

```
                          Mean    SE Mean
Pressure
 300                  0.000039   0.000009
 600                  0.000187   0.000009
Solvent Flow rate
  80                  0.000107   0.000009
 160                  0.000119   0.000009
Pressure*Solvent Flow rate
 300   80             0.000033   0.000013
 600   80             0.000180   0.000013
 300  160             0.000044   0.000013
 600  160             0.000194   0.000013


Mean for Center Point = 0.000070
```

Analysis of Variance for Selectivity (coded units)

```
Source                           DF    Seq SS   Adj SS   Adj MS      F       P
```

```
Main Effects                     2    25270    25270    12635   0.02  0.977
  Pressure                       1     2686     2686     2686   0.00  0.946
  Solvent Flow rate              1    22584    22584    22584   0.04  0.845
2-Way Interactions               1    17648    17648    17648   0.03  0.863
  Pressure*Solvent Flow rate     1    17648    17648    17648   0.03  0.863
  Curvature                      1  7013247  7013247  7013247  12.90  0.011
Residual Error                   6  3261830  3261830   543638
  Pure Error                     6  3261830  3261830   543638
Total                           10 10317995
```

Estimated Coefficients for Selectivity using data in uncoded units

```
Term                          Coef
Constant                    2804.19
Pressure                   -0.81719
Solvent Flow rate           -4.8509
Pressure*Solvent Flow rate 0.0078279
Ct Pt                       1792.88
```

Least Squares Means for Selectivity

```
                          Mean   SE Mean
Pressure
 300                      2259    368.7
 600                      2295    368.7
Solvent Flow rate
  80                      2330    368.7
 160                      2224    368.7
Pressure*Solvent Flow rate
 300  80                  2359    521.4
 600  80                  2302    521.4
 300 160                  2159    521.4
 600 160                  2289    521.4


Mean for Center Point = 4070
```

Analysis of Variance for % Recovery (coded units)

```
Source                      DF   Seq SS   Adj SS   Adj MS      F      P
Main Effects                 2  1.24132  1.24132  0.62066   9.92  0.013
  Pressure                   1  0.55053  0.55053  0.55053   8.79  0.025
  Solvent Flow rate          1  0.69079  0.69079  0.69079  11.04  0.016
2-Way Interactions           1  0.08794  0.08794  0.08794   1.40  0.281
  Pressure*Solvent Flow rate 1  0.08794  0.08794  0.08794   1.40  0.281
  Curvature                  1  0.13223  0.13223  0.13223   2.11  0.196
Residual Error               6  0.37558  0.37558  0.06260
  Pure Error                 6  0.37558  0.37558  0.06260
Total                       10  1.83707
```

Estimated Coefficients for % Recovery using data in uncoded units

```
Term                            Coef
Constant                    0.186470
Pressure                  0.00384582
Solvent Flow rate         0.00051731
Pressure*Solvent Flow rate -1.74747E-05
Ct Pt                       0.246179
```

Least Squares Means for % Recovery

```
                          Mean   SE Mean
Pressure
 300                    0.7732    0.1251
 600                    1.2979    0.1251
Solvent Flow rate
  80                    1.3294    0.1251
 160                    0.7417    0.1251
Pressure*Solvent Flow rate
 300   80               0.9622    0.1769
 600   80               1.6966    0.1769
 300  160               0.5842    0.1769
 600  160               0.8992    0.1769


Mean for Center Point = 1.2817
```

122

References

1. Alexander Stern, S. (1994). Polymers for gas separations: The next decade. *Journal of Membrane Science, 94*(1), 1-65.

2. Baker, R. (2012). *Membrane technology and applications* Wiley.

3. Baker, R. W. (2002). Future directions of membrane gas separation technology. *Industrial & Engineering Chemistry Research, 41*(6), 1393-1411.

4. Basu, R., & Sirkar, K. (1991). Hollow fiber contained liquid membrane separation of citric acid. *AIChE Journal, 37*(3), 383-393.

5. Bessarabov, D. (1999). Membrane gas-separation technology in the petrochemical industry. *Membrane Technology, 1999*(107), 9-13.

6. Bhide, B., Voskericyan, A., & Stern, S. (1998). Hybrid processes for the removal of acid gases from natural gas. *Journal of Membrane Science, 140*(1), 27-49.

7. Breckenridge, W., Holiday, A., Ong, J. O., & Sharp, C. (2000). Use of SELEXOL® process in coke gasification to ammonia project. Paper presented at the *PROCEEDINGS OF THE LAURANCE REID GAS CONDITIONING CONFERENCE,* 397-418.

8. Brunetti, A., Scura, F., Barbieri, G., & Drioli, E. (2010). Membrane technologies for CO_2 separation. *Journal of Membrane Science, 359*(1), 115-125.

9. Bucklin, R., & Schendel, R. (1985). *Comparison of physical solvents used for gas processing* Gulf Publishing Company, Houston, TX.

10. Burr, B., & Lyddon, L. (2008). A comparison of physical solvents for acid gas removal. Paper presented at the *Gas Processors' Association Convention, Grapevine, TX,*

11. Chern, R., Sheu, F., Jia, L., Stannett, V., & Hopfenberg, H. (1987). Transport of gases in unmodified and arylbrominated 2, 6-dimethyl-1, 4-poly (phenylene oxide). *Journal of Membrane Science, 35*(1), 103-115.

12. *CO₂ EMISSIONS FROM FUEL COMBUSTION.* (2012). (). Paris, France: International energy Agency.

13. Coleman, M., & Koros, W. (1990). Isomeric polyimides based on fluorinated dianhydrides and diamines for gas separation applications. *Journal of Membrane Science, 50*(3), 285-297.

14. Collins, J. P., Schwartz, R. W., Sehgal, R., Ward, T. L., Brinker, C., Hagen, G. P., & Udovich, C. A. (1996). Catalytic dehydrogenation of propane in hydrogen permselective membrane reactors. *Industrial & Engineering Chemistry Research, 35*(12), 4398-4405.

15. COONEY, D. O., & POUFOS, M. G. (1987). Liquid-liquid extraction in a hollow-fiber device. *Chemical Engineering Communications, 61*(1-6), 159-167.

16. Dastgir, M. G., Ferreira, F. C., Peeva, L. G., & Livingston, A. G. (2004). Recovery of 2, 4   -dichlorophen
system (MARS). *Journal of Chemical Technology and Biotechnology, 79*(4), 381-390.

17. Dastgir, M. G., Peeva, L. G., & Livingston, A. G. (2005). The performance of composite supported polymeric liquid membranes in the membrane aromatic recovery system (MARS). *Chemical Engineering Science, 60*(24), 7034-7044.

18. Doctor, R., Molburg, J., & Thimmapuram, P. (1994). *Gasification Combined Cycle: Carbon Dioxide Recovery, Transport,*

19. Eldridge, R. B. (1993). Olefin/paraffin separation technology: A review. *Industrial & Engineering Chemistry Research, 32*(10), 2208-2212.

20. Epps, R. (1994). Use of selexol solvent for hydrocarbon dewpoint control and dehydration of natural gas. Paper presented at the *Laurance Reid Gas Conditioning Conference, Norman, OK,*

21. Epps, R. Union Carbide Chemicals & Plastics Technology Corporation. (1992). Processing of landfill gas for commercial applications: The SELEXOL solvent process. Washington D. C.

22. Feron, P., & Jansen, A. (1995). Capture of carbon dioxide using membrane gas absorption and reuse in the horticultural industry. *Energy Conversion and Management, 36*(6), 411-414.

23. Figueroa, J. D., Fout, T., Plasynski, S., McIlvried, H., & Srivastava, R. D. (2008). Advances in CO_2 capture technology—The US department of energy's carbon sequestration program. *International Journal of Greenhouse Gas Control, 2*(1), 9-20.

24. Freeman, B., Yampolskii, Y., & Pinnau, I. (2006). *Materials science of membranes for gas and vapor separation* Wiley.

25. Gabelman, A., & Hwang, S. (1999). Hollow fiber membrane contactors. *Journal of Membrane Science, 159*(1–2), 61-106. doi:10.1016/S0376-7388(99)00040-X

26. Gainar, I., & Anitescu, G. (1995). The solubility of CO_2 , N_2 and H_2 in a mixture of dimethylether polyethylene glycols at high pressures. *Fluid Phase Equilibria, 109*(2), 281-289.

27. Han, S., Ferreira, F. C., & Livingston, A. (2001). Membrane aromatic recovery system (MARS)—a new membrane process for the recovery of phenols from wastewaters. *Journal of Membrane Science, 188*(2), 219-233.

28. Han, S., Puech, L., Law, R. V., Steinke, J. H., & Livingston, A. (2002). Selection of elastomeric membranes for the separation of organic compounds in acidic media. *Journal of Membrane Science, 199*(1), 1-11.

29. Heintz, Y. J., Sehabiague, L., Morsi, B. I., Jones, K. L., & Pennline, H. W. (2008). Novel physical solvents for selective CO_2 Capture from fuel gas streams at elevated pressures and temperatures†. *Energy & Fuels, 22*(6), 3824-3837.

30. Hellums, M., Koros, W., Husk, G., & Paul, D. (1991). Gas transport in halogen - containing aromatic polycarbonates. *Journal of Applied Polymer Science, 43*(11), 1977-1986.

31. Henis, J. M., & Tripodi, M. K. (1980). A novel approach to gas separations using composite hollow fiber membranes. *Separation Science and Technology, 15*(4), 1059-1068.

32. Henni, A., Tontiwachwuthikul, P., & Chakma, A. (2006). Solubility study of methane and ethane in promising physical solvents for natural gas sweetening operations. *Journal of Chemical & Engineering Data, 51*(1), 64-67.

33. Herzog, H. (1999). An introduction to CO_2 separation and capture technologies. *Energy Laboratory Working Paper,*

34. Hu, L., Xu, X., & Coleman, M. R. (2007). Impact of H ion beam irradiation on matrimid®. II. evolution in gas transport properties. *Journal of Applied Polymer Science, 103*(3), 1670-1680.

35. Ilinitch, O., Semin, G., Chertova, M., & Zamaraev, K. (1992). Novel polymeric membranes for separation of hydrocarbons. *Journal of Membrane Science, 66*(1), 1-8.

36. *International energy statistics.* (2010). ().Energy Information Administration.

37. *INVENTORY OF U.S. GREENHOUSE GAS EMISSIONS AND SINKS: 1990-2011 .* (2013). (). washington, DC: U.S. Environmental Protection Agency.

38. Itoh, N. (1987). A membrane reactor using palladium. *AIChE Journal, 33*(9), 1576-1578.

39. Jia, J., & Baker, G. L. (1998). Crosslinking of poly [1 (trimethylsilyl) 1 propyne] membranes using bis (aryl azides). *Journal of Polymer Science Part B: Polymer Physics, 36*(6), 959-968.

40. Judd, D. K. (1978). Selexol unit saves energy. *Journal of Hydrocarbon Processing, 57*(NO. 4, April), 122-124.

41. Kelman, S. D., Rowe, B. W., Bielawski, C. W., Pas, S. J., Hill, A. J., Paul, D., & Freeman, B. (2008). Crosslinking poly [1-(trimethylsilyl)-1-propyne] and its effect on physical stability. *Journal of Membrane Science, 320*(1), 123-134.

42. Kesting, R., Fritzsche, A., Murphy, M., Cruse, C., Handermann, A., Malon, R., & Moore, M. (1990). The second-generation polysulfone gas-separation membrane. I. the use of lewis acid: Base complexes as transient templates to increase free volume. *Journal of Applied Polymer Science, 40*(9 -10), 1557-1574.

43. Kikuchi, E. (1995). Palladium/ceramic membranes for selective hydrogen permeation and their application to membrane reactor. *Catalysis Today, 25*(3), 333-337.

44. Kim, T., Koros, W., Husk, G., & O'brien, K. (1988). Relationship between gas separation properties and chemical structure in a series of aromatic polyimides. *Journal of Membrane Science, 37*(1), 45-62.

45. Kohl, A. L., & Nielsen, R. (1997). *Gas purification* Gulf Professional Publishing.

46. Korens, N., Simbeck, D. R., Wilhelm, D. J., Longanbach, J. R., & Stiegel, G. J. (2002). SFA pacific, inc.

47. Koros, W., & Fleming, G. (1993). Membrane-based gas separation. *Journal of Membrane Science, 83*(1), 1-80.

48. Kumar, P., Hogendoorn, J., Feron, P., & Versteeg, G. (2002). New absorption liquids for the removal of CO_2 from dilute gas streams using membrane contactors. *Chemical Engineering Science, 57*(9), 1639-1651.

49. Lebo, J., Zajicek, J., Huckins, J., Petty, J., & Peterman, P. (1992). Use of semipermeable membrane devices for in situ monitoring of polycyclic aromatic hydrocarbons in aquatic environments. *Chemosphere, 25*(5), 697-718.

50. Li, J., & Chen, B. (2005). Review of CO_2 absorption using chemical solvents in hollow fiber membrane contactors. *Separation and Purification Technology, 41*(2), 109-122. doi:10.1016/j.seppur.2004.09.008

51. Matsuura, T. (1994). *Synthetic membranes and membrane separation processes* CRC PressI Llc.

52. *Meeting staged CO_2 Capture requirements with the UOP SELEXOL™ process.* (2009). ().UOP. A Honeywell company.

53. Meindersma, G., & Kuczynski, M. (1996). Implementing membrane technology in the process industry: Problems and opportunities. *Journal of Membrane Science, 113*(2), 285-292.

54. Miller, M. B., Chen, D., Xie, H., Luebke, D. R., Karl Johnson, J., & Enick, R. M. (2009). Solubility of CO_2 in CO_2 -philic oligomers; COSMOtherm predictions and experimental results. *Fluid Phase Equilibria, 287*(1), 26-32. doi:10.1016/j.fluid.2009.08.022

55. Mulder, M. (1991). Basic principles of membrane technology.

56. Muruganandam, N., & Paul, D. (1987). Evaluation of substituted polycarbonates and a blend with polystyrene as gas separation membranes. *Journal of Membrane Science, 34*(2), 185-198.

57. NETL, D. (May 2011). Advanced carbon dioxide capture R&D program: Technology update.

58. Newman, S. (1985). *Acid and sour gas treating processes* Gulf Publishing Co., Houston, TX.

59. Nunes, S. P., & Peinemann, K. (2006). *Membrane technology: In the chemical industry* Wiley-VCH.

127

60. Okamoto, K., Tanihara, N., Watanabe, H., Tanaka, K., Kita, H., Nakamura, A., . . . Nakagawa, K. (1992). Vapor permeation and pervaporation separation of water-ethanol mixtures through polyimide membranes. *Journal of Membrane Science, 68*(1), 53-63.

61. Okamoto, K., Semoto, T., Tanaka, K., & Kita, H. (1991). Application of pervaporation to Phenol–Acetone condensation reaction. *Chemistry Letters, 20*(1), 167-170.

62. Olajire, A. A. (2010). CO_2 capture and separation technologies for end-of-pipe applications–A review. *Energy, 35*(6), 2610-2628.

63. Pankhania, M., Stephenson, T., & Semmens, M. J. (1994). Hollow fibre bioreactor for wastewater treatment using bubbleless membrane aeration. *Water Research, 28*(10), 2233-2236.

64. Park, Y. S., Won, J., & Kang, Y. S. (2001). Facilitated transport of olefin through solid PAAm and PAAm-graft composite membranes with silver ions. *Journal of Membrane Science, 183*(2), 163-170.

65. Percec, S. (1987). Chemical modification of poly (2, 6-dimethyl-1, 4-phenylene oxide) by friedel–crafts reactions. *Journal of Applied Polymer Science, 33*(1), 191-203.

66. Perry, R. H., Green, D. W., & Maloney, J. O. (2008). *Perry's chemical engineers' handbook* McGraw-Hill New York.

67. Pixton, M., & Paul, D. (1994). *Relationships between structure and transport properties for polymers with aromatic backbones* CRC Press, Boca Raton, FL.

68. Porter, K., Sitthiosoth, S., & Jenkins, J. (1991). Designing a solvent for gas absorption. *Chemical Engineering Research & Design, 69*(A3), 229-236.

69. *Power plant carbon capture with CHEMCAD.* (No. rev. 031109).CHEMCAD.

70. Prasad, R., & Sirkar, K. (1987). Microporous membrane solvent extraction. *Separation Science and Technology, 22*(2-3), 619-640.

71. Prasad, R., & Sirkar, K. (1990). Hollow fiber solvent extraction: Performances and design. *Journal of Membrane Science, 50*(2), 153-175.

72. Prasad, R., & Sirkar, K. (1989). Hollow fiber solvent extraction of pharmaceutical products: A case study. *Journal of Membrane Science, 47*(3), 235-259.

73. Puri, P. S. (1996). Gas separation membranes-current status. *멤브레인, 6*(3), 117-126.

74. Raney, D. R. (1976). Remove carbon dioxide with selexol. *Journal of Hydrocarbon Processing, 55*(4), 73.

75. Rousseau, R., Matange, J., & Ferrell, J. (1981). Solubilities of carbon dioxide, hydrogen sulfide and nitrogen mixtures in methanol. *AIChE Journal, 27*(4), 605-613.

76. Sciamanna, S. F., & Lynn, S. (1988). Solubility of hydrogen sulfide, sulfur dioxide, carbon dioxide, propane, and n-butane in poly (glycol ethers). *Industrial & Engineering Chemistry Research, 27*(3), 492-499.

77. Solomon, S., Qin, D., Manning, M., Chen, Z., Marquis, M., Averyt, K., . . . Miller, H. (2007). IPCC climate change 2007: The physical science basis. *Contribution of Working Group I to the Fourth Assessment Report of the Intergovernmental Panel on Climate Change, Cambridge University Press, Cambridge, United Kingdom and New York, NY, USA,*

78. Spillman, R. W. (1989). Economics of gas separation membranes. *Chemical Engineering Progress, 85*(1), 41-62.

79. Stanojević, M., Lazarević, B., & Radić, D. (2003). Review of membrane contactors designs and applications of different modules in industry. *FME Transactions, 31*(2), 91-98.

80. Stern, S., Mi, Y., Yamamoto, H., & Clair, A. K. S. (1989). Structure/permeability relationships of polyimide membranes. applications to the separation of gas mixtures. *Journal of Polymer Science Part B: Polymer Physics, 27*(9), 1887-1909.

81. Stewart, C., & Hessami, M. (2005). A study of methods of carbon dioxide capture and sequestration—the sustainability of a photosynthetic bioreactor approach. *Energy Conversion and Management, 46*(3), 403-420.

82. Story, B. J., & Koros, W. (1992). Sorption and transport of CO_2 and CH_4 in chemically modified poly (phenylene oxide). *Journal of Membrane Science, 67*(2), 191-210.

83. Strube, R., & Manfrida, G. (2011). CO_2 capture in coal-fired power plants—Impact on plant performance. *International Journal of Greenhouse Gas Control, 5*(4), 710-726.

84. Sweny, J. W. (1976). The SELEXOL process in fuel gas treating. *81st National Meeting of the American Institute of Chemical Engineers,*

85. Sweny, J. W. (1980). High CO_2- high H_2S removal with selexol solvent. *59th Annual GPA Convention,*

86. Sweny, J. (1976). Synthetic fuel gas purification by the SELEXOL process. *Am.Chem.Soc., Div.Fuel Chem., Prepr.;(United States), 18*(2)

87. Toshima, N. (1992). *Polymers for gas separation* VCH Weinheim.

88. VAN DEN, B., & Smolders, C. (1988). Flux decline in membrane processes. *Filtration & Separation, 25*(2), 115-121.

89. Wankat, P. C. (2006). *Separation process engineering* Prentice Hall.

90. Wijmans, J. G., & Baker, R. W. (1995). The solution-diffusion model: A review. *Journal of Membrane Science, 107*(1–2), 1-21. doi:10.1016/0376-7388(95)00102-I

91. Wikol, M. J., Kobayashi, M., & Hardwick, S. J. (1998). Application of PTFE membrane contactors to the infusion of ozone into ultra-high purity water. *Contamination Control, ,* 172-177.

92. Yamasaki, A. (2003). An overview of CO_2 mitigation options for global warming-emphasizing CO_2 sequestration options. *Journal of Chemical Engineering of Japan, 36*(4), 361-375.

93. Yan, S., Fang, M., Zhang, W., Wang, S., Xu, Z., Luo, Z., & Cen, K. (2007). Experimental study on the separation of CO_2 from flue gas using hollow fiber membrane contactors without wetting. *Fuel Processing Technology, 88*(5), 501-511. doi:10.1016/j.fuproc.2006.12.007

94. Zhu, Y., Minet, R. G., & Tsotsis, T. T. (1996). A continuous pervaporation membrane reactor for the study of esterification reactions using a composite polymeric/ceramic membrane. *Chemical Engineering Science, 51*(17), 4103-4113. doi:10.1016/0009-2509(96)00252-7